MINISTÉRIO DA EDUCAÇÃO
UNIVERSIDADE FEDERAL RURAL DA AMAZÔNIA - UFRA
DOUTORADO EM AGRONOMIA

LUCILENE RODRIGUES DOS SANTOS

HOW BRASSINOSTEROIDS ACT IN SOYBEAN PLANTS SUBMITTED TO THE INADEQUATE ZINC AND IRON SUPPLIES?

BELÉM
2020

LUCILENE RODRIGUES DOS SANTOS

HOW BRASSINOSTEROIDS ACT IN SOYBEAN PLANTS SUBMITTED TO THE INADEQUATE ZINC AND IRON SUPPLIES?

Thesis submitted to Universidade Federal Rural da Amazônia, as part of the requirements for obtaining the *Doctor Scientiae* degree in Agronomy.
Concentration area: Plant Physiology.
Advisor: Prof. Dr. Allan Klynger da Silva Lobato

BELÉM
2020

Dados Internacionais de Catalogação na Publicação (CIP)
Bibliotecas da Universidade Federal Rural da Amazônia
Gerada automaticamente mediante os dados fornecidos pelo(a) autor(a)

S237h Santos, Lucilene Rodrigues dos Santos
HOW BRASSINOSTEROIDS ACT IN SOYBEAN PLANTS SUBMITTED TO THE INADEQUATE ZINC AND IRON SUPPLIES? / Lucilene Rodrigues dos Santos . - 2020.
61 f.

Tese (Doutorado) - Programa de Pós-Graduação em Agronomia (PPGA), Campus Universitário de Belém, Universidade Federal Rural Da Amazônia, Belém, 2020.
Orientador: Prof. Dr. Allan Klynger da Silva Lobato

1. Glycine max. 2. Brassinosteróides. 3. Micronutrientes. 4. Anatomia radicular. 5. Clorofila I. Lobato, Allan Klynger da Silva, *orient.* II. Título

CDD 630

LUCILENE RODRIGUES DOS SANTOS

HOW BRASSINOSTEROIDS ACT IN SOYBEAN PLANTS SUBMITTED TO THE INADEQUATE ZINC AND IRON SUPPLIES?

Thesis submitted to Universidade Federal Rural da Amazônia, as part of the requirements for obtaining the Doctor Scientiae degree in Agronomy.
Concentration area: Plant Physiology.
Advisor: Prof. Dr. Allan Klynger da Silva Lobato

EXAMINATION BOARD

Allan Klynger da S. Lobato

Prof. Dr. Allan Klynger da Silva Lobato – Advisor
UNIVERSIDADE FEDERAL RURAL DA AMAZÔNIA – UFRA

Flávio José Rodrigues Cruz

Prof. Dr. Flávio José Rodrigues Cruz – 1st Examiner
UNIVERSIDADE FEDERAL RURAL DE PERNAMBUCO – UFRPE

João Rodrigo C. Nobre

Prof. Dr. João Rodrigo Coimbra Nobre – 2rd Examiner
UNIVERSIDADE DO ESTADO DO PARÁ – UEPA

Rafaela Cabral dos Santos

Dra Rafaela Cabral dos Santos da Trindade – 3rd Examiner
MEMBRO EXTERNO A INSTITUIÇÃO

Seidel Ferreira dos Santos

Prof. Dr. Seidel Ferreira dos Santos – 4rd Examiner
UNIVERSIDADE DO ESTADO DO PARÁ – UEPA

Ao Mestre dos mestres,
pela minha existência, amor e proteção divina.

Aos meus amados pais, Lídia e Pedro,

expresso minha gratidão por todo amor, incentivo em todos os momentos da minha vida e por serem pilares em minha educação.

À minha filha Lídia Helena,

amor incondicional e motivo da minha resiliência.

Às minhas amadas irmãs, Luciane e Sinara,

pelo carinho, apoio e confiança indispensáveis para esta conquista.

À minha vovó Maria Letícia,

por me colocar sempre em suas orações e por me transmitir sua fé e sua alegria em todas as minhas conquistas.

A Lecides Henrique,

obrigada por todo seu carinho e companheirismo.

DEDICO

*Ao meu amado **DEUS**, toda honra e toda glória.*

OFEREÇO

*"**SENHOR**, eu reconheço que para ti nada é impossível e que nenhum dos teus planos pode ser impedido"*

Jó 42.1-2

AGRADECIMENTOS

À Deus, acima de todas as coisas, por ter me concedido a proteção celestial, a saúde, a força e a sabedoria para conduzir essa pesquisa e ter feito desse sonho realidade em minha vida. Obrigada meu Deus por todas as graças alcançadas.

À Universidade Federal Rural da Amazônia, pela oportunidade e acolhida no curso de doutorado em Agronomia e por toda a estrutura concedida na realização dessa Pesquisa.

A Coordenação de Aperfeiçoamento de Pessoal de Nível Superior (CAPES) pela concessão da bolsa de doutorado.

Ao meu orientador, Prof. Dr. Allan Klynger da Silva Lobato, pela amizade, por todos os ensinamentos, estímulo, paciência e pelo exemplo de profissionalismo e dedicação a serem seguidos.

Aos membros da Banca Examinadora, pela atenção e, principalmente, pelas críticas e sugestões que fizeram enriquecer esta pesquisa.

Aos meus pais, Lídia e Pedro por todo amor, ensinamento e dedicação a mim confiados durante toda a minha formação e por todo apoio incondicional.

A minha filha Lídia Helena, que me trouxe força e persistência.

As minhas irmãs pelo carinho e confiança.

À Lecides, por sua amizade e companheirismo.

À minha avó Maria Leticia, obrigada por todos os terços rezados.

Aos professores do Programa de Pós-Graduação em Agronomia (PGagro) pelos ensinamentos adquiridos durante o curso.

A todos que contribuíram direta ou indiretamente para a realização deste trabalho e concretização deste sonho.

Meu muito obrigada!

SUMÁRIO

RESUMO

A produção global da soja atingiu na safra 2017/2018, a segunda maior produção já registrada graças às colheitas nos Estados Unidos e no Brasil. Entre os fatores que têm contribuído para alavancar a produção e produtividade desta commodity, além das condições favoráveis do solo, a disponibilidade dos nutrientes, em especial dos micronutrientes, tem sido um fator determinante a ser considerado. Micronutrientes essenciais como zinco (Zn) e ferro (Fe) desempenham um papel crucial na produção da soja, pois estão envolvidos durante todo o ciclo de desenvolvimento da cultura. Contudo, suprimentos inadequados de Zn e Fe têm se tornado fatores de estresse para cultura devido à deficiência ou excesso destes elementos na planta. Nos últimos anos, estratégias e tecnologias têm sido desenvolvidas para o tratamento de plantas estressadas por fatores abióticos, entre eles, a aplicação de esteroides vegetais tem sido discutida como um método eficaz e menos danoso. Dos esteróides vegetais, uma considerável atenção tem sido dada aos Brassinosteroides (BRs). Neste contexto, objetivou-se avaliar os efeitos de Zn e Fe na cultura da soja exposta a suprimentos baixo/alto destes elementos no solo, assim como investigar o comportamento fisiológico e bioquímico do BRs em plantas de soja submetidas à deficiência e ao excesso de Zn e Fe e identificar quais os possíveis benefícios provocados pelo esteroide. Para isso, foram realizados dois experimentos em casa de vegetação. O experimento I seguiu um planejamento fatorial completamente casualizado com duas concentrações de 24-epibrassinolídeo (0 e 100 nM EBR) e três suprimentos de Zn (0,2, 20 e 2000 μM Zn). O experimento II foi realizado em um delineamento inteiramente casualizado com quatro tratamentos (0 nM EBR + 250 μM Fe, 0 nM EBR + 2,5 μM Fe, 100 nM EBR + 250 μM Fe e 100 nM EBR + 2,5 μM Fe). Em geral, suprimentos baixos de Zn e Fe e altos de Zn produziram efeitos deletérios. Contudo, os resultados revelaram que o BRs exógeno (100 nM EBR) minimizou os danos causados pela deficiência de Zn e Fe e pelos níveis tóxicos de Zn em plantas de soja. No experimento I, o EBR aliviou o impacto produzido pelo estresse do zinco no sistema radicular agindo positivamente sobre epiderme, endoderme, córtex, cilindro vascular e metaxilema, melhorando intrisecamente o status nutricional nas plantas. EBR promoveu melhoras no maquinário fotossintético de plantas expostas ao estresse de zinco, estimulando a atividade das enzimas antioxidantes que desempenham papéis cruciais na proteção das membranas do cloroplastos, com repercussões positivas sobre as clorofilas, rendimento quântico efetivo da fotoquímica do PSII e taxa de transporte de elétrons. No experimento II, o EBR maximizou o teor de Fe na folha, caule e raiz, bem como melhorou o teor de nutrientes e a homeostase do metal, conforme confirmado pela detecção aumentada de $Fe^{2+/}Mg^{2+}$, Fe^{2+}/Mn^{2+} e Fe^{2+}/Cu^{2+} em plantas com deficiência de Fe. O esteróide também promoveu melhorias nos pigmentos cloroplásticos e aumentou a eficiência fotoquímica, regulando positivamente o transporte de elétrons e reduzindo os impactos negativos associados à fotoinibição do PSII.

Palavras chave: *Glycine max*, Brassinosteróides, Micronutrientes, Anatomia da raiz, Clorofila

ABSTRACT

Global soy production reached the 2017/2018 crop, the second highest production ever recorded thanks to harvests in the United States and Brazil. Among the factors that have contributed to leverage the production and productivity of this commodity, in addition to favorable soil conditions, the availability of nutrients, especially micronutrients, has been a determining factor to be considered. Essential micr-onutrients such as zinc (Zn) and iron (Fe) play a crucial role in soybean production, as they are involved throughout the crop's development cycle. However, inadequate supplies of Zn and Fe have become stress factors for culture due to the deficiency or excess of these elements in the plant. In recent years, strategies and technologies have been developed for the treatment of plants stressed by abiotic factors, among them, the application of plant steroids has been discussed as an effective and less harmful method. From plant steroids, considerable attention has been paid to brassinosteroids (BRs). In this context, the objective was to evaluate the effects of Zn and Fe in the soybean culture exposed to low/high supplies of these elements in the soil, as well as to investigate the physiological and biochemical behavior of BRs in soybean plants submitted to Zn deficiency and excess and Fe and identify the possible benefits caused by the steroid. For this, two experiments were carried out in a greenhouse. Experiment I followed a completely randomized factorial design with two concentrations of 24-epibrassinolide (0 and 100 nM EBR) and three supplies of Zn (0.2, 20 and 2000 μM Zn). Experiment II was carried out in a completely randomized design with four treatments (0 nM EBR + 250 μM Fe, 0 nM EBR + 2.5 μM Fe, 100 nM EBR + 250 μM Fe and 100 nM EBR + 2.5 μM Fe). In general, low supplies of Zn and Fe and high supplies of Zn produced deleterious effects. However, the results revealed that exogenous BRs (100 nM EBR) minimized the damage caused by Zn and Fe deficiency and by toxic Zn levels in soybean plants. In experiment I, EBR alleviated the impact produced by zinc stress on the root system by acting positively on the epidermis, endoderm, cortex, vascular cylinder and metaxylem, intrinsically improving the nutritional status in plants. EBR promoted improvements in the photosynthetic machinery of plants exposed to zinc stress, stimulating the activity of antioxidant enzymes that play crucial roles in the protection of chloroplast membranes, with positive repercussions on chlorophylls, effective quantum yield of PSII photochemistry and transport rate of PSII electrons. In experiment II, EBR maximized the Fe content in the leaf, stem and root, as well as improved the nutrient content and the metal homeostasis, as confirmed by the increased detection of Fe^{2+}/Mg^{2+}, Fe^{2+}/Mn^{2+} and Fe^{2+}/Cu^{2+} in plants with Fe deficiency. The steroid also promoted improvements in chloroplastic pigments and increased photochemical efficiency, positively regulating electron transport and reducing the negative impacts associated with PSII photoinhibition.

Keywords: *Glycine max*, Brassinosteróides, Micronutrients, Root anatomy, Chlorophyll

,

CONTEXTUALIZATION

The soybean (Glycine max (L.) Merrill) is an oleaginous plant that has great importance for human and animal feeding (HUANG et al., 2017) because it has a large capacity to produce grains rich in proteins (XU et al., 2016), besides being also used as energy source in biofuels (PEREIRA et al., 2017). According to the FAO (2018) in the 2017/2018 harvest, approximately 338 million tons were produced, and is currently the world's most consumed and cultivated legume. In the world ranking, the main producing countries are the United States of America and Brazil (HART, 2017).

Brazil stands out for being the world's largest soybean producer with a production of 124.845 million tons in the 2019/2020 harvest. The planted area in this harvest period was 36,950 million hectares, reaching an average productivity of 3,379 kg / ha (CONAB, 2020). In Pará, planting began in the last half of December 2019, in the main producing municipalities, Paragominas being the largest soybean pole in the state, with an expected planting of 162,000 hectares in 2020 (CONAB, 2020).

Under field conditions, it is often observed that the growth and development of this species can be affected by abiotic stresses induced by the water restriction (KUNERT et al., 2016, WIJEWARDANA et al. 2019), salinity (SHU et al., 2017), temperature (ALLEN Jr. et al., 2018), toxic metals (BALASARASWATHI et al., 2017, REIS et al., 2018), mainly because of the nutritional stress caused by the deficiency or excess of the minerals required by the soybean crop.

The nutrients play structural and metabolic functions in soybean plants and their availability is directly related to the best performance of the species. Nutritional disorders cause reduced productivity and are associated with symptoms characteristic of the lack of each nutrient (CARMELLO and OLIVEIRA, 2006). Essential micronutrients, such as zinc (Zn) and iron (Fe), are absorbed in small amounts by plants, when compared to macronutrients, but play a crucial role in soybean production (HANSEL and OLIVEIRA, 2016).

Zinc is a nutrient absorbed actively by roots as $Zn^{2+,}$ with the absorption process being highly dependent on soil pH (SFREDO and BORKERT, 2004). Zn is important in the activation of enzymes in plants, such as the synthesis of tryptophan, indole acetic acid precursor enzyme (IAA), dehydrogenase and carbonic anhydrase (MASCARENHAS et al., 2014). Symptoms of deficiency are characterized by the light yellow-brown coloration on the leaves and the small size of the young leaves, due to the

low mobility of this micronutrient in the phloem of the plant. Another symptom of disability is the shortening of the internodes (rosette) (HANSEL and OLIVEIRA, 2016). In addition, excess Zn also promotes damaging effects on crop yield (TRIPATHI et al., 2015), because Zn toxicity negatively affects CO_2 assimilation and stomatal mechanism (AZZARELLO et al., 2012), reducing the rate of the transpiration and content of water in the leaf (SAGARDOY et al., 2009), resulting in low biomass content (MARQUES et al., 2017).

Iron (Fe), an essential nutrient for plants, is necessary for physiological processes in plants (KIM, GUERINOT, 2007). The main function of Fe in plants is to be an enzymatic component, where most participate in oxidation processes (KOBAYASHI; NISHIZAWA, 2012). The enzymes that act in the transfer of electrons use the Fe as cofactor of choice, being these enzymes involved in a variety of reversible redox reactions (FOURCROY et al., 2014), participates in the route of chlorophyll synthesis (ABADÍA et al., 2011), in the photosynthesis (LIU et al., 2017), DNA synthesis, respiration (BRIAT et al., 2015), biosynthesis of phytohormones (gibberellic acid, jasmonic acid and ethylene) in the production and the elimination of reactive oxygen species (ERO) (DIXON; STOCKWELL, 2014). In Fe deficiency, 75% of Fe is found in chloroplasts and, consequently, in its deficiency, there is a uniform chlorosis of young leaves, due to a decrease in the amount of chloroplast and chlorophyll content (SFREDO and BORKERT, 2004).

In recent years, various strategies and technologies have been developed for the treatment of plants exposed to nutritional stress, between them, the application of plant hormones have been discussed as an effective and less harmful method. Of plant hormones, a considerable attention has been given to Brassinosteroids (BRs) (HAYAT et al., 2012).

Brassinosteroids (BRs) are currently considered a new group of vegetable steroids that have significant growth-promoting properties. Your role in the plant protection against environmental stresses has become, in recent years, the subject of scientific research to clarify its mode of action and that has contributed to the use of this phytohormone in agricultural production (SHARMA et al., 2011).

BRs are associated with various physiological processes of the plant. Act directly on the cell elongation, cell expansion, differentiation of xylem, and promote the increase in yield and biomass production, accelerate plant ripening process, stimulate

the activity of antioxidant enzymes against oxidative damage to cells and also induce plant tolerance to biotic and abiotic stresses (FREITAS et al., 2012; HASAN et al., 2011; MAZORRA, 2008). Among the abiotic stresses, they are effective on increase resistance to high and low temperatures, drought, salinity, toxic heavy metal and nutrition imbalance (LARRÉ et al., 2014).

In rice, 24-epibrassinolide increases resistance at temperatures between 1-5^{0} C and tolerance is associated with increased ATP production, increased proline levels and increased enzyme activity, indicating that this growth regulator is involved in stability of membranes and osmoregulation (RAO et al., 2011).

Another fact that arouses the interest of physiologists and biochemists is related to the potentiation of antioxidant enzymes of plants exposed to abiotic stresses (FARIDUDDIN et al., 2012), as well as reports of attenuation of the drought-induced damages associated with gas exchange plants of Oryza sativa (FAROOQ et al., 2011), making brassinosteroids ecologically safe and amenable to extensive agricultural use.

Eucalyptus urophylla plants treated with 24-epibrinosinolide subjected to saline stress had positive changes on nutritional homeostasis, antioxidant metabolism and leaf anatomy, suggesting that this steroid mitigated the deleterious effects of saline stress, improving the increase of photosynthetic pigments and photochemical efficiency, which is explained by the antioxidant system, specifically through the significant increase observed in the activity of SOD, CAT, APX and POX enzymes (OLIVEIRA et al., 2019).

In *Brassica juncea* plants, the action of 24-epibrassinolide minimized stress by Cu, in which relief was associated with an increase in the photosynthetic rate, reduction in ROS levels by increasing the activity of antioxidant enzymes and raising the rates of growth in mustard plants, revealing the positive action of this steroid on the Cu phytotoxicity (YUSUF et al., 2016).

The exogenous application of 24-epibrinsinolide (EBR) attenuated the negative effects caused by Fe deficiency on the nutritional condition and on the physiological and biochemical behavior of *Eucalyptus urophylla* plants, increasing the macronutrient and micronutrient contents, including Fe. EBR also improved the photochemical efficiency of PSII, gas exchanges, photosynthetic pigments inducing less accumulation of oxidative compounds (LIMA et al., 2018)

The general hypothesis of the work is that the exogenous application of EBR is able to attenuate the negative impacts caused by the deficiency and excess of Zn and Fe in soybean plants. The objective of this work was to investigate the performance of EBR in soybean plants submitted to different Zn and Fe supplements, as well as to reveal the physiological and biochemical behavior of plants submitted to nutritional stress, and to identify the possible benefits of Brassinosteroids. For this, the thesis was divided into two chapters.

The hypothesis of the first article is that the EBR may be a possible solution to mitigate the damages caused by the deficiency and excess of Zn in soybean plants. The objective of this first chapter was to answer whether the EBR can reduce oxidative stress in soybean plants submitted to different Zn supplements, evaluating the possible repercussions on the anatomical, nutritional, biochemical, physiological and biomass parameters.

The hypothesis of the second article is that the EBR can attenuate the damages caused by the deficiency Fe in soybean plants. This second chapter aimed to answer whether epibrassinolide (EBR) can alleviate Fe deficiency in *Glycine max* plants and to evaluate the repercussions on nutritional conditions and physiological, biochemical and anatomical behavior.

REFERENCES

ALLEN JR. LH; ZHANG, L; BOOTE, KJ; HAUSER, BA. Elevated temperature intensity, timing, and duration of exposure affect soybean internode elongation, mainstem node number, and pod number per plant. **Crop J** 6:148–161, 2018.

AZZARELLO, E; PANDOLFI, C; GIORDANO, C. Ultramorphological and physiological modifications induced by high zinc levels in *Paulownia tomentosa*. **Environ Exp Bot** 81:11–17, 2012.

ABADÍA, J; VÁZQUEZ, S; RELLÁN-ÁLVAREZ, R; EL-JENDOUBI, H; ABADÍA, A., ÁLVAREZ-FERNÁNDEZ, A. Towards a knowledge-based correction of iron chlorosis. **Plant Physiology and Biochemistry**, v. 49, n. 5, p. 471-482, 2011.

ANURADHA, S; RAO, SER. Amelioration of Lead Toxicity in Radish (*Raphanus sativus* L) Plants by Brassinolide. **J App Biolog Scien** 5 (3): 43-48, 2011.

BALASARASWATHI, K; JAYAVENI, S; SRIDEVI, J. Cr–induced cellular injury and necrosis in *Glycine max* L.: Biochemical mechanism of oxidative damage in chloroplast. **Plant Physiol Biochem** 118:653–666, 2017.

CONAB. Compania Nacional de abastecimento. V.7 - SAFRA 2019/20 - N. 4 - **Quarto levantamento**. Janeiro 2020.

CONAB. Compania Nacional de abastecimento. V.7 - SAFRA 2019/20 - N. 12 - **Décimo segundo levantamento**. Setembro 2020.

DIXON, SJ; STOCKWELL, BR. The role of iron and reactive oxygen species in cell death. **Nature Chemical Biology**, v. 10, n. 1, p. 9-17, 2014.

CARMELLO, QAC; OLIVEIRA, FA. Nutrição de lavouras de soja: situação atual e perspectivas. **Visão agrícola**, 2006.

FAO. Food and agriculture organization of the united nations. Food outlook: Biannual report on global food markets, 2018.

FAROOQ, M; WAHID, A; BASRA, SMA; ISLAM-UD-DIN. Improving water relations and gas Exchange with brassinosteroids in rice under drought stress. **Journal of Agronomy and Crop Science** ,v. 195, n. 4, p. 262-269, 2009.

HART, C. The economic evolution of the soybean industry. In: The Soybean Genome. **Compendium of Plant Genomes, Springer**, p. 1-9, 2017.

HAYAT, S; ALYEMENI, MN; HASAN, SA. Foliar spray of brassinosteroid enhances yield and quality of *Solanum lycopersicum* under cadmium stress. . **Saudi J Biol Sci** 19: 325-335, 2012.

HASAN, SA; HAYAT, S; AHMAD, A. Brassinosteroids protect photosynthetic machinery against the cadmium induced oxidative stress in two tomato cultivars. **Chemosphere**, v. 82, n. 10, p. 1446-1451, 2011.

KIM, SA; GUERINOT, ML. Mining iron: Iron uptake and transport in plants. **FEBS Letters**, v. 581, n. 12, p. 2273–2280, 2007.

KUNERT, KJ; VORSTER, BJ; FENTA, BA. Drought Stress Responses in Soybean Roots and Nodules. Front Plant Sci 7:1–7. 2017.

LARRÉ, CF; MARINI, P; MORAES, CL; AMARANTE, L; MORAES, DM. Influência do 24-epibrassinolídeo na tolerância ao estresse salino em plântulas de arroz. **Semina: Ciências Agrárias**, v. 35, n. 1, p. 67-76, 2014.

LIMA, MDR; JUNIOR, UOB; BATISTA, BL; LOBATO, AKS. Brassinosteroids mitigate iron deficiency improving nutritional status and photochemical efficiency in *Eucalyptus urophylla* plants. **Trees,** V. **32**, p. 1681-1694, 2018.

MAZORRA, LM; NÚÑEZ, M. Estado actual sobre el conocimiento de la biosintesis y los mecanismos moleculares de acción de los brassinosteroids em las plantas. **Cultivos Tropicales**, v. 29, n. 1, p. 91-105, 2008.

OLIVEIRA, VP; LIMA, MDR; SILVA, BRS. Brassinosteroids confer tolerance to salt stress in *Eucalyptus urophylla* plants enhancing homeostasis, antioxidant metabolism and leaf anatomy. **J Plant Growth Regul** In press:19, 2019.

PEREIRA, GG; GARCIA, RK; FERREIRA, LL; BARRERA-ARELLANO, D. Soybean and soybean/beef-tallow biodiesel: a comparative study on oxidative degradation during long-term storage. **Journal of the American Oil Chemists' Society**, v. 94, n. 4, p. 587-593, 2017.

SHARMA, P; JHA, AB; DUBEY, RS; PESSARAKLI, M. Reactive oxygen species, oxidative damage, and antioxidative defense mechanism in plants under stressful conditions. **Journal of Botany**, v. 47, p. 172-177, 2011.

SAGARDOY, R; MORALES, F; LÓPEZ-MILLÁN, AF. Effects of zinc toxicity on sugar beet (*Beta vulgaris* L.) plants grown in hydroponics. **Plant Biol** 11:339–350, 2009.

SFREDO, GJ; BORKERT, CM. Deficiências e Toxicidades de Nutrientes em Plantas de soja. **Embrapa soja**, 2004.

TRIPATHI, DK; SINGH, S; SINGH, S. Micronutrients and their diverse role in agricultural crops: advances and future prospective. **Acta Physiol Plant** 37:14, 2015.

WIJEWARDANA, C; REDDY, KR; BELLALOUI, N.Soybean seed physiology, quality, and chemical composition under soil moisture stress. Food Chem 278:92–100, 2019.

XU, D; ZHANG, J; CAO, Y; WANG, J; XIAO, J. Influence of microcrystalline cellulose on the microrheological property and freeze-thaw stability of soybean protein hydrolysate stabilized curcumin emulsion. **LWT-Food Science and Technology**, v. 66, p. 590-597, 2016.

CAPITULO I. 24-EPIBRASSINOLIDE IMPROVES ROOT ANATOMY AND ANTIOXIDANT ENZYMES IN SOYBEAN PLANTS SUBJECTED TO ZINC STRESS. Página 18 à 37.

Journal of Soil Science and Plant Nutrition
https://doi.org/10.1007/s42729-019-00105-z

ORIGINAL PAPER

24-Epibrassinolide Improves Root Anatomy and Antioxidant Enzymes in Soybean Plants Subjected to Zinc Stress

Lucilene Rodrigues dos Santos[1] · Breno Ricardo Serrão da Silva[1] · Tatiana Pedron[2] · Bruno Lemos Batista[2] · Allan Klynger da Silva Lobato[1]

Received: 19 June 2019 / Accepted: 16 September 2019

Abstract

The aim of this research was to determine whether 24-epibrassinolide can mitigate oxidative stress in soybean plants subjected to different zinc levels; to examine this, we evaluated the possible repercussions on anatomical, nutritional, biochemical, physiological and morphological behaviours. The experiment followed a completely randomized factorial design with two concentrations of 24-epibrassinolide (0 and 100 nM EBR, described as - EBR and + EBR, respectively) and three zinc supplies (0.2, 20 and 2000 μM Zn, described as low, control and a high supply of Zn). In general, low and high zinc supplies produced deleterious effects. However, plants exposed to high zinc +100 nM EBR presented increases of 25%, 7%, 9% 29% and 69% for root epidermis, root endodermis, root cortex, vascular cylinder and metaxylem, respectively, when compared to the same treatment without the steroid. The steroid spray alleviated the impact produced by zinc stress on nutritional status, and these results were intrinsically linked to incremental changes in root structure, mainly vascular cylinder and metaxylem. Antioxidant enzymes play crucial roles in the photosynthetic machinery of plants treated with 24-epibrassinolide and stressed by high and low zinc supply, modulating reactive oxygen species scavenging and protecting the chloroplast membranes, with clear positive repercussions on photosystem II efficiency and photosynthetic pigments. The stimulation induced by this steroid on gas exchange can be explained by the favourable conditions detected in stomatal performance and leaf anatomy, thus enhancing the diffusion of carbon dioxide.

Keywords 24-epibrassinolide · Antioxidant system · *Glycine max* · Root anatomy · Zinc supply

Abbreviations

APX	Ascorbate peroxidase
BRs	Brassinosteroids
CA	Carbonic anhydrase
CAR	Carotenoids
CAT	Catalase
Chl *a*	Chlorophyll a
Chl *b*	Chlorophyll b
C_i	Intercellular CO_2 concentration
CO_2	Carbon dioxide
E	Transpiration rate
EBR	24-epibrassinolide
EDS	Equatorial diameter of the stomata
EL	Electrolyte leakage
ETAb	Epidermis thickness from abaxial leaf side
ETAd	Epidermis thickness from adaxial leaf side
ETR	Electron transport rate
ETR/P_N	Ratio between the apparent electron transport rate and net photosynthetic rate
EXC	Relative energy excess at the PSII level
F_0	Minimal fluorescence yield of the dark-adapted state
F_m	Maximal fluorescence yield of the dark-adapted state
F_v	Variable fluorescence
F_v/fm	Maximal quantum yield of PSII photochemistry
g_s	Stomatal conductance
H_2O_2	Hydrogen peroxide
LDM	Leaf dry matter
MDA	Malondialdehyde
NPQ	Nonphotochemical quenching
O_2^-	Superoxide

✉ Allan Klynger da Silva Lobato
allanllobato@yahoo.com.br

[1] Núcleo de Pesquisa Vegetal Básica e Aplicada, Universidade Federal Rural da Amazônia, Rodovia PA, Paragominas, Pará 256, Brazil

[2] Centro de Ciências Naturais e Humanas, Universidade Federal do ABC, Santo André, São Paulo, Brazil

Published online: 22 October 2019

PDS	Polar diameter of the stomata
P_N	Net photosynthetic rate
P_N/C_i	Instantaneous carboxylation efficiency
POX	Peroxidase
PPT	Palisade parenchyma thickness
PSII	Photosystem II
q_P	Photochemical quenching
RCD	Root cortex diameter
RDM	Root dry matter
RMD	Root metaxylem diameter
RDT	Root endodermis thickness
RET	Root epidermis thickness
ROS	Reactive oxygen species
RuBisCO	Ribulose-1,5-bisphosphate carboxylase/oxygenase
SD	Stomatal density
SDM	Stem dry matter
SF	Stomatal functionality
SI	Stomatal index
SOD	Superoxide dismutase
SPT	Spongy parenchyma thickness
TDM	Total dry matter
Total Chl	Total Chlorophyll
VCD	Vascular cylinder diameter
WUE	Water-use efficiency
Φ_{PSII}	Effective quantum yield of PSII photochemistry

1 Introduction

Soybean (*Glycine max* L.) is the most widely cultivated legume around the world due to its high protein and oil content (Singh et al. 2008; Nisa et al. 2016; Baig et al. 2018). Its world production reached 338 million tons in the 2017/2018 harvest, with the United States, Brazil and Argentina being the main producers (FAO 2018). In field conditions, it has been frequently observed that the growth and development of this species can be affected by abiotic stresses induced by nutritional imbalances (Wang et al. 2015; Santos et al. 2017), metal toxicity (Balasaraswathi et al. 2017; Reis et al. 2018), water deficiency (Kunert et al. 2016; Wijewardana et al. 2019), salinity (Shu et al. 2017) and high temperatures (Allen Jr. et al. 2018).

Zinc is the second most necessary micronutrient for plants (Jain et al. 2010), being the deficiency of this element caused by the weathering process in tropical soils (Suhr et al. 2018). On the other hand, the zinc toxicity in plants is mainly determined by the anthropic activity associated to deposition of pollutants rich in heavy metals (Nagajyoti et al. 2010). Many plants contain 3 to 100 μg Zn g^{-1} dry matter, which is considered sufficient to promote adequate plant growth rates, while concentrations above 300 μg Zn g^{-1} are generally considered toxic (Noulas et al. 2018). The Zn content in soil is variable depending on its physical and chemical characteristics, but concentrations higher than 100 μg g^{-1} in soil are unusual (Rezapour et al. 2014; Antoniadis et al. 2018). However, plants frequently exhibit symptoms of Zn deficiency in shoots with concentrations lower than 2 μg Zn g^{-1} dry matter (Sinclair and Krämer 2012).

Zinc is essential for plant growth (Sadeghzadeh 2013; Hafeez et al. 2013) and plays important roles in essential processes, such as membrane biosynthesis, photosynthetic machinery, hormonal regulation, metabolism of lipids and nucleic acids, gene expression, and protein synthesis (Hänsch and Mendel 2009; Noulas et al. 2018; Manaf et al. 2019). Additionally, Zn is the single metal required in all six classes of the enzymes (oxidoreductases, transferases, hydrolases, lyases, isomerases and ligases) essential during photosynthesis processes and subsequent starch accumulation (Palmer and Guerinot 2009; Tripathi et al. 2015).

Deficiency linked to zinc frequently results in lower biomass and yield (Hidoto et al. 2017), reduces chlorophyll levels (Kosesakal and Unal 2009; Samreen et al. 2017) and minor efficiency linked to antioxidant system, more specifically related to superoxide dismutase (SOD) enzyme (Singh et al. 2019). Chloroplast ultrastructure is affected, resulting in abnormalities in leaf structure leading to leaf chlorosis (Kim and Wetzstein 2003; Fu et al. 2015). In relation to the photosynthetic machinery, decreases in the photochemical efficiency and the activities of ribulose-1,5-bisphosphate carboxylase/oxygenase (RuBisCO) and carbonic anhydrase (CA) enzymes have been reported (Salama et al. 2006; Tavallali et al. 2009; Hajiboland and Amirazad 2010). However, excess levels of Zn also promote deleterious effects on crop yield (Tripathi et al. 2015) because Zn toxicity negatively affects CO_2 assimilation and stomatal mechanisms (Azzarello et al. 2012), thus decreasing the transpiration rates and water content in the leaf (Sagardoy et al. 2009) and resulting in a lower biomass (Marques et al. 2017).

The root is a vital organ of the plant and has specialized tissues with important functions connected to influx of water and nutrients (Barberon et al. 2016). The exodermis and endodermis are tissues that act in regard to protection and selectivity of the root, thus contributing to the symplastic immobilization of excesses of Zn in the vacuoles of the root cells (Enstone et al. 2003; Arrivault et al. 2006; Sinclair and Krämer 2012). The cortex is a tissue with a storage capacity for water and nutrients in the root (Hameed et al. 2009). However, under conditions of oxidative stress, reduction and disintegration of cortical cells can occur (Singh et al. 2007; Talukdar 2013), negatively impacting the respiration and nutrient content of the root tissue (Schneider et al. 2017). In plants exposed to low/high availability of nutrients, the cortical tissue can be replaced by the cortical aerenchyma of the root, which allows for a higher allocation of the nutrients to other plant functions, such as growth and reproduction (Fan

et al. 2003; Lynch 2007; Postma and Lynch 2011; Saengwilai et al. 2014).

The exogenous application of 24-epibrassinolide (EBR) can be a possible solution to mitigate the damage caused by deficiencies and excess Zn in plants because EBR is one of the most bioactive forms of brassinosteroids (BRs); it is extracted from plants and is biodegradable (Azhar et al. 2017). This steroid presents a broad spectrum of systemic action on plant metabolism (Oh et al. 2012), including CO_2 (Li et al. 2016b), gas exchange (Swamy and Rao 2009), photochemical efficiency (Thussagunpanit et al. 2015), antioxidant metabolism (Xia et al. 2009) and growth rate (Abdullahi et al. 2003). In addition, BRs activate proton pumps, stimulate the synthesis of proteins and nucleic acids (Bajguz 2000) and modulate cellular expansion and division (Zhiponova et al. 2013).

This study has focused on the gap in the literature in relation to EBR's hypothetical effects in regard to Zn. Zn is the second most common micronutrient required by plants; however, deficiencies and excesses of Zn promote deleterious effects on soybean plants. Interestingly, EBR can be a possible solution to mitigate the damage caused by deficiencies and excesses of Zn in plants because this steroid presents a spectrum of actions linked to increments in nutrient content (Lima et al. 2018), reactive oxygen species scavenging (Oliveira et al. 2019) and stimulation of biomass (Maia et al. 2018). Therefore, the aim of this research was to determine whether EBR can mitigate oxidative stress in soybean plants subjected to different Zn supplies and to evaluate its possible repercussions on anatomical, nutritional, biochemical, physiological and morphological behaviours.

2 Materials and Methods

2.1 Location and Growth Conditions

The experiment was performed at the Campus of Paragominas of the Universidade Federal Rural da Amazônia, Paragominas, Brazil (2°55' S, 47°34' W). The study was conducted in a greenhouse with the temperature and humidity controlled. The minimum, maximum, and median temperatures were 21, 31 and 25.2 °C, respectively. The relative humidity during the experimental period varied between 60% and 80%.

2.2 Plants, Containers and Acclimation

Seeds of *Glycine max* (L.) Merr. var. M8644RR Monsoy™ were germinated and grown in 1.2-L pots filled with a mixed substrate of sand and vermiculite at a ratio of 3:1. The plants were cultivated under semi-hydroponic conditions containing 500 mL of distilled water for eight days. A modified Hoagland and Arnon (1950) solution was used for nutrients, with the ionic strength beginning at 50% (6th day) and later modified to 100% after two days (8th day). After this period, the nutritive solution remained at total ionic strength.

2.3 Experimental Design

The experiment followed a completely randomized factorial design with two concentrations of 24-epibrassinolide (0 and 100 nM EBR, described as - EBR and + EBR, respectively) and three Zn supplies (0.2, 20 and 2000 μM Zn, described as low, control and high supply of Zn). With five replicates for each of six treatments, a total of 30 experimental units were used in the experiment, with one plant in each unit.

2.4 24-Epibrassinolide (EBR) Preparation and Application

Ten-day-old seedlings were sprayed with 24-epibrassinolide (EBR) or Milli-Q water (containing a proportion of ethanol that was equal to that used to prepare the EBR solution) at 5-d intervals until day 35. The 0 and 100 nM EBR (Sigma-Aldrich, USA) solutions were prepared in agreement with Ahammed et al. (2013). Based on preliminary studies and literature available (Lima and Lobato 2017; Maia et al. 2018; Pereira et al. 2019; Oliveira et al. 2019), the EBR is more efficient in plants pretreated (10th day). On the other hand, Zn was applied only on 20th day after experimental implementation due to need of leaf area and plant tissue sufficient to make all analyses involved in this research.

2.5 Plant Conduction and Zn Supplies

The plants received the following macro- and micronutrients contained in the nutrient solution: 8.75 mM KNO_3, 7.5 mM $Ca(NO_3)_2{\cdot}4H_2O$, 3.25 mM $NH_4H_2PO_4$, 1.5 mM $MgSO_4{\cdot}7H_2O$, 62.50 μM KCl, 31.25 μM H_3BO_3, 2.50 μM $MnSO_4{\cdot}H_2O$, 0.63 μM $CuSO_4{\cdot}5H_2O$, 0.63 μM $NaMoO_4{\cdot}5H_2O$ and 250 μM $NaEDTAFe{\cdot}3H_2O$, with Zn concentrations adjusted to each treatment. For Zn treatments, $ZnCl_2$ was used at concentrations of 0.2 μM (low) and 20 μM (control) and 2000 μM (high) applied over 15 days (days 20–35 after the start of the experiment). Plants were maintained from 8th to 20th day under equal Zn concentration (20 μM Zn), considered as control treatment. One plant per pot was used to examine the plant parameters. On day 35 of the experiment, all plants were harvested and analysed.

2.6 Measurement of Chlorophyll Fluorescence and Gas Exchange

The chlorophyll fluorescence was measured in fully expanded leaves under light using a modulated chlorophyll fluorometer (model OS5p; Opti-Sciences). Preliminary tests determined

the location of the leaf, the part of the leaf and the time required to obtain the greatest F_v/fm ratio; therefore, the acropetal third of the leaves, which was the middle third of the plant and adapted to the dark for 30 min, was used in the evaluation. The intensity and duration of the saturation light pulse were 7500 μmol m^{-2} s^{-1} and 0.7 s, respectively. The gas exchange was evaluated in all plants, measuring expanded leaves in middle region of the plant under constant conditions of a CO_2 concentration, using an infrared gas analyser (model LCPro$^+$; ADC BioScientific), photosynthetically active radiation, air-flow rate and temperature in a chamber at 360 μmol mol^{-1} CO_2, 800 μmol photons m^{-2} s^{-1}, 300 μmol s^{-1} and 28 °C, respectively, between 10:00 and 12:00 h. Previous tests using equal soybean variety and greenhouse were conducted to configure the equipment and determinate the work conditions. The water-use efficiency (WUE) was estimated according to Ma et al. (2004), and the instantaneous carboxylation efficiency (P_N/C_i) was calculated using the formula that was described by Aragão et al. (2012).

2.7 Quantifications Linked to Anatomical Variables

Samples were collected from the middle region of the leaf limb of fully expanded leaves and roots 5 cm from the root apex, being used five samples to examine the anatomical variables. Subsequently, all collected botanical material was fixed in FAA 70 for 24 h, dehydrated in ethanol and embedded in historesin Leica™ (Leica, Nussloch, Germany). Transverse sections with a thickness of 5 μm were obtained with a rotating microtome (model Leica RM 2245, Leica Biosystems) and were stained with toluidine blue (O'Brien et al. 1964). For stomatal characterization, the epidermal impression method was used according to Segatto et al. (2004). The slides were observed and photomicrographed under an optical microscope (Motic BA 310, Motic Group Co. LTD.) coupled to a digital camera (Motic 2500, Motic Group Co., LTD.). The images were analysed with Motic plus 2.0, which was previously calibrated with a micrometre slide supplied by the manufacturer. The anatomical parameters evaluated were polar diameter of the stomata (PDS), equatorial diameter of the stomata (EDS), epidermis thickness from adaxial leaf side (ETAd), epidermis thickness from abaxial leaf side (ETAb), palisade parenchyma thickness (PPT), spongy parenchyma thickness (SPT), and the ratio PPT/SPT. In both leaf faces, the stomatal density (SD) was calculated as the number of stomata per unit area and the stomatal functionality (SF) as the ratio PDS/EDS according to Castro et al. (2009). The stomatal index (SI %) was calculated as the percentage of stomata in relation to total epidermal cells by area. In root samples, the root epidermis thickness (RET), root endodermis thickness (RDT), root cortex diameter (RCD), vascular cylinder diameter (VCD) and root metaxylem diameter (RMD) were measured.

2.8 Extraction of Antioxidant Enzymes, Superoxide and Soluble Proteins

Antioxidant enzymes (SOD, CAT, APX and POX), superoxide and soluble proteins were extracted from leaf tissues according to the method of (Badawi et al. 2004). The extraction mixture was prepared by homogenizing 500 mg of fresh plant material in 5 ml of extraction buffer, which consisted of 50 mM phosphate buffer (pH 7.6), 1.0 mM ascorbate and 1.0 mM EDTA. Samples were centrifuged at 14,000×*g* for 4 min at 3 °C, and the supernatant was collected. Quantification of the total soluble proteins was performed using the method described by (Bradford 1976). Absorbance was measured at 595 nm, using bovine albumin as a standard.

2.9 Superoxide Dismutase Assay

For the SOD assay (EC 1.15.1.1), 2.8 ml of a reaction mixture containing 50 mM phosphate buffer (pH 7.6), 0.1 mM EDTA, 13 mM methionine (pH 7.6), 75 μM NBT, and 4 μM riboflavin was mixed with 0.2 ml of supernatant. The absorbance was then measured at 560 nm (Giannopolitis and Ries 1977).One SOD unit was defined as the amount of enzyme required to inhibit 50% of the NBT photoreduction. The SOD activity was expressed in unit mg^{-1} protein.

2.10 Catalase Assay

For the CAT assay (EC 1.11.1.6), 0.2 ml of supernatant and 1.8 ml of a reaction mixture containing 50 mM phosphate buffer (pH 7.0) and 12.5 mM hydrogen peroxide were mixed, and the absorbance was measured at 240 nm (Havir and McHale 1987). The CAT activity was expressed in μmol H_2O_2 mg^{-1} protein min^{-1}.

2.11 Ascorbate Peroxidase Assay

For the APX assay (EC 1.11.1.11), 1.8 ml of a reaction mixture containing 50 mM phosphate buffer (pH 7.0), 0.5 mM ascorbate, 0.1 mM EDTA, and 1.0 mM hydrogen peroxide was mixed with 0.2 ml of supernatant, and the absorbance was measured at 290 nm (Nakano and Asada 1981). The APX activity was expressed in μmol AsA mg^{-1} protein min^{-1}.

2.12 Peroxidase Assay

For the POX assay (EC 1.11.1.7), 1.78 ml of a reaction mixture containing 50 mM phosphate buffer (pH 7.0) and 0.05% guaiacol was mixed with 0.2 ml of supernatant, followed by addition of 20 μL of 10 mM hydrogen peroxide. The absorbance was then measured at 470 nm (Cakmak and Marschner 1992). The POX activity was expressed in μmol tetraguaiacol mg^{-1} protein min^{-1}.

2.13 Determination of Superoxide Concentration

To determine O_2^-, 1 ml of extract was incubated with 30 mM phosphate buffer [pH 7.6] and 0.51 mM hydroxylamine hydrochloride for 20 min at 25 °C. Then, 17 mM sulphanilamide and 7 mM α-naphthylamine were added to the incubation mixture for 20 min at 25 °C. After the reaction, ethyl ether was added in the identical volume and centrifuged at 3000×g for 5 min. The absorbance was measured at 530 nm (Elstner and Heupel 1976).

2.14 Extraction of Nonenzymatic Compounds

Nonenzymatic compounds (H_2O_2 and MDA) were extracted as described by Wu et al. (2006). Briefly, a mixture for extraction of H_2O_2 and MDA was prepared by homogenizing 500 mg of fresh leaf materials in 5 mL of 5% (*w*/*v*) trichloroacetic acid. Then, the samples were centrifuged at 15,000 x g for 15 min at 3 °C to collect the supernatant.

2.15 Determination of Hydrogen Peroxide Concentration

To measure H_2O_2, 200 μL of supernatant and 1800 μL of reaction mixture (2.5 mM potassium phosphate buffer [pH 7.0] and 500 mM potassium iodide) were mixed, and the absorbance was measured at 390 nm (Velikova et al. 2000).

2.16 Quantification of Malondialdehyde Concentration

MDA was determined by mixing 500 μL of supernatant with 1000 μL of the reaction mixture, which contained 0.5% (*w*/*v*) thiobarbituric acid in 20% trichloroacetic acid. The mixture was incubated in boiling water at 95 °C for 20 min, with the reaction terminated by placing the reaction container in an ice bath. The samples were centrifuged at 10,000×g for 10 min, and the absorbance was measured at 532 nm. The nonspecific absorption at 600 nm was subtracted from the absorbance data. The MDA–TBA complex (red pigment) amount was calculated based on the method of Cakmak and Horst (1991), with minor modifications and using an extinction coefficient of 155 mM^{-1} cm^{-1}.

2.17 Determination of Electrolyte Leakage

Electrolyte leakage was measured according to the method of Gong et al. (1998) with minor modifications. Fresh tissue (200 mg) was cut into pieces 1 cm in length and placed in containers with 8 mL of distilled deionized water. The containers were incubated in a water bath at 40 °C for 30 min, and the initial electrical conductivity of the medium (EC_1) was measured. Then, the samples were boiled at 95 °C for 20 min to release the electrolytes. After cooling, the final electrical conductivity (EC_2) was measured. The percentage of electrolyte leakage was calculated using the formula EL (%) = (EC_1/EC_2) × 100.

2.18 Determination of Photosynthetic Pigments

The chlorophyll and carotenoid determinations were performed with 40 mg of leaf tissue, being used five samples per treatment. The samples were homogenized in the dark with 8 mL of 90% methanol (Nuclear). The homogenate was centrifuged at 6000×g for 10 min at 5 °C. The supernatant was removed, and chlorophyll *a* (Chl *a*) and *b* (Chl *b*), carotenoid (Car) and total chlorophyll (total Chl) contents were quantified using a spectrophotometer (model UV-M51; Bel Photonics), according to the methodology of Lichtenthaler and Buschmann (2001).

2.19 Determination of Nutrients

Samples with 100 mg of milled samples were weighed in 50-mL conical tubes (Falcon^R, Corning, Mexico) and predigested (48 h) with 2 ml of sub boiled HNO_3 (DST 1000, Savillex, USA). After, 8 ml of a solution containing 4 ml of H_2O_2 (30% *v*/v, Synth, Brasil) and 4 ml of ultra-pure water (Milli-Q System, Millipore, USA) were added, and the mixture was transferred to a Teflon digestion vessel, closed and heated in a block digester (EasyDigest®, Analab, France) according to the following program: i) 100 °C for 30 min; ii) 150 °C for 30 min; iii) 130 °C for 10 min; iv) 100 °C for 30 min and; and v) left to cool. The volume was made to 50 mL with ultra-pure water, and iridium was used as an internal standard at 10 μg l^{-1}. The determinations of Zn, P, K, Mg, Fe, Cu and Mo were carried out using an inductively coupled plasma mass spectrometer (ICP-MS 7900, Agilent, USA). Certified reference materials (NIST 1570a and NIST 1577c) were run in each batch for quality control purposes. All found values were in agreement with certified values.

2.20 Measurements of Morphological Parameters

The growth of roots, stems and leaves was measured based on constant dry weights (g) after drying in a forced-air ventilation oven at 65 °C.

2.21 Data Analysis

The data were submitted to ANOVA and applied Scott–Knott test at a probability level of 5% (Steel et al. 2006). All statistical procedures used the Assistat software.

3 Results

3.1 Zn Contents in Plants after EBR and Zn Treatments

The low and high Zn supplies promoted changes in the contents of this element in the root, stem and leaf tissues of soybean plants (Table 1). Plants sprayed with EBR and exposed to low Zn presented increases in Zn concentrations of 48% (root), 42% (stem) and 41% (leaf) when compared to the same treatment without EBR. However, the control + EBR treatment exhibited increases of 44%, 50% and 12% in root, stem and leaf, respectively. In relation to the high Zn with EBR, significant decreases were detected in the Zn contents in the stem and leaf by 21% and 10%, respectively, but there was an increase in the root tissue of 7%.

3.2 Root Structures Were Positively Modulated by EBR

The low and high Zn supplies resulted in negative changes in root anatomy (Fig. 1). However, the application of EBR in the plants submitted to the low Zn treatment promoted increases for RET, RDT, RCD, VCD and RMD of 16%, 3%, 14%, 33% and 74% (Table 2), respectively, when compared to the same treatment without EBR, while the control + EBR treatment had increases of 10%, 5%, 10%, 38% and 5%, respectively. Plants exposed to high Zn + EBR had increases of 25%, 7%, 9% 29% and 69%, respectively.

3.3 EBR Maximized the Nutrient Contents

Soybean plants exposed to low and high concentrations of Zn had reductions ($P < 0.05$) in nutrient contents in their tissues (Table 3). However, plants subjected to a low Zn supply and sprayed with EBR had increases in the values of K, P, Mg, Fe, Cu and Mo at 14%, 15%, 9%, 29%, 23% and 42% (root); 4%, 16%, 15%, 16%, 30% and 12% (stem); 25%, 13%, 12%, 10%, 7% and 55% (leaf), respectively, compared with the same treatment without EBR (Table 3). In the high Zn treatment with EBR, we also observed increases in K, P, Mg, Fe, Cu and Mo of 29%, 13%, 24%, 19%, 37% and 10% in roots; 7%, 12%, 50%, 9%, 9% and 4% in stems; and 6%, 28%, 15%, 17%, 17% and 50% in leaves compared with the equal treatment without EBR.

The steroid provoked benefits for the photosynthetic machinery of plants under Zn stress.

Plants with low and high Zn supplies exhibited reductions in F_m, F_v and F_v/fm, but increase in F_0, in relation control treatment (Fig. 2). In F_m, the EBR application resulted in increases of 2% and 2% in the low and high supplies, respectively, when related to the same treatment without EBR. For F_v, we detected increases of 3% and 3% in plants under low and high Zn supplies with EBR, respectively. In F_v/fm, a low Zn with EBR had an increase of 1%, while the control + EBR showed an increment of 2% in relation to the same treatment without EBR. Decreases in Φ_{PSII}, q_P and ETR and increases in NPQ, EXC and ETR/P_N were verified under low and high Zn in soybean plants (Table 4). However, plants treated with 100 nM EBR and exposed to low Zn had increases of 4%, 4%, and 5% for Φ_{PSII}, q_P and ETR, respectively, and reductions in NPQ (8%) and EXC (1%) compared to the low Zn without EBR. In relation to the high Zn with EBR, there were increases of 16%, 12%, and 14% for Φ_{PSII}, q_P and ETR, respectively, and decreases in NPQ (8%) and EXC (6%) and ETR/P_N (5%) compared with the same treatment in the absence of EBR.

3.4 Exogenous EBR Improved the Gas Exchange

The low and high Zn supplies had negative effects on gas exchange (Table 5). However, the application of EBR in plants with a low Zn supply resulted in increases of P_N, g_s, WUE and P_N/C_i of 5%, 14%, 10% and 32%, respectively, and decreases of 20% for C_i when compared to the same treatment without EBR. The high Zn + EBR had incremental changes in P_N, E, g_s, WUE and P_N/C_i of 20%, 9%, 13%, 10% and 59%, respectively, and a reduction of 19% in C_i.

EBR action enhanced the stomatal performance in plants exposed to different Zn supplies.

The stomatal characteristics showed decreases in SD, SF and SI, as well as increases in PDS and EDS on the adaxial and abaxial faces of soybean leaves exposed to the low and high Zn concentrations (Table 6). The action of EBR on the adaxial face of leaves in both treatments (low and high Zn) caused increases in SD (26% and 76%, respectively), SF (5% and 4%, respectively) and SI (24% and 57%, respectively) and reductions in PDS (4% and 8%, respectively) and EDS (9% and 12%, respectively). For the abaxial face, the low and high Zn supplies with 100 nM EBR spray promoted increases in SD (13% and 30%, respectively), SF (4% and 2%, respectively) and SI (6% and 8%, respectively) and decreases in values of PDS (5% and 8%, respectively) and EDS (10% and 11%, respectively) when compared to the same treatment in the absence of EBR.

Beneficial repercussions on leaf anatomy promoted by the steroids in plants under Zn stress.

The low and high concentrations of Zn promoted negative changes in the leaf anatomy (Fig. 3). However, plants under low Zn and EBR had increases in ETAd (21%), ETAb (25%), PPT (11%) and SPT (12%) and a reduction in PPT/SPT (2%) compared with the same treatment without EBR (Table 7). For the high Zn with EBR, we observed significant increases in ETAd (19%), ETAb (14%), PPT (10%) and SPT (16%) and a decrease in PPT/SPT (6%).

Antioxidant enzymes were stimulated after EBR spray in plants treated with different Zn concentrations.

Table 1 Zn contents in soybean plants sprayed with EBR and exposed to different Zn supplies

EBR	Zn supply	Zn in root (μg g DM^{-1})	Zn in stem (μg g DM^{-1})	Zn in leaf (μg g DM^{-1})
_	Low	8.21 ± 0.19Bb	3.28 ± 0.24Cb	4.33 ± 0.19Cb
_	Control	9.24 ± 0.52Bb	4.65 ± 0.26Bb	9.12 ± 0.20Bb
_	High	2636.76 ± 124.22Aa	342.73 ± 9.02Aa	665.87 ± 6.46Aa
+	Low	12.15 ± 0.93Ba	4.67 ± 0.19Ca	6.10 ± 0.34Ca
+	Control	13.27 ± 0.76Ba	6.96 ± 0.29Ba	10.20 ± 0.33Ba
+	High	2834.10 ± 157.69Aa	270.99 ± 9.77Ab	598.71 ± 7.34Ab

Zn = Zinc. Columns with different uppercase letters between Zn supplies (low, control and high Zn supply under equal EBR level) and lowercase letters between EBR level (with and without EBR under equal Zn supply) indicate significant differences from the Scott-Knott test ($P < 0.05$). Means ± SD, $n = 5$

Soybean plants exposed to low and high Zn supplies had increases ($P < 0.05$) in SOD, CAT, APX and POX values (Fig. 4). The application of 100 nM EBR in plants under a low Zn supply provoked significant increases of 26% 18%, 66% and 25%, respectively, when compared to the low supplement Zn with 0 nM EBR. The high Zn + EBR resulted in significant increases in the activities of SOD (29%), CAT (24%), APX (72%) and POX (44%) compared with the same treatment in the absence of EBR (Fig. 4).

Oxidative stress induced by different Zn supplies was alleviated after treatment with the steroid.

The oxidant compounds (O_2^- and H_2O_2) and indicators of cell damage (MDA and EL) in plants exposed to low and high Zn supplies showed increases (Fig. 5). However, plants with a low supply of Zn and 100 nM EBR had reductions in O_2^- (46%), H_2O_2 (6%), MDA (17%) and EL (10%) levels compared to the low Zn and 0 nM EBR plants. In relation to the high Zn with EBR, decreases were verified in O_2^- (29%), H_2O_2 (2%), MDA (15%) and EL (6%) in comparison with the same treatment in the absence of EBR.

EBR prevented the degradation of photosynthetic pigments in plants under Zn stress.

In both treatments (low and high Zn), a concentration of 100 nM EBR promoted maximization of the photosynthetic pigments (Table 8), increasing the levels of Chl *a* (29% and 31%, respectively), Chl *b* (95% and 65%, respectively), Chl total (38% and 35%, respectively) and Car (38% and 45%, respectively) when compared with equal treatment without EBR (0 nM). In addition, there were reductions in the Chl *a*/Chl *b* ratio of 31% and 14% and in the Chl/Car ratio of 4% and 5%, respectively.

Effects deleterious on the biomass were mitigated in plants treated with EBR and subjected to Zn stress.

Plants under low and high Zn supplies presented improvements in growth when receiving EBR application, for the low Zn + EBR increases of 25%, 32%, 5% and 22% of LDM, RDM, SDM and TDM, respectively, compared to low Zn + 0 nM EBR (Fig. 6). In the high Zn with EBR, we also detected increases in the values of LDM, RDM, SDM and TDM of 14%, 5%, 12% and 10%, respectively.

4 Discussion

Plants exposed to low and control Zn + 100 nM EBR had increases in Zn content, suggesting that this steroid improved the absorption, transport and accumulation of Zn in the evaluated tissues. This result can be associated with the intense interaction between Zn^{2+} ions and organic acids, such as histidine, to form soluble Zn complexes, favouring the absorption and accumulation of this metal in the cytosol of the root cells (Khodamoradi et al. 2015). Histidine is an amino acid that plays a central role in the homeostasis of $^{Zn2+}$ ions, facilitating the mobility of this element in the xylem sap via symplastic transport (Kozhevnikova et al. 2014; Khodamoradi et al. 2015). On the other hand, exogenous EBR also minimized the toxic effects of Zn, reducing the Zn content in the tissues exposed to a high Zn supply. This reduction is related to higher synthesis of phytochelatins (PC) in the root cells (Anwar et al. 2018). PC contributes to detoxification mechanisms of heavy metals (Rajewska et al. 2016), chelating the metal ions and forming complexes, with consequent immobilization of this metal in the cytoplasm of root cells (Bajguz and Hayat 2009; Bajguz 2010). Tadayon and Moafpourian (2019) verified that foliar application of 0.4 mg L^{-1} EBR increased the efficiency of foliar application of Zn and B, affecting the chemical and reproductive characteristics of *Vitis vinifera* plants.

EBR revealed beneficial effects on root tissues (RET, RDT, RCD, VCD and RMD). Increases in the expression of RET, RDT and RCD demonstrated that EBR modulated growth linked to the root meristem through cellular expansion and differentiation, conferring higher protection to this organ (Wei and Li 2016). The epidermis, endoderm and cortex are tissues that are associated with the mechanism of protection and selectivity in the roots, and the increases detected in these tissues contribute to forming a barrier against biotic and abiotic stresses (Cui 2015; Barberon et al. 2016). EBR has positive effects on VCD and RMD, suggesting that the higher densities of these tissues must facilitate transport of water and nutrients via the symplast (Meyer et al. 2011). Reductions in RET and RCD promoted by the high Zn supply

Table 2 Root anatomy in soybean plants sprayed with EBR and exposed to different Zn supplies

EBR	Zn supply	RET (μm)	RDT (μm)	RCD (μm)	VCD (μm)	RMD (μm)
_	Low	11.8 ± 0.6Bb	17.84 ± 0.6Ba	279.7 ± 15.0Bb	250.8 ± 13.0Bb	25.6 ± 1.5Bb
_	Control	13.2 ± 0.6Ab	19.22 ± 0.5Aa	333.9 ± 09.0Ab	282.3 ± 16.0Ab	47.3 ± 2.2Aa
_	High	10.2 ± 0.5Cb	16.82 ± 0.7Ba	252.6 ± 15.2Ba	221.1 ± 14.0Cb	21.8 ± 1.3Cb
+	Low	13.7 ± 0.3Aa	18.43 ± 0.6Ba	319.6 ± 21.2Ba	334.2 ± 12.7Ba	44.6 ± 1.8Ba
+	Control	14.5 ± 0.6Aa	20.20 ± 0.5Aa	366.9 ± 22.5Aa	388.8 ± 31.3Aa	49.5 ± 2.0Aa
+	High	12.8 ± 0.3Ba	17.94 ± 0.7Ba	276.3 ± 16.0Ca	285.3 ± 15.1Ca	36.8 ± 2.2Ca

RET = Root epidermis thickness; RDT = Root endodermis thickness; RCD = Root cortex diameter; VCD = Vascular cylinder diameter; RMD = Root metaxylem diameter. Columns with different uppercase letters between Zn supplies (low, control and high Zn supply under equal EBR level) and lowercase letters between EBR level (with and without EBR under equal Zn supply) indicate significant differences from the Scott-Knott test ($P < 0.05$). Means ± SD, n = 5

(500 μM ZnSO4) were verified by Bazihizina et al. (2014) after studying the impacts of this metal on the cellular structure of *Nicotiana tabacum* roots. Maia et al. (2018) observed in a study with *Solanum lycopersicum* plants that a spray with 100 nM EBR promoted increases in RET (9%), RDT (14%), RCD (12%), VCD (7%) and RMD (17%).

Plants treated with low and high concentrations of Zn and sprayed with 100 nM EBR presented increases in the contents of macronutrients (K, P, and Mg) and micronutrients (Fe, Cu and Mo). The increments induced by the EBR on Zn contents (mainly under low and control Zn supplies) can be explained by the increases in RDM, suggesting higher amounts of root hairs, because this tissue have large contact surface exposed to substrate, facilitating the uptake and mobility of the Zn in plant tissues (Tanaka et al. 2014). These results revealed that the EBR mitigated the negative impacts of Zn on the ionic homeostasis of these essential elements in the absorption channels, optimizing the transport and assimilation process

Table 3 Nutrient contents in soybean plants sprayed with EBR and exposed to different Zn supplies

EBR	Zn supply	K (mg g DM^{-1})	P (mg g DM^{-1})	Mg (mg g DM^{-1})	Fe (μg g DM^{-1})	Cu (μg g DM^{-1})	Mo (μg g DM^{-1})
Contents in root							
_	Low	23.1 ± 0.7Bb	5.9 ± 0.1Bb	5.7 ± 0.2Ab	943.2 ± 28.1Bb	4.84 ± 0.34Cb	2.6 ± 0.2Cb
_	Control	25.7 ± 0.5Ab	9.3 ± 0.3Ab	6.0 ± 0.3Ab	1670.6 ± 36.5Ab	8.92 ± 0.45Ab	4.5 ± 0.2Bb
_	High	23.5 ± 0.8Bb	6.3 ± 0.2Bb	4.5 ± 0.2Bb	864.9 ± 25.3Cb	6.72 ± 0.36Bb	5.0 ± 0.1Ab
+	Low	26.3 ± 0.7Ca	6.8 ± 0.2Ba	6.2 ± 0.1Ba	1215.5 ± 45.9Ba	5.95 ± 0.34Ca	3.7 ± 0.1Ca
+	Control	35.7 ± 1.6Aa	12.7 ± 1.0Aa	6.7 ± 0.1Aa	2333.8 ± 81.9Aa	10.11 ± 0.40Aa	6.0 ± 0.2Aa
+	High	30.2 ± 0.7Ba	7.1 ± 0.3Ba	5.6 ± 0.1Ca	1032.6 ± 42.9Ca	9.22 ± 0.36Ba	5.5 ± 0.1Ba
Contents in stem							
_	Low	26.9 ± 0.9Ba	5.92 ± 0.2Ab	3.4 ± 0.1Bb	58.2 ± 2.1Ab	1.35 ± 0.10Bb	7.7 ± 0.2Cb
_	Control	31.8 ± 1.5Ab	6.12 ± 0.3Ab	3.7 ± 0.1Ab	58.9 ± 2.0Ab	1.69 ± 0.11Ab	9.6 ± 0.1Ab
_	High	16.1 ± 0.7Ca	3.13 ± 0.1Bb	1.2 ± 0.1Cb	23.2 ± 1.8Ba	1.11 ± 0.05Cb	8.9 ± 0.2Ba
+	Low	27.9 ± 1.8Ba	6.85 ± 0.1Aa	3.9 ± 0.2Aa	67.3 ± 3.0Aa	1.75 ± 0.07Ba	8.6 ± 0.1Ca
+	Control	39.0 ± 0.4Aa	7.05 ± 0.3Aa	4.2 ± 0.2Aa	69.4 ± 0.9Aa	1.98 ± 0.08Aa	10.7 ± 0.3Aa
+	High	17.3 ± 1.7Ca	3.50 ± 0.1Ba	1.8 ± 0.1Ba	25.4 ± 1.5Ba	1.21 ± 0.03Ca	9.3 ± 0.3Ba
Contents in leaf							
_	Low	17.4 ± 0.1Bb	7.1 ± 0.1Bb	4.1 ± 0.1Bb	77.6 ± 1.2Bb	1.22 ± 0.02Bb	3.1 ± 0.1Cb
_	Control	18.6 ± 0.2Aa	7.7 ± 0.1Ab	4.4 ± 0.1Ab	114.7 ± 1.6Ab	1.43 ± 0.05Ab	4.3 ± 0.1Ab
_	High	14.1 ± 0.5Ca	2.9 ± 0.1Cb	3.3 ± 0.1Cb	52.0 ± 0.9Cb	1.16 ± 0.01Cb	3.6 ± 0.1Bb
+	Low	21.7 ± 0.6Aa	8.0 ± 0.1Ba	4.6 ± 0.1Ba	85.5 ± 2.4Ba	1.31 ± 0.04Ba	4.8 ± 0.1Ca
+	Control	19.3 ± 0.9Ba	8.5 ± 0.1Aa	4.8 ± 0.0Aa	127.6 ± 0.2Aa	1.69 ± 0.04Aa	6.1 ± 0.2Aa
+	High	15.0 ± 0.9Ca	3.7 ± 0.1Ca	3.8 ± 0.1Ca	61.0 ± 3.7Ca	1.36 ± 0.05Ba	5.4 ± 0.1Ba

Mg = Magnesium; P = Phosphorus; K = Potassium; Fe = Iron; Cu = Copper; Mo = Molybdenum. Columns with different uppercase letters between Zn supplies (low, control and high Zn supply under equal EBR level) and lowercase letters between EBR level (with and without EBR under equal Zn supply) indicate significant differences from the Scott-Knott test ($P < 0.05$). Means ± SD, n = 5

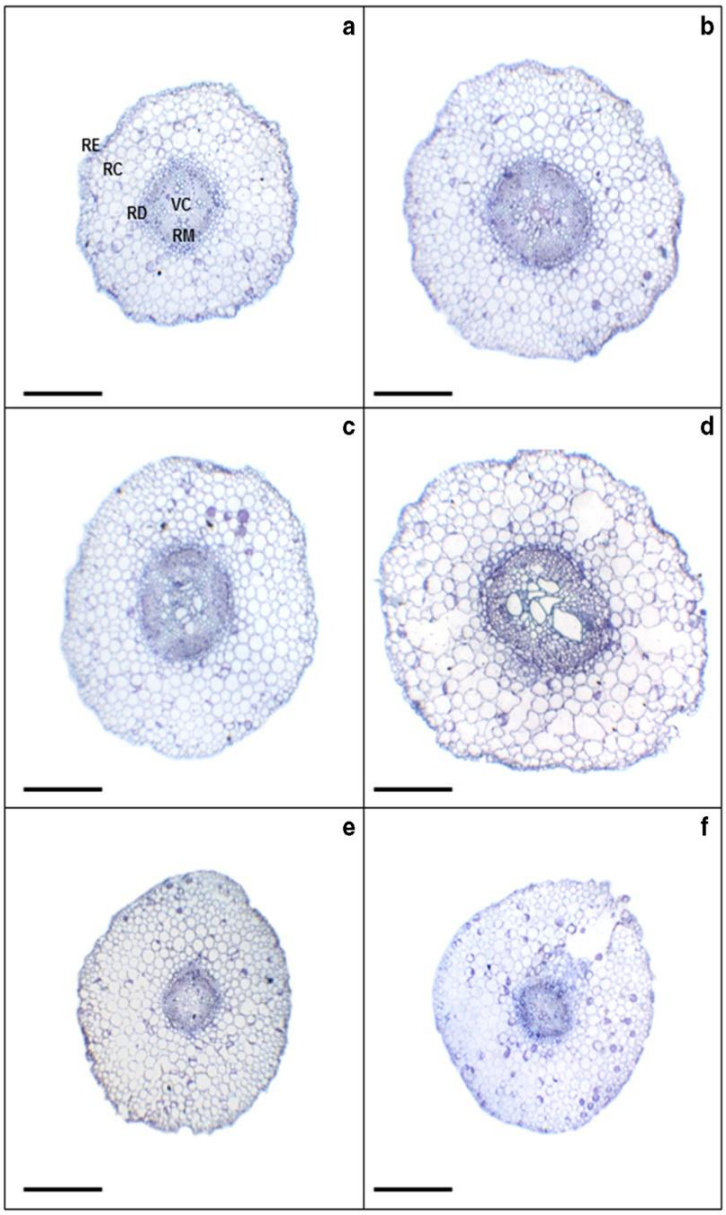

Fig. 1 Root cross sections in soybean plants sprayed with EBR and exposed to different Zn supplies. Low Zn without EBR (A), Low Zn with EBR (B), Control Zn without EBR (C), Control Zn with EBR (D), High Zn without EBR (E), High Zn with EBR (F). RE = Root epidermis; RC = Root cortex; RD = Root endodermis; VC = Vascular cylinder; RM = Root metaxylem. Bars: 300 μm

of $H_2PO_4^-$, Ca^{2+}, Mg^{2+}, Mn^{2+} Fe^{3+}, Cu^{2+} and Zn^{2+} ions by the roots (Karlidag et al. 2011). The exogenous steroid increased the uptake of the Mg^{2+} ion in the root and improved the transport of this element from root to shoot, increasing the chlorophyll levels and improving the photosynthetic characteristics (Fiedor et al. 2008; Yuan et al. 2015). In addition, increases in Fe, Cu, Zn and Mn contribute to a better response related to the antioxidant system because they are metal cofactors of the three main forms of SOD (Fe-SOD, Cu / Zn-SOD and Mn-SOD) (Hänsch and Mendel 2009; Abreu and Cabelli 2010). A study conducted by Samreen et al. (2017) evaluating the effect of Zn stress (0, 1 and 2 μM Zn) on the growth, chlorophyll content and mineral content of *Vigna radiata* plants verified that Zn toxicity had deleterious effects on P, K, and Fe contents in plants. Billard et al. (2015) investigated the impacts of Zn deficiency on nutritional status and protein modifications in *Brassica napus* plants and found that Zn-deficient plants exhibited a lower absorption of elements (K, Mg and Fe).

The exogenous application of 100 nM EBR mitigated the negative effects of low and high Zn supplies on F_0, F_m, F_v and F_v/fm, indicating that EBR reduced photoinhibition and improved photochemical efficiency. Reductions in F_0 and increases in F_m suggested that EBR enhanced the electron transfer from the primary plastoquinone acceptor (Q_A) to the secondary plastoquinone acceptor (Q_B) on the acceptor side of PSII, reflecting positively on F_v/fm (Shu et al. 2016). Andrejić et al. (2018), studying the impact of Zn excess (250, 500 and

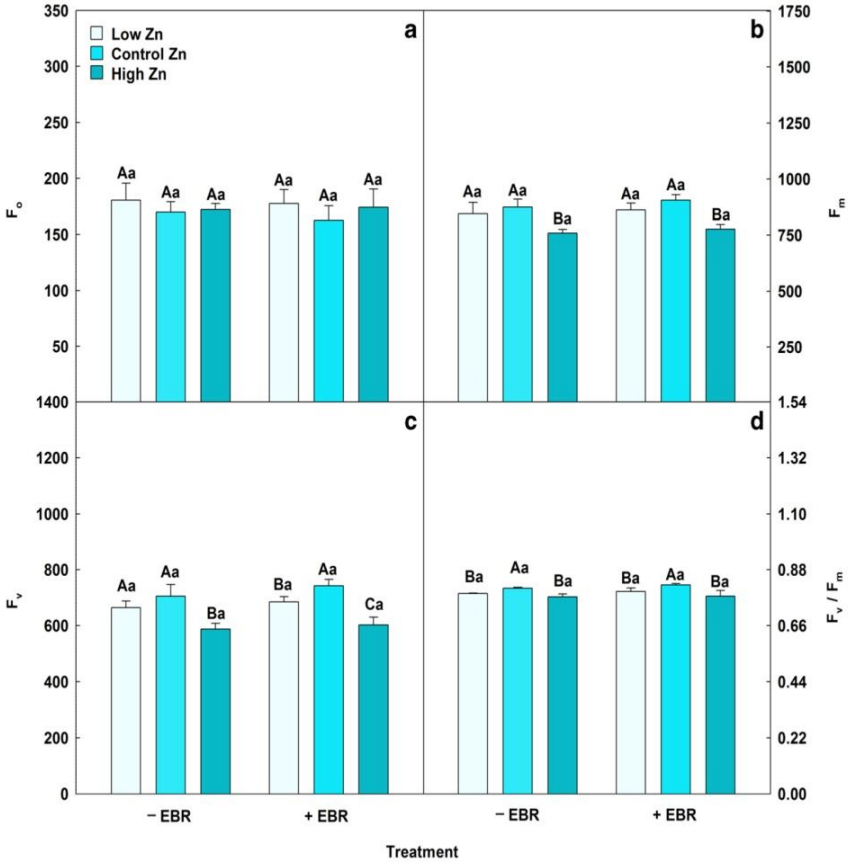

Fig. 2 Minimal fluorescence yield of the dark-adapted state (F_0), maximal fluorescence yield of the dark-adapted state (F_m), variable fluorescence (F_v) and maximal quantum yield of PSII photochemistry (F_v/fm) in soybean plants sprayed with EBR and exposed to different Zn supplies. Columns with different letters indicate significant differences from the Scott-Knott test ($P < 0.05$). Columns corresponding to means from five repetitions and standard deviations

1000 mg Zn kg-1) on gas exchange and chlorophyll fluorescence in plants *Miscanthus* × *giganteus*, verified reductions in F_m, F_v and F_v/fm, while Xia et al. (2009) confirmed in a study with *Cucumis sativus* that 0.1 μM EBR increased the F_v/fm values, optimizing the activity of PSII.

The highest values of Φ_{PSII}, q_p and ETR are intrinsically related to the increase in F_v/fm, as previously described in this study. These results confirm that exogenous EBR maximized the energy capture efficiency by the PSII open-reaction centres in Zn-stressed plants (Zhang et al. 2013; Jia et al. 2015). In addition, the increase in ETR, as indicated by higher values of $\Phi_{PSII,}$ corroborates that EBR increased the capacity of the photosynthetic apparatus to maintain the Q_A in the oxidized state, optimizing the transport of electrons through PSII (Dobrikova et al. 2014). Siddiqui et al. (2018), investigating the chlorophyll fluorescence of *Brassica juncea* plants pretreated with two BRs, detected increases promoted by EBR (10^{-8} M) in Φ_{PSII} (19%), q_p (17%) and ETR (19%), while

Table 4 Chlorophyll fluorescence in soybean plants sprayed with EBR and exposed to different Zn supplies

EBR	Zn supply	Φ_{PSII}	q_P	NPQ	ETR (μmol m^{-2} s^{-1})	EXC (μmol m^{-2} s^{-1})	ETR/P_N
_	Low	0.26 ± 0.02Aa	0.69 ± 0.03Ba	0.96 ± 0.02Aa	38.2 ± 3.5Aa	0.67 ± 0.04Aa	2.49 ± 0.22Aa
_	Control	0.28 ± 0.01Ab	0.80 ± 0.02Aa	0.68 ± 0.02Ca	40.4 ± 2.3Ab	0.66 ± 0.01Aa	2.36 ± 0.22Aa
_	High	0.25 ± 0.01Ab	0.68 ± 0.01Bb	0.75 ± 0.01Ba	36.9 ± 2.3Ab	0.67 ± 0.01Aa	2.61 ± 0.16Aa
+	Low	0.27 ± 0.03Ba	0.72 ± 0.04Ba	0.88 ± 0.02Ab	40.0 ± 3.5Ba	0.66 ± 0.01Aa	2.50 ± 0.08Aa
+	Control	0.32 ± 0.01Aa	0.84 ± 0.03Aa	0.61 ± 0.02Cb	47.3 ± 2.0Aa	0.61 ± 0.02Bb	2.35 ± 0.16Aa
+	High	0.29 ± 0.01Ba	0.76 ± 0.01Ba	0.69 ± 0.01Bb	42.1 ± 1.7Ba	0.63 ± 0.01Bb	2.48 ± 0.11Aa

Φ_{PSII} = Effective quantum yield of PSII photochemistry; q_P = Photochemical quenching coefficient; NPQ = Nonphotochemical quenching; ETR = Electron transport rate; EXC = Relative energy excess at the PSII level; ETR/P_N = Ratio between the electron transport rate and net photosynthetic rate. Columns with different uppercase letters between Zn supplies (low, control and high Zn supply under equal EBR level) and lowercase letters between EBR level (with and without EBR under equal Zn supply) indicate significant differences from the Scott-Knott test ($P < 0.05$). Means ± SD, n = 5

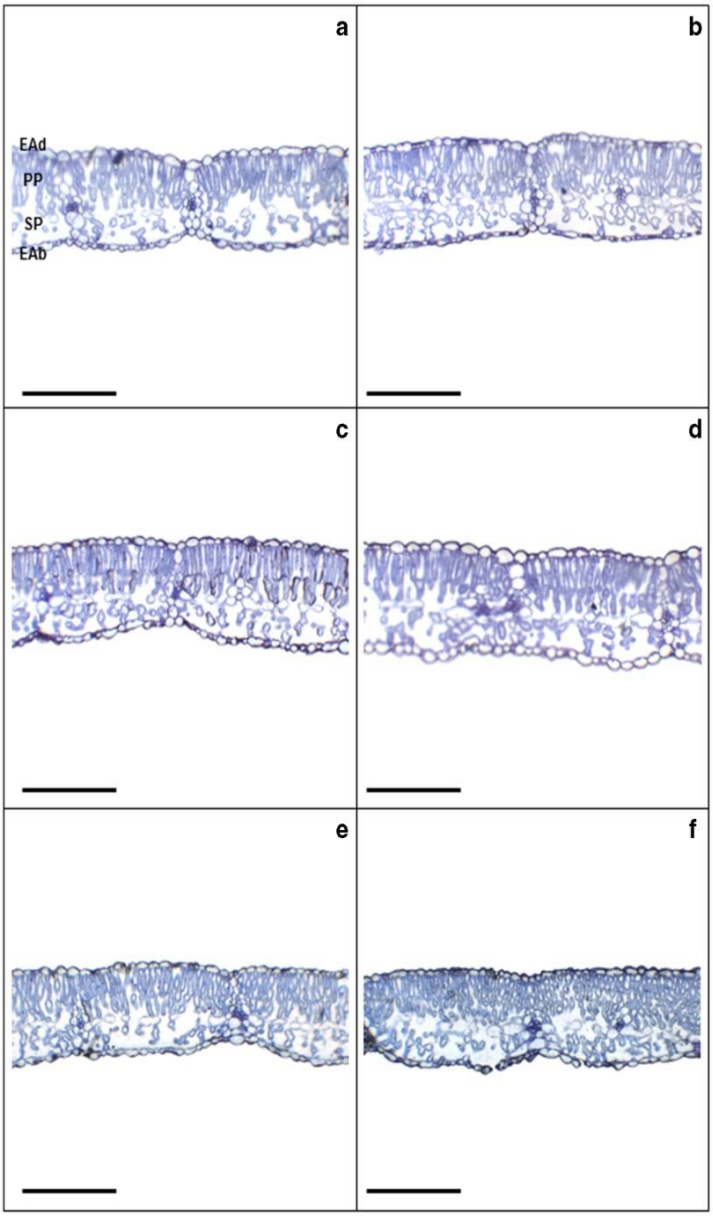

Fig. 3 Leaf cross sections in soybean plants sprayed with EBR and exposed to different Zn supplies. Low Zn without EBR (A), Low Zn with EBR (B), Control Zn without EBR (C), Control Zn with EBR (D), High Zn without EBR (E), High Zn with EBR (F). EAd = adaxial epidermis; EAb = Abaxial epidermis; PP = Palisade parenchyma; SP = Spongy parenchyma. Bars: 200 μm

Table 5 Gas exchange in soybean plants sprayed with EBR and exposed to different Zn supplies

EBR	Zn supply	P_N (μmol m^{-2} s^{-1})	E (mmol m^{-2} s^{-1})	g_s (mol m^{-2} s^{-1})	C_i (μmol mol^{-1})	WUE (μmolmmol^{-1})	P_N/C_i (μmol m^{-2} s^{-1} Pa^{-1})
_	Low	15.4 ± 0.8Ba	2.88 ± 0.10Aa	0.21 ± 0.02Ba	302 ± 12Ba	5.38 ± 0.43Ab	0.056 ± 0.002Bb
_	Control	17.3 ± 0.7Ab	3.02 ± 0.11Aa	0.39 ± 0.01Aa	270 ± 14Ca	5.73 ± 0.32Ab	0.065 ± 0.003Ab
_	High	14.2 ± 0.9Bb	2.63 ± 0.06Bb	0.23 ± 0.02Ba	338 ± 13Aa	5.40 ± 0.20Ab	0.041 ± 0.002Cb
+	Low	16.2 ± 1.5Ba	2.75 ± 0.11Ba	0.24 ± 0.02Ba	243 ± 13Ab	5.91 ± 0.18Ba	0.074 ± 0.003Ba
+	Control	20.2 ± 1.2Aa	3.08 ± 0.04Aa	0.39 ± 0.01Aa	252 ± 21Aa	6.58 ± 0.19Aa	0.089 ± 0.006Aa
+	High	17.1 ± 1.4Ba	2.87 ± 0.07Ba	0.26 ± 0.02Ba	273 ± 19Ab	5.95 ± 0.20Ba	0.065 ± 0.002Ca

P_N = Net photosynthetic rate; E = Transpiration rate; g_s = Stomatal conductance; C_i = Intercellular CO_2 concentration; WUE = Water-use efficiency; P_N/C_i = Carboxylation instantaneous efficiency. Columns with different uppercase letters between Zn supplies (low, control and high Zn supply under equal EBR level) and lowercase letters between EBR level (with and without EBR under equal Zn supply) indicate significant differences from the Scott-Knott test ($P < 0.05$). Means ± SD, n = 5

Table 6 Stomatal characteristics in soybean plants sprayed with EBR and exposed to different Zn supplies

EBR	Zn supply	SD (stomata per mm^2)	PDS (μm)	EDS (μm)	SF	SI (%)
Adaxial face						
_	Low	178 ± 6Bb	13.4 ± 0.3Ba	23.5 ± 0.9Ba	0.57 ± 0.01Ba	7.5 ± 0.6Bb
_	Control	242 ± 3Ab	12.9 ± 0.8Ba	21.3 ± 0.8Ca	0.61 ± 0.01Aa	9.7 ± 0.4Ab
_	High	85 ± 7Cb	14.4 ± 0.2Aa	25.8 ± 0.6Aa	0.56 ± 0.03Ba	4.7 ± 0.3Cb
+	Low	225 ± 9Ba	12.8 ± 0.9Aa	21.4 ± 0.5Bb	0.60 ± 0.05Aa	9.3 ± 0.5Ba
+	Control	250 ± 2Aa	12.3 ± 0.5Aa	20.2 ± 1.5Ba	0.61 ± 0.03Aa	10.7 ± 0.2Aa
+	High	150 ± 8Ca	13.2 ± 0.4Ab	22.8 ± 0.2Ab	0.58 ± 0.04Aa	7.4 ± 0.3Ca
Abaxial face						
_	Low	357 ± 2Bb	13.2 ± 0.4Ba	24.1 ± 0.8Ba	0.55 ± 0.04Aa	34.3 ± 0.8Bb
_	Control	427 ± 8Ab	12.2 ± 0.3Ca	21.6 ± 1.0Ca	0.57 ± 0.04Aa	36.5 ± 0.6Ab
_	High	257 ± 8Cb	14.3 ± 0.2Aa	26.8 ± 0.9Aa	0.54 ± 0.04Aa	33.1 ± 0.9Bb
+	Low	404 ± 9Ba	12.5 ± 0.3Aa	21.8 ± 0.7Bb	0.57 ± 0.04Aa	36.5 ± 0.7Ba
+	Control	457 ± 7Aa	11.2 ± 0.4Bb	18.8 ± 1.2Cb	0.60 ± 0.05Aa	38.8 ± 0.4Aa
+	High	335 ± 6Ca	13.1 ± 0.6Ab	23.9 ± 0.5Ab	0.55 ± 0.04Aa	35.9 ± 0.8Ba

SD = Stomatal density; PDS = Polar diameter of the stomata; EDS = Equatorial diameter of the stomata; SF = Stomatal functionality; SI = Stomatal index. Columns with different uppercase letters between Zn supplies (low, control and high Zn supply under equal EBR level) and lowercase letters between EBR level (with and without EBR under equal Zn supply) indicate significant differences from the Scott-Knott test ($P < 0.05$). Means ± SD, n = 5

foliar spray of HBL (10^{-8} M) promoted increases of 17%, 16% and 18% for Φ_{PSII}, q_p and ETR, respectively.

The decrease induced by EBR in the NPQ, EXC and ETR/P_N of plants exposed to the low and high Zn supplies revealed that the application of this steroid resulted in less excitation energy dissipation in the form of heat, avoiding the damage by photoinhibition in the centres of reaction (Ogweno et al. 2008; Zhang et al. 2015). Additionally, reductions of the expression of EXC and ETR/P_N indicated that the excess electrons were used less often for secondary processes, such as photorespiration, and thus were potentially available for primary processes, such as reductions of $NADP^+$ during the biochemical fixation of CO_2 (Silva et al. 2012). Lima et al. (2018) found that the application of 100 nM EBR in *Eucalyptus urophylla* under Fe deficiency significantly reduced the values of NPQ (19%), EXC (14%) and ETR/P_N (16%), promoting protection of PSII against possible damages caused by the excess of excitation and improving the use of electrons during the photochemical activity.

EBR minimized the damage caused by Zn concentrations (low and high) on gas exchange. Increases in P_N and E are positively related to the improvements expressed in g_s, and these effects are explained by the positive impact of EBR on the enzymatic activities of CA (Hayat et al. 2011) and RuBisCO (Yu et al. 2004), which are key enzymes in the initial process of photosynthesis. The high CA activity increases the carboxylation state of RuBisCO in the Calvin cycle, consequently decreasing C_i and inducing P_N maximization (Hasan et al. 2011; Alyemeni and Al-Quwaiz 2016). The increase in WUE is associated with the benefits promoted by EBR on P_N. In addition, P_N/C_i values were increased in EBR-treated plants due to

Table 7 Leaf anatomy in soybean plants sprayed with EBR and exposed to different Zn supplies

EBR	Zn supply	ETAd (μm)	ETAb (μm)	PPT (μm)	SPT (μm)	Ratio PPT/SPT
_	Low	15.6 ± 1.3Bb	14.2 ± 0.2Bb	84.4 ± 2.0Bb	77.6 ± 3.2Bb	1.09 ± 0.03Ba
_	Control	18.5 ± 0.7Aa	17.4 ± 0.2Ab	93.3 ± 5.0Aa	88.0 ± 4.0Aa	1.06 ± 0.01Ba
_	High	14.9 ± 1.0Bb	13.8 ± 0.9Bb	76.8 ± 3.0Cb	65.4 ± 4.7Cb	1.18 ± 0.01Aa
+	Low	18.8 ± 0.6Aa	17.7 ± 0.7Aa	93.6 ± 2.4Aa	87.2 ± 1.7Aa	1.07 ± 0.03Aa
+	Control	18.9 ± 1.3Aa	18.9 ± 0.5Aa	95.5 ± 5.4Aa	91.8 ± 4.1Aa	1.04 ± 0.03Aa
+	High	17.8 ± 0.7Aa	15.8 ± 0.4Ba	84.1 ± 3.5Ba	75.8 ± 3.9Ba	1.11 ± 0.01Ab

ETAd = Epidermis thickness from adaxial leaf side; ETAb = Epidermis thickness from abaxial leaf side; PPT = Palisade parenchyma thickness; SPT = Spongy parenchyma thickness. Columns with different uppercase letters between Zn supplies (low, control and high Zn supply under equal EBR level) and lowercase letters between EBR level (with and without EBR under equal Zn supply) indicate significant differences from the Scott-Knott test ($P < 0.05$). Means ± SD, n = 5

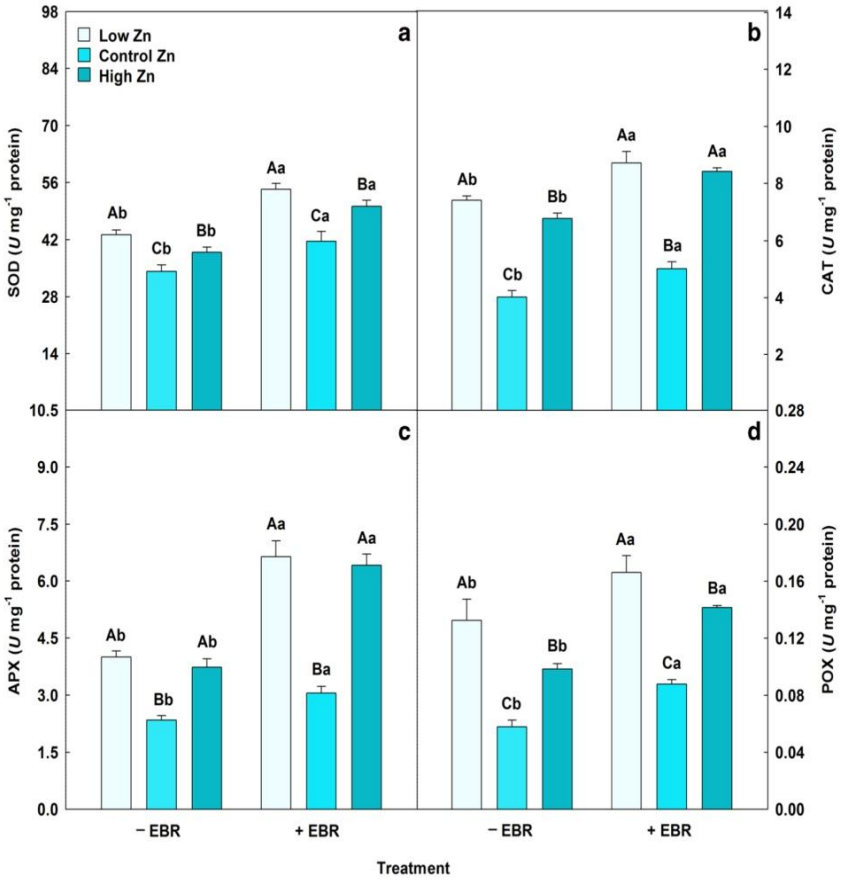

Fig. 4 Activities of superoxide dismutase (SOD), catalase (CAT), ascorbate peroxidase (APX) and peroxidase (POX) in soybean plants sprayed with EBR and exposed to different Zn supplies. Columns with different letters indicate significant differences from the Scott-Knott test ($P < 0.05$). Columns corresponding to means from five repetitions and standard deviations

increased P_N and a simultaneous reduction in C_i. Fei et al. (2016) detected reductions in P_N, g_s and E, as well as increases in C_i promoted by the low Zn supplement in *Citrus sinensis* plants. Ouni et al. (2016), analysing the effects of Zn concentrations (100 and 300 ppm) on the gas exchange of *Polypogon monspeliensis*, observed reductions in P_N, g_s and WUE values under the highest concentration of Zn (300 ppm). However, Jiang et al. (2012) demonstrated that the effects of EBR foliar spraying (0.1 μM) improved the gas exchange (P_N, g_s and C_i) in *Cucumis sativus* plants.

Exogenous EBR (100 nM) had positive effects on stomatal characteristics (SD, PDS, EDS, SF and SI). The increases of SD, SF and SI revealed that the EBR improved stomatal performance, corroborated by higher values detected for g_s. This steroid regulates stomatal development, activating specific proteins that act on the stomatal intracellular signalling pathway (Kim et al. 2012; Casson and Hetherington 2012), maximizing the gas exchange and increasing the opportunity for CO_2 uptake by the mesophyll cells (PPT and SPT) (Flexas et al. 2008, 2012). Additionally, the reductions observed in PDS and EDS reveal beneficial interferences of the EBR in the stomata form, inducing stomata to be more elliptic and providing increases in SF (Martins et al. 2015). Subba et al. (2014), investigating physiological and biochemical changes induced by nine concentrations of Zn (0–20 mM Zn) in *Citrus reticulata* seedlings, observed reductions in SD in the leaves of plants exposed to deficiency (0, 1, 2, 3 and 4 mM Zn) and excess (10, 15 and 20 mM Zn) when compared to a sufficient concentration (5 mM Zn).

Plants treated with EBR (100 nM) and exposed to Zn supplies (low and high) had beneficial effects on leaf anatomy (ETAd, ETAb, PPT and SPT). The increases in PPT and SPT are connected to increments shown in P_N and P_N/C_i because the gas exchange has an influence on the mesophyll, facilitating CO_2 diffusion from the environment to the carboxylation sites in the chloroplasts (Ennajeh et al. 2010). The high values of ETAd and ETAb in plants sprayed with EBR can be explained by the higher values of E and WUE, in which the epidermis is a coating tissue, clearly contributing to the use of water and avoiding excessive loss of water during the transpiration process (Javelle et al. 2011). Kim and Wetzstein (2003) investigated *Carya illinoinensis* plants subjected to Zn deficiency and reported decreases in PPT and SPT

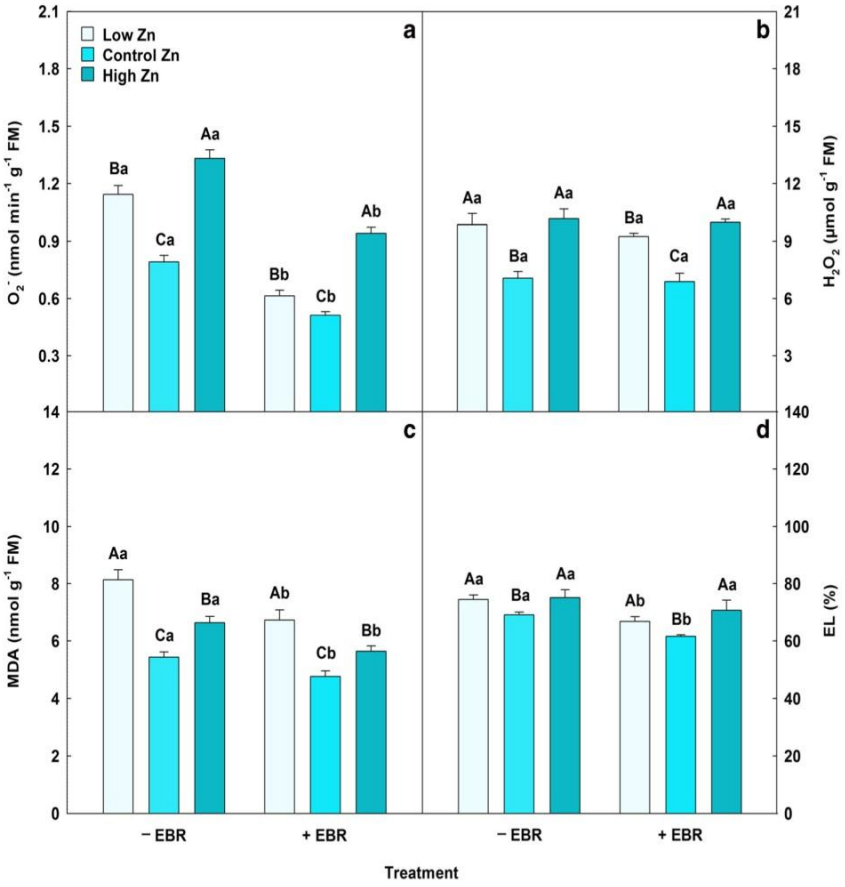

Fig. 5 Superoxide ($O_2^{\cdot-}$), hydrogen peroxide (H_2O_2), malondialdehyde (MDA) and electrolyte leakage (EL) in soybean plants sprayed with EBR and exposed to different Zn supplies. Columns with different letters indicate significant differences from the Scott-Knott test ($P < 0.05$). Columns corresponding to means from five repetitions and standard deviations

and found a reduction in the number of cells of the palisade parenchyma per length in leaf. Mattiello et al. (2015) examined the impacts of Zn deficiency on physiological and anatomical characteristics of *Zea mays* leaves during 0, 2, 6, 10, 14, 18 and 22 days after the Zn omission; they reported intense reductions in their size, composed of 44% mesophyll and 8% intercellular space. In addition, the epidermal area on the adaxial and abaxial surfaces corresponded to 15% and 10%, respectively.

The application of EBR (100 nM) contributed to an increase in the activities of the SOD, CAT, APX and POX enzymes of the plants exposed to the low and high Zn supplies, revealing the intrinsic action of this substance on antioxidant metabolism. These changes contribute to a higher photochemical efficiency, as evidenced by the increases in F_v/fm and ETR. A study conducted by He et al. (2016) evaluating the enzymatic responses and growth of *Solanum melongena* seedlings

Table 8 Photosynthetic pigments in soybean plants sprayed with EBR and exposed to different Zn supplies

EBR	Zn supply	Chl *a* (mg g^{-1} FM)	Chl *b* (mg g^{-1} FM)	Total Chl (mg g^{-1} FM)	Car (mg g^{-1} FM)	Ratio Chl *a*/Chl *b*	Ratio Total Chl/Car
_	Low	8.19 ± 0.36Bb	1.37 ± 0.05Bb	9.56 ± 0.31Bb	0.48 ± 0.01Bb	6.06 ± 0.41Aa	20.88 ± 0.50Aa
_	Control	12.38 ± 1.12Aa	3.04 ± 0.06Ab	15.42 ± 0.83Aa	0.84 ± 0.02Ab	4.33 ± 0.10Ba	19.60 ± 0.24Ba
_	High	7.41 ± 0.50Bb	1.17 ± 0.04Cb	8.59 ± 0.19Cb	0.42 ± 0.01Cb	6.36 ± 0.41Aa	21.07 ± 0.60Aa
+	Low	10.53 ± 0.30Ba	2.67 ± 0.14Ba	13.20 ± 0.57Ba	0.66 ± 0.02Ba	4.20 ± 0.24Bb	19.96 ± 0.54Aa
+	Control	12.45 ± 0.44Aa	3.21 ± 0.08Aa	15.67 ± 1.10Aa	0.91 ± 0.02Aa	3.95 ± 0.15Ba	18.15 ± 0.44Bb
+	High	9.69 ± 0.20Ca	1.93 ± 0.15Ca	11.62 ± 0.39Ca	0.61 ± 0.01Ca	5.46 ± 0.33Ab	20.04 ± 0.49Aa

Chl *a* = Chlorophyll *a*; Chl *b* = Chlorophyll *b*; Total chl = Total chlorophyll; Car = Carotenoids. Columns with different uppercase letters between Zn supplies (low, control and high Zn supply under equal EBR level) and lowercase letters between EBR level (with and without EBR under equal Zn supply) indicate significant differences from the Scott-Knott test ($P < 0.05$). Means ± SD, n = 5

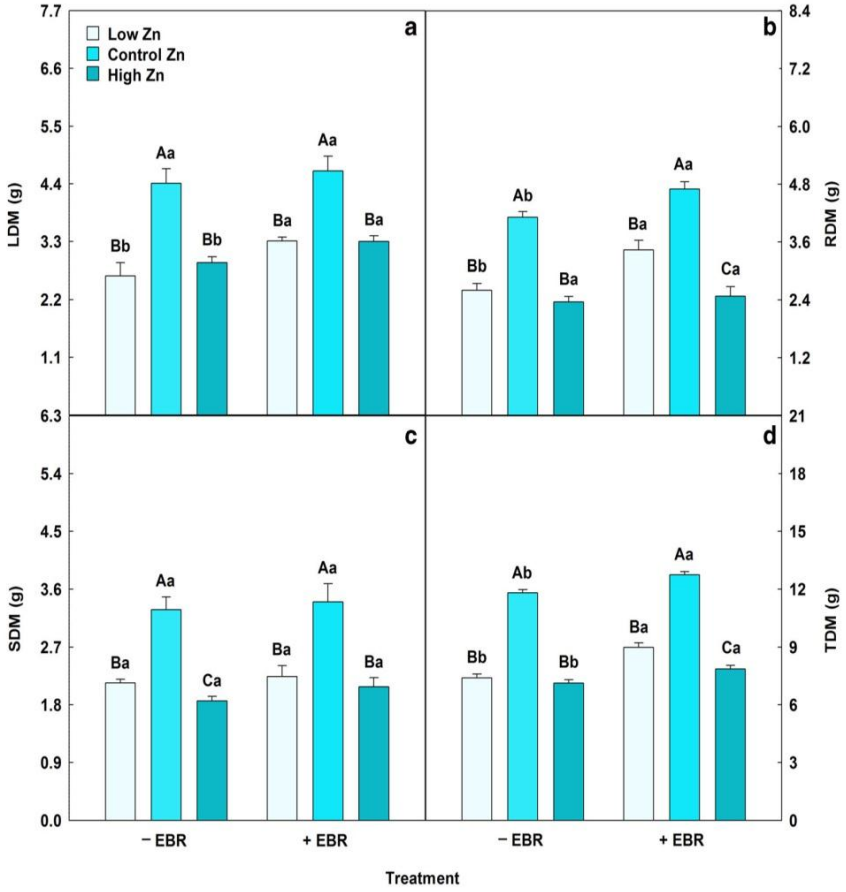

Fig. 6 Leaf dry matter (LDM), root dry matter (RDM), stem dry matter (SDM) and total dry matter (TDM) in soybean plants sprayed with EBR and exposed to different Zn supplies. Columns with different letters indicate significant differences from the Scott-Knott test ($P < 0.05$). Columns corresponding to means from five repetitions and standard deviations

subjected to Zn toxicity (10% Zn) + 0.1 μM EBR detected increases in the activities of SOD (20%), CAT (25%), APX (11%) and POX (17%). Li et al. (2016a), investigating the exogenous effects of EBR on *Solanum lycopersicum* seedlings, also found benefits on the antioxidant system, in which 5 nM EBR notably increased the activities of the SOD, CAT and APX enzymes under Zn stress.

Exogenous EBR (100 nM) promoted reductions in ROS levels (O_2^- and H_2O_2) and mitigated the membrane damage (MDA and EL) in *Glycine max* plants exposed to Zn stress (low and high), and these results were attributed to higher activity of the antioxidant enzymes (SOD, CAT, APX and POX) as previously detected in this study. In cells, the SOD enzyme rapidly converts O_2^- to H_2O_2, while the CAT and APX enzymes act to dissociate H_2O_2, with consequent formation of H_2O and O_2, reducing the concentrations of oxidizing compounds (Li et al. 2016a). On the other hand, high concentrations of O_2^- and H_2O_2 often promote lipid peroxidation (MDA), inducing electrolyte leakage (EL) and negatively impacting the membrane function (Kumari et al. 2010; Gallego et al. 2012). Ramakrishna and Rao (2012) evaluated *Raphanus sativus* seedlings subjected to three concentrations of EBR (0.5, 1.0 and 2 μM) and exposed to Zn stress and verified significant reductions in O_2^- (57%), H_2O_2 (27%) and EL.

Plants under Zn stress (low and high) and sprayed with EBR had increases in the levels of Chl *a*, Chl *b*, Chl total and Car, and these effects were related to lower accumulation of ROS (O_2^- and H_2O_2) in leaf tissue, reducing the oxidative damage to the structures and functions of the thylakoid membranes (Ramakrishna and Rao 2012). This result was confirmed by the decreases in the MDA and EL levels previously described in this study. In addition, EBR promoted an increase in Mg content, which is a structural element of the chlorophyll molecule (Fiedor et al. 2008). These benefits induced by EBR enhanced pigment biosynthesis and promoted a positive impact on the photosynthetic apparatus. Mateos-Naranjo et al. (2018) found reductions in Chl *a*, Chl *b* and Car levels in *Juncus acutus* plants exposed to Zn toxicity (100 mM Zn). However, Ramakrishna and Rao (2015) demonstrated that foliar application of EBL and HBL at concentrations of 0.5, 1.0 and 2.0 μM effectively alleviated the deleterious effects of Zn toxicity on *Raphanus sativus*, protecting mainly the chloroplast membranes and increasing Chl *a*, Chl *b* and Car.

The EBR application reduced the deleterious effects on plant biomass (LDM, RDM, SDM and TDM) caused by low and high Zn supplementation. These results suggest

that EBR stimulated cell division and elongation in roots, stems and leaves, increasing the rate of growth and development (Müssig 2005; Que. et al. 2018). The increase in biomass can be explained by the benefits to root anatomy, gas exchange, antioxidant enzymes (SOD, CAT, APX and POX) and nutrient contents demonstrated in this study (Shahbaz et al. 2008; Hayat et al. 2012; Santos et al. 2018). Pascual et al. (2016) reported significant reductions in the LDM and RDM values of *Glycine max* plants subjected to Zn deficiency. Research conducted by Marques et al. (2017) studying *Jatropha curcas* plants subjected to different concentrations of Zn (100, 200, 300, 400 and 600 μM) observed a decrease in plant biomass (leaf, stem and root) after exposure to a higher concentration of Zn (600 μM).

5 Conclusion

Our study proved that 24-epibrassinolide mitigated the oxidative stress induced by different zinc supplies in soybean plants. In other hand, plants exposed to high zinc supply without 24-epibrassinolide application presented deleterious effects more intense. The steroid spray alleviated the impact produced by zinc stress on nutritional status because these results were intrinsically linked to improvements on vascular cylinder and metaxylem, improving the magnesium, phosphorus, potassium, iron, copper and molybdenum contents. In relation to the photosynthetic machinery of plants treated with 24-epibrassinolide and exposed to high and low zinc supplies, antioxidant enzymes play crucial roles, dismutating superoxide and hydrogen peroxide, and protecting the chloroplast membranes, with clear positive repercussions on chlorophylls, effective quantum yield of photosystem II photochemistry and electron transport rate. The stimulation induced by this substance on gas exchange can be explained by the favourable conditions detected for stomatal density, stomatal index, palisade parenchyma and spongy parenchyma, enhancing the carbon dioxide diffusion in the chloroplasts. Finally, an interesting result found in this research is related to 24-epibrassinolide application on leaves promoting beneficial effects on root anatomy, validating the systemic action of this steroid.

Acknowledgements This research had financial supports from Fundação Amazônia de Amparo a Estudos e Pesquisas (FAPESPA/Brazil), Conselho Nacional de Desenvolvimento Científico e Tecnológico (CNPq/Brazil), Programa de Pós-Graduação em Agronomia (PGAGRO/Brazil) and Universidade Federal Rural da Amazônia (UFRA/Brazil) to AKSL. In other hand, LRS was supported with scholarship from Coordenação de Aperfeiçoamento de Pessoal de Nível Superior (CAPES/Brazil).

Author Contribution Statement AKSL was the advisor of this project, planning all phases of this research. LRS conducted the experiment in the greenhouse and performed physiological, biochemical and morphological determinations, while BRSS measured anatomical parameters. TP and BLB performed nutritional determinations and helped in drafting the manuscript and in interpreting the results.

Data Availability Statement Data are available upon request to the corresponding author.

Compliance with Ethical Standards

Conflict of Interest The authors declare that they have no competing interests.

References

Abdullahi BA, Gu X, Gan Q, Yang Y (2003) Brassinolide amelioration of aluminum toxicity in mungbean seedling growth. J Plant Nutr 26: 1725–1734. https://doi.org/10.1081/PLN-120023278

Abreu IA, Cabelli DE (2010) Superoxide dismutases—a review of the metal-associated mechanistic variations. Biochim Biophys Acta, Proteins Proteomics 1804:263–274. https://doi.org/10.1016/j.bbapap.2009.11.005

Ahammed GJ, Choudhary SP, Chen S et al (2013) Role of brassinosteroids in alleviation of phenanthrene–cadmium co-contamination-induced photosynthetic inhibition and oxidative stress in tomato. J Exp Bot 64:199–213. https://doi.org/10.1093/jxb/ers323

Allen LH Jr, Zhang L, Boote KJ, Hauser BA (2018) Elevated temperature intensity, timing, and duration of exposure affect soybean internode elongation, mainstem node number, and pod number per plant. Crop J 6:148–161. https://doi.org/10.1016/j.cj.2017.10.005

Alyemeni MN, Al-Quwaiz SM (2016) Effect of 28-homobrassinolide on the performance of sensitive and resistant varieties of Vigna radiata. Saudi J Biol Sci 23:698–705. https://doi.org/10.1016/j.sjbs.2016.01.002

Andrejić G, Gajić G, Prica M, Dželetović Ž, Rakić T (2018) Zinc accumulation, photosynthetic gas exchange, and chlorophyll a fluorescence in Zn-stressed Miscanthus × giganteus plants. Photosynthetica 56:1249–1258. https://doi.org/10.1007/s11099-018-0827-3

Antoniadis V, Shaheen SM, Tsadilas CD et al (2018) Zinc sorption by different soils as affected by selective removal of carbonates and hydrous oxides. Appl Geochem 88:49–58. https://doi.org/10.1016/j.apgeochem.2017.04.007

Anwar A, Liu Y, Dong R, Bai L, Yu X, Li Y (2018) The physiological and molecular mechanism of brassinosteroid in response to stress: a review. Biol Res 51:1–15. https://doi.org/10.1186/s40659-018-0195-2

Aragão RM, Silva EN, Vieira CF, Silveira JAG (2012) High supply of NO3 − mitigates salinity effects through an enhancement in the efficiency of photosystem II and CO2 assimilation in Jatropha curcas plants. Acta Physiol Plant 34:2135–2143. https://doi.org/10.1007/s11738-012-1014-y

Arrivault S, Senger T, Krämer U (2006) The Arabidopsis metal tolerance protein AtMTP3 maintains metal homeostasis by mediating Zn exclusion from the shoot under Fe deficiency and Zn oversupply. Plant J 46:861–879. https://doi.org/10.1111/j.1365-313X.2006.02746.x

Azhar N, Su N, Shabala L, Shabala S (2017) Exogenously applied 24-epibrassinolide (EBL) ameliorates detrimental effects of salinity by reducing K+ efflux via depolarization-activated K+ channels. Plant Cell Physiol 58:802–810. https://doi.org/10.1093/pcp/pcx026

Azzarello E, Pandolfi C, Giordano C et al (2012) Ultramorphological and physiological modifications induced by high zinc levels in

Paulownia tomentosa. Environ Exp Bot 81:11–17. https://doi.org/10.1016/j.envexpbot.2012.02.008

Badawi GH, Yamauchi Y, Shimada E et al (2004) Enhanced tolerance to salt stress and water deficit by overexpressing superoxide dismutase in tobacco (Nicotiana tabacum) chloroplasts. Plant Sci 166:919–928. https://doi.org/10.1016/j.plantsci.2003.12.007

Baig MA, Ahmad J, Bagheri R, Ali AA, al-Huqail AA, Ibrahim MM, Qureshi MI (2018) Proteomic and ecophysiological responses of soybean (Glycine max L.) root nodules to Pb and hg stress. BMC Plant Biol 18:283–221. https://doi.org/10.1186/s12870-018-1499-7

Bajguz A (2000) Effect of brassinosteroids on nucleic acids and protein content in cultured cells of Chlorella vulgaris. Plant Physiol Biochem 38:209–215. https://doi.org/10.1016/S0981-9428(00)00733-6

Bajguz A (2010) An enhancing effect of exogenous brassinolide on the growth and antioxidant activity in Chlorella vulgaris cultures under heavy metals stress. Environ Exp Bot 68:175–179. https://doi.org/10.1016/j.envexpbot.2009.11.003

Bajguz A, Hayat S (2009) Effects of brassinosteroids on the plant responses to environmental stresses. Plant Physiol Biochem 47:1–8. https://doi.org/10.1016/j.plaphy.2008.10.002

Balasaraswathi K, Jayaveni S, Sridevi J et al (2017) Cr–induced cellular injury and necrosis in Glycine max L.: biochemical mechanism of oxidative damage in chloroplast. Plant Physiol Biochem 118:653–666. https://doi.org/10.1016/j.plaphy.2017.08.001

Barberon M, Vermeer JEM, De Bellis D et al (2016) Adaptation of root function by nutrient-induced plasticity of endodermal differentiation. Cell 164:447–459. https://doi.org/10.1016/j.cell.2015.12.021

Bazihizina N, Taiti C, Marti L et al (2014) Zn2+−induced changes at the root level account for the increased tolerance of acclimated tobacco plants. J Exp Bot 65:4931–4942. https://doi.org/10.1093/jxb/eru251

Billard V, Maillard A, Garnica M et al (2015) Zn deficiency in Brassica napus induces Mo and Mn accumulation associated with chloroplast proteins variation without Zn remobilization. Plant Physiol Biochem 86:66–71. https://doi.org/10.1016/j.plaphy.2014.11.005

Bradford MM (1976) A rapid and sensitive method for the quantitation of microgram quantities of protein utilizing the principle of protein-dye binding. Anal Biochem 72:248–254. https://doi.org/10.1016/0003-2697(76)90527-3

Cakmak I, Horst WJ (1991) Effect of aluminium on lipid peroxidation, superoxide dismutase, catalase, and peroxidase activities in root tips of soybean (Glycine max). Physiol Plant 83:463–468. https://doi.org/10.1111/j.1399-3054.1991.tb00121.x

Cakmak I, Marschner H (1992) Magnesium deficiency and high light intensity enhance activities of superoxide dismutase, ascorbate peroxidase, and glutathione reductase in bean leaves. Plant Physiol 98:1222–1227. https://doi.org/10.1104/pp.98.4.1222

Casson SA, Hetherington AM (2012) GSK3-like kinases integrate brassinosteroid signaling and stomatal development. Sci Signal 5:1–3. https://doi.org/10.1126/scisignal.2003311

Castro EM, Pereira FJ, Paiva R (2009) Plant histology: structure and function of vegetative organs. Lavras

Cui H (2015) Cortex proliferation in the root is a protective mechanism against abiotic stress. Plant Signal Behav 10:e1011949. https://doi.org/10.1080/15592324.2015.1011949

Dobrikova AG, Vladkova RS, Rashkov GD et al (2014) Effects of exogenous 24-epibrassinolide on the photosynthetic membranes under non-stress conditions. Plant Physiol Biochem 80:75–82. https://doi.org/10.1016/j.plaphy.2014.03.022

Elstner EF, Heupel A (1976) Inhibition of nitrite formation from hydroxylammoniumchloride: a simple assay for superoxide dismutase. Anal Biochem 70:616–620. https://doi.org/10.1016/0003-2697(76)90488-7

Ennajeh M, Vadel AM, Cochard H, Khemira H (2010) Comparative impacts of water stress on the leaf anatomy of a drought-resistant and a drought-sensitive olive cultivar. J Hortic Sci Biotechnol 85:289–294. https://doi.org/10.1080/14620316.2010.11512670

Enstone DE, Peterson CA, Ma F (2003) Root endodermis and exodermis: structure, function, and responses to the environment. J Plant Growth Regul 21:335–351. https://doi.org/10.1007/s00344-003-0002-2

Fan M, Zhu J, Richards C et al (2003) Physiological roles for aerenchyma in phosphorus-stressed roots. Funct Plant Biol 30:493–506. https://doi.org/10.1071/FP03046

FAO (2018) Food and agriculture organization of the united nations. Food outlook: Biannual report on global food markets. FAO, Rome

Fei X, Xing-zheng F, Nan-qi W et al (2016) Physiological changes and expression characteristics of ZIP family genes under zinc deficiency in navel orange (Citrus sinensis). J Integr Agric 15:803–811. https://doi.org/10.1016/S2095-3119(15)61276-X

Fiedor L, Kania A, Mysliwa-Kurdziel B et al (2008) Understanding chlorophylls: central magnesium ion and phytyl as structural determinants. Biochim Biophys Acta Bioenerg 1777:1491–1500. https://doi.org/10.1016/j.bbabio.2008.09.005

Flexas J, Ribas-carbó M, Diaz-espejo A et al (2008) Mesophyll conductance to CO 2 : current knowledge and future prospects. Plant Cell Environ 31:602–621. https://doi.org/10.1111/j.1365-3040.2007.01757.x

Flexas J, Barbour MM, Brendel O et al (2012) Mesophyll diffusion conductance to CO2: an unappreciated central player in photosynthesis. Plant Sci 193–194:70–84. https://doi.org/10.1016/j.plantsci.2012.05.009

Fu C, Li M, Zhang Y et al (2015) Morphology, photosynthesis, and internal structure alterations in field apple leaves under hidden and acute zinc deficiency. Sci Hortic (Amsterdam) 193:47–54. https://doi.org/10.1016/j.scienta.2015.06.016

Gallego SM, Pena LB, Barcia RA et al (2012) Unravelling cadmium toxicity and tolerance in plants: insight into regulatory mechanisms. Environ Exp Bot 83:33–46. https://doi.org/10.1016/j.envexpbot.2012.04.006

Giannopolitis CN, Ries SK (1977) Superoxide dismutases: I. occurrence in higher plants. Plant Physiol 59:309–314

Gong M, Li Y-J, Chen S-Z (1998) Abscisic acid-induced thermotolerance in maize seedlings is mediated by calcium and associated with antioxidant systems. J Plant Physiol 153:488–496. https://doi.org/10.1016/S0176-1617(98)80179-X

Hafeez B, Khanif YM, Saleem M (2013) Role of zinc in plant nutrition- a review. Am J Exp Agric 3:374–391. https://doi.org/10.9734/AJEA/2013/2746

Hajiboland R, Amirazad F (2010) Growth, photosynthesis and antioxidant defense system in Zn-deficient red cabbage plants. Plant Soil Environ 56:209–217

Hameed M, Ashraf M, Naz N (2009) Anatomical adaptations to salinity in cogon grass [Imperata cylindrica (L.) Raeuschel] from the salt range, Pakistan. Plant Soil 322:229–238. https://doi.org/10.1007/s11104-009-9911-6

Hänsch R, Mendel RR (2009) Physiological functions of mineral micronutrients (cu, Zn, Mn, Fe, Ni, Mo, B, cl). Curr Opin Plant Biol 12:259–266. https://doi.org/10.1016/j.pbi.2009.05.006

Hasan SA, Hayat S, Ahmad A (2011) Brassinosteroids protect photosynthetic machinery against the cadmium induced oxidative stress in two tomato cultivars. Chemosphere 84:1446–1451. https://doi.org/10.1016/j.chemosphere.2011.04.047

Havir EA, McHale NA (1987) Biochemical and developmental characterization of multiple forms of catalase in tobacco leaves. Plant Physiol 84:450–455. https://doi.org/10.1104/pp.84.2.450

Hayat S, Yadav S, Wani AS et al (2011) Comparative effect of 28-homobrassinolide and 24-epibrassinolide on the growth, carbonic anhydrase activity and photosynthetic efficiency of Lycopersicon esculentum. Photosynthetica 49:397–404. https://doi.org/10.1007/s11099-011-0051-x

Hayat S, Alyemeni MN, Hasan SA (2012) Foliar spray of brassinosteroid enhances yield and quality of Solanum lycopersicum under cadmium stress. Saudi J Biol Sci 19:325–335

He J, Wang Y, Ding H, Ge C (2016) Epibrassinolide confers zinc stress tolerance by regulating antioxidant enzyme responses, osmolytes, and hormonal balance in Solanum melongena seedlings. Brazilian J Bot 39:295–303. https://doi.org/10.1007/s40415-015-0210-6

Hidoto L, Worku W, Mohammed H, Taran B (2017) Effects of zinc application strategy on zinc content and productivity of chickpea grown under zinc deficient soils. J Soil Sci Plant Nutr 17:112–126. https://doi.org/10.4067/S0718-95162017005000009

Hoagland DR, Arnon DI (1950) The water-culture method for growing plants without soil, 2nd edn. California Agricultural Experiment Station, Riverside

Jain R, Srivastava S, Solomon S et al (2010) Impact of excess zinc on growth parameters, cell division, nutrient accumulation, photosynthetic pigments and oxidative stress of sugarcane (Saccharum spp.). Acta Physiol Plant 32:979–986. https://doi.org/10.1007/s11738-010-0487-9

Javelle M, Vernoud V, Rogowsky PM, Ingram GC (2011) Epidermis: the formation and functions of a fundamental plant tissue. New Phytol 189:17–39. https://doi.org/10.1111/j.1469-8137.2010.03514.x

Jia L, Liu Z, Chen W et al (2015) Hormesis effects induced by cadmium on growth and photosynthetic performance in a hyperaccumulator, Lonicera japonica Thunb. J Plant Growth Regul 34:13–21. https://doi.org/10.1007/s00344-014-9433-1

Jiang YP, Cheng F, Zhou YH et al (2012) Interactive effects of CO2 enrichment and brassinosteroid on CO2 assimilation and photosynthetic electron transport in Cucumis sativus. Environ Exp Bot 75: 98–106. https://doi.org/10.1016/j.envexpbot.2011.09.002

Karlidag H, Yildirim E, Turan M (2011) Role of 24-epibrassinolide in mitigating the adverse effects of salt stress on stomatal conductance, membrane permeability, and leaf water content, ionic composition in salt stressed strawberry (Fragaria×ananassa). Sci Hortic (Amsterdam) 130:133–140. https://doi.org/10.1016/j.scienta.2011.06.025

Khodamoradi K, Khoshgoftarmanesh AH, Dalir N et al (2015) How do glycine and histidine in nutrient solution affect zinc uptake and root-to-shoot translocation by wheat and triticale? Crop Pasture Sci 66: 1105. https://doi.org/10.1071/CP14227

Kim T, Wetzstein HY (2003) Cytological and ultrastructural evaluations of zinc deficiency in leaves. J Am Soc Hortic Sci 128:171–175. https://doi.org/10.21273/JASHS.128.2.0171

Kim T-W, Michniewicz M, Bergmann DC, Wang Z-Y (2012) Brassinosteroid regulates stomatal development by GSK3- mediated inhibition of a MAPK pathway. Nature 482:419–422. https://doi.org/10.1038/nature10794.Brassinosteroid

Kosesakal T, Unal M (2009) Role of zinc deficiency in photosynthentic pigments and peroxidase activity of tomato seedlings. Istanbul Univ Fac Sci J Biol 68:113–120

Kozhevnikova AD, Seregin IV, Erlikh NT et al (2014) Histidine-mediated xylem loading of zinc is a species-wide character in Noccaea caerulescens. New Phytol 203:508–519. https://doi.org/10.1111/nph.12816

Kumari A, Sheokand S, Swaraj K (2010) Nitric oxide induced alleviation of toxic effects of short term and long term cd stress on growth, oxidative metabolism and cd accumulation in chickpea. Braz J Plant Physiol 22:271–284. https://doi.org/10.1590/S1677-04202010000400007

Kunert KJ, Vorster BJ, Fenta BA et al (2016) Drought stress responses in soybean roots and nodules. Front Plant Sci 7:1–7. https://doi.org/10.3389/fpls.2016.01015

Li M, Ahammed GJ, Li C et al (2016a) Brassinosteroid ameliorates zinc oxide nanoparticles-induced oxidative stress by improving antioxidant potential and redox homeostasis in tomato seedling. Front Plant Sci 7:1–13. https://doi.org/10.3389/fpls.2016.00615

Li X, Guo X, Zhou Y et al (2016b) Overexpression of a brassinosteroid biosynthetic gene dwarf enhances photosynthetic capacity through activation of Calvin cycle enzymes in tomato. BMC Plant Biol 16: 33–12. https://doi.org/10.1186/s12870-016-0715-6

Lichtenthaler HK, Buschmann C (2001) Chlorophylls and carotenoids: measurement and characterization by UV-VIS spectroscopy. In: Current protocols in food analytical chemistry. Wiley, Hoboken, pp 431–438

Lima JV, Lobato AKS (2017) Brassinosteroids improve photosystem II efficiency, gas exchange, antioxidant enzymes and growth of cowpea plants exposed to water deficit. Physiol Mol Biol Plants 23:59–72. https://doi.org/10.1007/s12298-016-0410-y

Lima MDR, Barros Junior UO, Batista BL, Lobato AKS (2018) Brassinosteroids mitigate iron deficiency improving nutritional status and photochemical efficiency in Eucalyptus urophylla plants. Trees 32:1681–1694. https://doi.org/10.1007/s00468-018-1743-7

Lynch JP (2007) Rhizoeconomics: the roots of shoot growth limitations. Hortscience 42:1107–1109

Ma JF, Mitani N, Nagao S et al (2004) Characterization of the silicon uptake system and molecular mapping of the silicon transporter gene in rice. Plant Physiol 136:3284–3289. https://doi.org/10.1104/pp.104.047365

Maia CF, Silva BRS, Lobato AKS (2018) Brassinosteroids positively modulate growth: physiological, biochemical and anatomical evidence using two tomato genotypes contrasting to dwarfism. J Plant Growth Regul 37:1–14. https://doi.org/10.1007/s00344-018-9802-2

Manaf A, Raheel M, Sher A et al (2019) Interactive effect of zinc fertilization and cultivar on yield and nutritional attributes of canola (Brassica napus L.). J Soil Sci Plant Nutr 19:in press. https://doi.org/10.1007/s42729-019-00067-2

Marques MC, Nascimento CWA, da Silva AJ, da Silva G-NA (2017) Tolerance of an energy crop (Jatropha curcas L.) to zinc and lead assessed by chlorophyll fluorescence and enzyme activity. South African J Bot 112:275–282. https://doi.org/10.1016/j.sajb.2017.06.009

Martins JPR, Verdoodt V, Pasqual M, De Proft M (2015) Impacts of photoautotrophic and photomixotrophic conditions on in vitro propagated Billbergia zebrina (Bromeliaceae). Plant Cell Tissue Organ Cult 123:121–132. https://doi.org/10.1007/s11240-015-0820-5

Mateos-Naranjo E, Pérez-Romero JA, Redondo-Gómez S et al (2018) Salinity alleviates zinc toxicity in the saltmarsh zinc-accumulator Juncus acutus. Ecotoxicol Environ Saf 163:478–485. https://doi.org/10.1016/j.ecoenv.2018.07.092

Mattiello EM, Ruiz HA, Neves JCL et al (2015) Zinc deficiency affects physiological and anatomical characteristics in maize leaves. J Plant Physiol 183:138–143. https://doi.org/10.1016/j.jplph.2015.05.014

Meyer CJ, Peterson CA, Steudle E (2011) Permeability of Iris germanica's multiseriate exodermis to water, NaCl, and ethanol. J Exp Bot 62:1911–1926. https://doi.org/10.1093/jxb/erq380

Müssig C (2005) Brassinosteroid-promoted growth. Plant Biol 7:110–117. https://doi.org/10.1055/s-2005-837493

Nagajyoti PC, Lee KD, Sreekanth TVM (2010) Heavy metals, occurrence and toxicity for plants: a review. Environ Chem Lett 8:199–216. https://doi.org/10.1007/s10311-010-0297-8

Nakano Y, Asada K (1981) Hydrogen peroxide is scavenged by ascorbate-specific peroxidase in spinach chloroplasts. Plant Cell Physiol 22:867–880

Nisa Z, Chen C, Yu Y et al (2016) Constitutive overexpression of myo-inositol-1-phosphate synthase gene (GsMIPS2) from Glycine soja confers enhanced salt tolerance at various growth stages in Arabidopsis. J Northeast Agric Univ (English Ed 23:28–44. https://doi.org/10.1016/S1006-8104(16)30045-9

Noulas C, Tziouvalekas M, Karyotis T (2018) Zinc in soils, water and food crops. J Trace Elem Med Biol 49:252–260. https://doi.org/10.1016/j.jtemb.2018.02.009

O'Brien TP, Feder N, McCully ME (1964) Polychromatic staining of plant cell walls by toluidine blue O. Protoplasma 59:368–373

Ogweno JO, Song XS, Shi K et al (2008) Brassinosteroids alleviate heat-induced inhibition of photosynthesis by increasing carboxylation efficiency and enhancing antioxidant systems in Lycopersicon esculentum. J Plant Growth Regul 27:49–57. https://doi.org/10.1007/s00344-007-9030-7

Oh K, Yamada K, Asami T, Yoshizawa Y (2012) Synthesis of novel brassinosteroid biosynthesis inhibitors based on the ketoconazole scaffold. Bioorg Med Chem Lett 22:1625–1628. https://doi.org/10.1016/j.bmcl.2011.12.120

Oliveira VP, Lima MDR, Silva BRS et al (2019) Brassinosteroids confer tolerance to salt stress in Eucalyptus urophylla plants enhancing homeostasis, antioxidant metabolism and leaf anatomy. J Plant Growth Regul 19 In press. https://doi.org/10.1007/s00344-018-9870-3

Ouni Y, Mateos-Naranjo E, Abdelly C, Lakhdar A (2016) Interactive effect of salinity and zinc stress on growth and photosynthetic responses of the perennial grass, Polypogon monspeliensis. Ecol Eng 95:171–179. https://doi.org/10.1016/j.ecoleng.2016.06.067

Palmer CM, Guerinot ML (2009) Facing the challenges of cu, Fe and Zn homeostasis in plants. Nat Chem Biol 5:333–340. https://doi.org/10.1038/nchembio.166

Pascual MB, Echevarria V, Gonzalo MJ, Hernández-Apaolaza L (2016) Silicon addition to soybean (Glycine max L.) plants alleviate zinc deficiency. Plant Physiol Biochem 108:132–138. https://doi.org/10.1016/j.plaphy.2016.07.008

Pereira YC, Rodrigues WS, Lima EJA et al (2019) Brassinosteroids increase electron transport and photosynthesis in soybean plants under water deficit. Photosynthetica 57:1–11

Postma JA, Lynch JP (2011) Root cortical aerenchyma enhances the growth of maize on soils with suboptimal availability of nitrogen, phosphorus, and potassium. Plant Physiol 156:1190–1201. https://doi.org/10.1104/pp.111.175489

Rajewska I, Talarek M, Bajguz A (2016) Brassinosteroids and response of plants to heavy metals action. Front Plant Sci 7:1–5. https://doi.org/10.3389/fpls.2016.00629

Ramakrishna B, Rao SSR (2012) 24-Epibrassinolide alleviated zinc-induced oxidative stress in radish (Raphanus sativus L.) seedlings by enhancing antioxidative system. Plant Growth Regul 68:249–259. https://doi.org/10.1007/s10725-012-9713-3

Ramakrishna B, Rao SSR (2015) Foliar application of brassinosteroids alleviates adverse effects of zinc toxicity in radish (Raphanus sativus L.) plants. Protoplasma 252:665–677. https://doi.org/10.1007/s00709-014-0714-0

Reis AR, Lisboa LAM, Reis HPG et al (2018) Depicting the physiological and ultrastructural responses of soybean plants to Al stress conditions. Plant Physiol Biochem 130:377–390. https://doi.org/10.1016/j.plaphy.2018.07.028

Rezapour S, Golmohammad H, Ramezanpour H (2014) Impact of parent rock and topography aspect on the distribution of soil trace metals in natural ecosystems. Int J Environ Sci Technol 11:2075–2086. https://doi.org/10.1007/s13762-014-0663-3

Sadeghzadeh B (2013) A review of zinc nutrition and plant breeding. J Soil Sci Plant Nutr 13:905–927. https://doi.org/10.4067/S0718-95162013005000072

Saengwilai P, Nord EA, Chimungu JG et al (2014) Root cortical aerenchyma enhances nitrogen acquisition from low-nitrogen soils in maize. Plant Physiol 166:726–735. https://doi.org/10.1104/pp.114.241711

Sagardoy R, Morales F, López-Millán AF et al (2009) Effects of zinc toxicity on sugar beet (Beta vulgaris L.) plants grown in hydroponics. Plant Biol 11:339–350. https://doi.org/10.1111/j.1438-8677.2008.00153.x

Salama ZA, El-Fouly MM, Lazova G, Popova LP (2006) Carboxylating enzymes and carbonic anhydrase functions were suppressed by zinc deficiency in maize and chickpea plants. Acta Physiol Plant 28:445–451. https://doi.org/10.1007/BF02706627

Samreen T, Humaira, Shah HU et al (2017) Zinc effect on growth rate, chlorophyll, protein and mineral contents of hydroponically grown mungbeans plant (Vigna radiata). Arab J Chem 10:S1802–S1807. https://doi.org/10.1016/j.arabjc.2013.07.005

Santos EF, Santini JMK, Paixão AP et al (2017) Physiological highlights of manganese toxicity symptoms in soybean plants: Mn toxicity responses. Plant Physiol Biochem 113:6–19. https://doi.org/10.1016/j.plaphy.2017.01.022

Santos LR, Batista BL, Lobato AKS (2018) Brassinosteroids mitigate cadmium toxicity in cowpea plants. Photosynthetica 56:591–605. https://doi.org/10.1007/s11099-017-0700-9

Schneider HM, Wojciechowski T, Postma JA et al (2017) Root cortical senescence decreases root respiration, nutrient content and radial water and nutrient transport in barley. Plant Cell Environ 40:1392–1408. https://doi.org/10.1111/pce.12933

Segatto FB, Bisognin DA, Benedetti M et al (2004) A technique for the anatomical study of potato leaf epidermis. Ciência Rural 34:1597–1601. https://doi.org/10.1590/S0103-84782004000500042

Shahbaz M, Ashraf M, Athar H-U-R (2008) Does exogenous application of 24-epibrassinolide ameliorate salt induced growth inhibition in wheat (Triticum aestivum L.)? Plant Growth Regul 55:51–64. https://doi.org/10.1007/s10725-008-9262-y

Shu S, Tang Y, Yuan Y et al (2016) The role of 24-epibrassinolide in the regulation of photosynthetic characteristics and nitrogen metabolism of tomato seedlings under a combined low temperature and weak light stress. Plant Physiol Biochem 107:344–353. https://doi.org/10.1016/j.plaphy.2016.06.021

Shu K, Qi Y, Chen F et al (2017) Salt stress represses soybean seed germination by negatively regulating GA biosynthesis while positively mediating ABA biosynthesis. Front Plant Sci 8:1–12. https://doi.org/10.3389/fpls.2017.01372

Siddiqui H, Ahmed KBM, Hayat S (2018) Comparative effect of 28-homobrassinolide and 24-epibrassinolide on the performance of different components influencing the photosynthetic machinery in Brassica juncea L. Plant Physiol Biochem 129:198–212. https://doi.org/10.1016/j.plaphy.2018.05.027

Silva EN, Ribeiro RV, Ferreira-Silva SL et al (2012) Coordinate changes in photosynthesis, sugar accumulation and antioxidative enzymes improve the performance of Jatropha curcas plants under drought stress. Biomass Bioenergy 45:270–279. https://doi.org/10.1016/j.biombioe.2012.06.009

Sinclair SA, Krämer U (2012) The zinc homeostasis network of land plants. Biochim Biophys Acta, Mol Cell Res 1823:1553–1567. https://doi.org/10.1016/j.bbamcr.2012.05.016

Singh HP, Batish DR, Kohli RK, Arora K (2007) Arsenic-induced root growth inhibition in mung bean (Phaseolus aureus Roxb.) is due to oxidative stress resulting from enhanced lipid peroxidation. Plant Growth Regul 53:65–73. https://doi.org/10.1007/s10725-007-9205-z

Singh P, Kumar R, Sabapathy SN, Bawa AS (2008) Functional and edible uses of soy protein products. Compr Rev Food Sci Food Saf 7:14–28. https://doi.org/10.1111/j.1541-4337.2007.00025.x

Singh P, Shukla AK, Behera SK, Tiwari PK (2019) Zinc application enhances superoxide dismutase and carbonic anhydrase activities in zinc-efficient and zinc-inefficient wheat genotypes. J soil Sci plant Nutr 19:in press. https://doi.org/10.1007/s42729-019-00038-7

Steel RG, Torrie JH, Dickey DA (2006) Principles and procedures of statistics: a biometrical approach, 3rd edn. Academic Internet Publishers, Moorpark

Subba P, Mukhopadhyay M, Mahato SK, Bhutia KD, Mondal TK, Ghosh SK (2014) Zinc stress induces physiological, ultra-structural and biochemical changes in mandarin orange (Citrus reticulata Blanco) seedlings. Physiol Mol Biol Plants 20:461–473. https://doi.org/10.1007/s12298-014-0254-2

Suhr N, Schoenberg R, Chew D et al (2018) Elemental and isotopic behaviour of Zn in Deccan basalt weathering profiles: chemical weathering from bedrock to laterite and links to Zn deficiency in tropical soils. Sci Total Environ 619–620:1451–1463. https://doi.org/10.1016/j.scitotenv.2017.11.112

Swamy KN, Rao SSR (2009) Effect of 24-epibrassinolide on growth, photosynthesis, and essential oil content of Pelargonium graveolens (L.) Herit. Russ J Plant Physiol 56:616–620. https://doi.org/10.1134/S1021443709050057

Tadayon MS, Moafpourian G (2019) Effects of exogenous epibrassinolid, zinc and boron foliar nutrition on fruit development and ripening of grape (Vitis vinifera L. clv. "Khalili"). Sci Hortic (Amsterdam) 244:94–101. https://doi.org/10.1016/j.scienta.2018.09.036

Talukdar D (2013) Arsenic-induced oxidative stress in the common bean legume, Phaseolus vulgaris L. seedlings and its amelioration by exogenous nitric oxide. Physiol Mol Biol Plants 19:69–79. https://doi.org/10.1007/s12298-012-0140-8

Tanaka N, Kato M, Tomioka R et al (2014) Characteristics of a root hairless line of Arabidopsis thaliana under physiological stresses. J Exp Bot 65:1497–1512. https://doi.org/10.1093/jxb/eru014

Tavallali V, Rahemi M, Maftoun M et al (2009) Zinc influence and salt stress on photosynthesis, water relations, and carbonic anhydrase activity in pistachio. Sci Hortic (Amsterdam) 123:272–279. https://doi.org/10.1016/j.scienta.2009.09.006

Thussagunpanit J, Jutamanee K, Sonjaroon W et al (2015) Effects of brassinosteroid and brassinosteroid mimic on photosynthetic efficiency and rice yield under heat stress. Photosynthetica 53:312–320. https://doi.org/10.1007/s11099-015-0106-5

Tripathi DK, Singh S, Singh S, Mishra S, Chauhan DK, Dubey NK (2015) Micronutrients and their diverse role in agricultural crops: advances and future prospective. Acta Physiol Plant 37:14–14. https://doi.org/10.1007/s11738-015-1870-3

Velikova V, Yordanov I, Edreva A (2000) Oxidative stress and some antioxidant systems in acid rain-treated bean plants protective role of exogenous polyamines. Plant Sci 151:59–66. https://doi.org/10.1016/S0168-9452(99)00197-1

Wang X, Zhao X, Jiang C et al (2015) Effects of potassium deficiency on photosynthesis and photoprotection mechanisms in soybean (Glycine max (L.) Merr.). J Integr Agric 14:856–863. https://doi.org/10.1016/S2095-3119(14)60848-0

Wei Z, Li J (2016) Brassinosteroids regulate root growth, development, and Symbiosis. Mol Plant 9:86–100. https://doi.org/10.1016/j.molp.2015.12.003

Wijewardana C, Reddy KR, Bellaloui N (2019) Soybean seed physiology, quality, and chemical composition under soil moisture stress. Food Chem 278:92–100. https://doi.org/10.1016/j.foodchem.2018.11.035

Wu Q-S, Xia R-X, Zou Y-N (2006) Reactive oxygen metabolism in mycorrhizal and non-mycorrhizal citrus (Poncirus trifoliata) seedlings subjected to water stress. J Plant Physiol 163:1101–1110. https://doi.org/10.1016/j.jplph.2005.09.001

Xia X-J, Huang L-F, Zhou Y-H et al (2009) Brassinosteroids promote photosynthesis and growth by enhancing activation of Rubisco and expression of photosynthetic genes in Cucumis sativus. Planta 230:1185–1196. https://doi.org/10.1007/s00425-009-1016-1

Yu JQ, Huang L-F, Hu WH et al (2004) A role for brassinosteroids in the regulation of photosynthesis in Cucumis sativus. J Exp Bot 55:1135–1143. https://doi.org/10.1093/jxb/erh124

Yuan L, Zhu S, Shu S et al (2015) Regulation of 2,4-epibrassinolide on mineral nutrient uptake and ion distribution in Ca(NO3)2 stressed cucumber plants. J Plant Physiol 188:29–36. https://doi.org/10.1016/j.jplph.2015.06.010

Zhang YP, Zhu XH, Ding HD et al (2013) Foliar application of 24-epibrassinolide alleviates high-temperature-induced inhibition of photosynthesis in seedlings of two melon cultivars. Photosynthetica 51:341–349. https://doi.org/10.1007/s11099-013-0031-4

Zhang Y, Xu S, Yang S, Chen Y (2015) Salicylic acid alleviates cadmium-induced inhibition of growth and photosynthesis through upregulating antioxidant defense system in two melon cultivars (Cucumis melo L.). Protoplasma 252:911–924. https://doi.org/10.1007/s00709-014-0732-y

Zhiponova MK, Vanhoutte I, Boudolf V et al (2013) Brassinosteroid production and signaling differentially control cell division and expansion in the leaf. New Phytol 197:490–502. https://doi.org/10.1111/nph.12036

CAPITULO II. BRASSINOSTEROIDS-MEDIATED AMELIORATION OF IRON DEFICIENCY IN SOYBEAN PLANTS: BENEFICIAL EFFECTS ON THE NUTRITIONAL STATUS, PHOTOSYNTHETIC PIGMENTS AND CHLOROPHYLL FLUORESCENCE. Página 39 à 59.

Journal of Plant Growth Regulation
https://doi.org/10.1007/s00344-020-10232-y

Brassinosteroids-Mediated Amelioration of Iron Deficiency in Soybean Plants: Beneficial Effects on the Nutritional Status, Photosynthetic Pigments and Chlorophyll Fluorescence

Lucilene Rodrigues dos Santos[1] · Lucélia de Sousa Paula[1] · Ynglety Cascaes Pereira[1] · Breno Ricardo Serrão da Silva[1] · Bruno Lemos Batista[2] · Abdulaziz Abdullah Alsahli[3] · Allan Klynger da Silva Lobato[1]

Received: 19 June 2020 / Accepted: 17 September 2020

Abstract
Iron (Fe) is essential for chlorophyll biosynthesis and functions in chloroplasts. Fe deficiency provokes negative effects on photochemical efficiency and electron transport. 24-Epibrassinolide (EBR) is a natural molecule with potential advantages, including a natural origin, biodegradability and high plant steroid bioactivity, improving metabolism and inducing tolerance during stress. Present study was aimed to investigate whether pre-treatment with EBR can trigger protective roles in soybean plants cultivated under the conditions of Fe deficiency and to evaluate the responses linked to the nutritional status, photosynthetic pigments and chlorophyll fluorescence. The study was carried out using a completely randomized design with four treatments (0 nM EBR + 250 µM Fe, 0 nM EBR + 2.5 µM Fe, 100 nM EBR + 250 µM Fe and 100 nM EBR + 2.5 µM Fe). Results revealed that the exogenous EBR minimized the damage caused by Fe deficiency. This steroid maximized the Fe content in the leaf, stem and root, as well as improved the nutrient content and metal homeostasis, as confirmed by the increased detection of Fe^{2+}/Mg^{2+}, Fe^{2+}/Mn^{2+} and Fe^{2+}/Cu^{2+} ratios in plants under Fe deficiency. Additionally, plants under Fe deficiency and sprayed with EBR had improvements on chloroplastic pigments, with significant increases in chlorophyll *a* (14%), chlorophyll *b* (23%), total chlorophyll (15%) and carotenoids (28%). Steroid also increased the photochemical efficiency, positively regulating electron transport and reducing the negative impacts associated with photoinhibition in photosystem II. Therefore, pre-treatment with EBR improved the nutrient contents and physiological performance of soybean plants under the conditions of Fe limitation.

Keywords Chlorophyll · Electron transport rate · Fe supply · Gas exchange · Ionic homeostasis · 24-Epibrassinolide

Abbreviations

APX	Ascorbate peroxidase
BRs	Brassinosteroids
CA	Carbonic anhydrase
CAR	Carotenoids
CAT	Catalase
Chl *a*	Chlorophyll a
Chl *b*	Chlorophyll b
C_i	Intercellular CO_2 concentration
CO_2	Carbon dioxide
Cu	Copper
E	Transpiration rate
EBR	24-Epibrassinolide
EDS	Equatorial diameter of the stomata
EL	Electrolyte leakage
ETAb	Epidermis thickness from abaxial leaf side
ETAd	Epidermis thickness from adaxial leaf side
ETR	Electron transport rate
ETR/P_N	Ratio between the apparent electron transport rate and net photosynthetic rate
EXC	Relative energy excess at the PSII level
F_0	Minimal fluorescence yield of the dark-adapted state
Fe	Iron

✉ Allan Klynger da Silva Lobato
allanllobato@yahoo.com.br

[1] Núcleo de Pesquisa Vegetal Básica e Aplicada, Universidade Federal Rural da Amazônia, Rodovia PA 256, Paragominas, PA, Brazil

[2] Centro de Ciências Naturais e Humanas, Universidade Federal do ABC, Santo André, SP, Brazil

[3] Department of Botany and Microbiology, College of Science, King Saud University, Riyadh 11451, Saudi Arabia

Published online: 29 September 2020

F_m	Maximal fluorescence yield of the dark-adapted state
F_v	Variable fluorescence
F_v/F_m	Maximal quantum yield of PSII photochemistry
g_s	Stomatal conductance
H_2O_2	Hydrogen peroxide
K	Potassium
LDM	Leaf dry matter
MDA	Malondialdehyde
Mg	Magnesium
Mn	Manganese
Mo	Molybdenum
NPQ	Nonphotochemical quenching
O_2^-	Superoxide
P	Phosphorus
PDS	Polar diameter of the stomata
P_N	Net photosynthetic rate
P_N/C_i	Instantaneous carboxylation efficiency
POX	Peroxidase
PPT	Palisade parenchyma thickness
PSII	Photosystem II
q_P	Photochemical quenching
RCD	Root cortex diameter
RDM	Root dry matter
RMD	Root metaxylem diameter
RDT	Root endodermis thickness
RET	Root epidermis thickness
ROS	Reactive oxygen species
RuBisCO	Ribulose-1,5-bisphosphate carboxylase/oxygenase
SD	Stomatal density
SDM	Stem dry matter
SF	Stomatal functionality
SI	Stomatal index
SOD	Superoxide dismutase
SPT	Spongy parenchyma thickness
TDM	Total dry matter
Total Chl	Total Chlorophyll
VCD	Vascular cylinder diameter
WUE	Water-use efficiency
Zn	Zinc
Φ_{PSII}	Effective quantum yield of PSII photochemistry

Introduction

Soybean (*Glycine max* L.) is one of the most important leguminous crops. In general, grains are composed by high contents of proteins (42%), oil (22%) and iron (Singh et al. 2008; Anwar et al. 2016; Aksoy et al. 2017). Grain global production had reached 338 million tons in the 2017/2018 harvest, representing the second largest production recorded and driven by the United States and Brazil (Ekpei et al. 2018). However, the yield of this leguminous crop has been primarily affected by nutrient deficiency (Santos et al. 2015; Keino et al. 2015; Bai et al. 2018) and adequate mineral nutrition plays a vital role in the growth and development of this agricultural crop.

Iron (Fe) is the fourth most abundant element found in the Earth's crust and the second-most abundant metal in soil (López-Millán et al. 2013). Despite the high Fe content in soil, Fe is mainly found as oxyhydroxide polymers, such as $Fe(OH)^{2+}$, $Fe(OH)_3$ e $Fe(OH)_4^-$, which have low solubility, limiting the absorption and Fe supply to plants (Silveira et al. 2007; Rout and Sahoo 2015; Tsai and Schmidt 2017). This problem is critical, especially in areas with limestone soils under high pH, where approximately 30% of the world's arable land presents this restriction. Therefore, Fe deficiency has been one of the most widespread nutritional deficiencies among crops (Jin et al. 2007; Morrissey and Guerinot 2009; Aksoy et al. 2017).

Fe is the micronutrient most absorbed by higher plants (Baker et al. 2003). This metal is involved in the synthesis of chlorophylls and is essential for the maintenance of the structure and function of chloroplasts (Rout and Sahoo 2015; Chen et al. 2015), catalysing enzymatic reactions linked to respiration, synthesis of DNA, hormone synthesis and redox metabolism (Barberon et al. 2014; Xiong et al. 2014). However, when this micronutrient is not available to the plants, frequent detection of yellowing of the upper leaves, chlorosis in the leaf nervure and a lower growth rate occurs (Jeong and Connolly 2009). In addition, Fe deficiency causes negative effects on chloroplast constitutive proteins, such as cytochrome *b6f* complex (Cyt b6f) and ferredoxin (Fd), reducing the efficiencies of photosystem II and electron transport (López-Millán et al. 2013; Roncel et al. 2016).

24-Epibrassinolide (EBR) is the most bioactive form of brassinosteroids (BRs) (Bishop and Koncz 2002), which are classified as polyhydroxylated steroids (Clouse 2002), mainly located in the meristem and found under low concentrations in plant tissues (Janeczko et al. 2016). Additionally, these steroids are essentials for division and cell elongation (Zhiponova et al. 2013), increases on antioxidant enzyme activities (Ahanger et al. 2018), regulation and allocation of carbohydrates (Pociecha et al. 2016), improvement in gas exchange and the efficiency of photosystem II (Wu et al. 2014). EBR also promotes beneficial effects on plant tolerance to different abiotic stresses, such as water deficit (Lima and Lobato 2017; Kaya et al. 2019), salinity (Ahmad et al. 2018a; Alam et al. 2019; Ahanger et al. 2020), extreme temperature (Fariduddin et al. 2011), pesticide stress (Sharma et al. 2016), heavy metal (Kohli et al. 2018a; Ahmad et al. 2018b) and nutritional deficiency (Borges et al. 2019).

Our hypothesis focused on metabolic problems caused by Fe deficiency, declining nutrient contents (Lima et al. 2018), chloroplast pigments (Roncel et al. 2016) and performance of photosystem II (Osório et al. 2014). However, considering the available literature, EBR is associated with root anatomy (Ribeiro et al. 2019), ionic homeostasis (Oliveira et al. 2019) and the electron transport rate (Pereira et al. 2019). Based on this overview, we aimed to investigate whether pretreatment with EBR can trigger protective roles in *Glycine max* plants cultivated under the conditions of Fe deficiency, evaluating the responses linked to the nutritional status, photosynthetic pigments and chlorophyll fluorescence.

Materials and Methods

Location and Environmental Conditions

The study was performed at the Campus of Paragominas of the Universidade Federal Rural da Amazônia, Paragominas, Brazil (2° 55′ S, 47° 34′ W). The experiments were conducted in a temperature- and humidity-controlled greenhouse. The minimum, maximum, and median temperatures were 25 °C, 35 °C and 26.2 °C, respectively. The relative humidity during the experimental period varied between 60 and 80%.

Plants, Containers and Acclimation

Glycine max (L.) Merr. var. M8644RR Monsoy™ seeds were germinated and grown in 1.2-L pots (0.15 m in height and 0.10 m in diameter) filled with a mixed substrate of sand and vermiculite at a ratio of 3:1. Plants were cultivated under semi-hydroponic conditions with water aeration at 500 mL of distilled water for 8 days. A modified Hoagland and Arnon (1950) solution was used for supply nutrients, with the ionic strength beginning at 50% (5th day) and later modified to 100% after 2 days (7th day). After this period, the nutritive solution remained at the total ionic strength.

Experimental Design

Experiment was performed using a completely randomized design with four treatments (0 nM EBR + 250 µM Fe, 0 nM EBR + 2.5 µM Fe, 100 nM EBR + 250 µM Fe and 100 nM EBR + 2.5 µM Fe, described as – EBR/Fe adequate (Control), – EBR/Fe deficiency, + EBR/Fe adequate and + EBR/Fe deficiency, respectively. With five replicates for each one of four treatments, 20 experimental units were used in the experiment, being one plant in each experimental unit. Fe concentrations were chosen based in research of Lima et al. (2018) and preliminary assays. While EBR treatments were defined using the recommendation of Pereira et al. (2019).

24-Epibrassinolide (EBR) Preparation and Application

Ten-day-old seedlings were sprayed with 24-epibrassinolide (EBR) or Milli-Q water (containing a proportion of ethanol that was equal to that used to prepare the EBR solution) at 5-days intervals until day 25. The 0- and 100-nM EBR (Sigma-Aldrich, USA) solutions were prepared by dissolving the solute in ethanol 100%, followed by dilution with Milli-Q water [ethanol:water (v/v) = 1:10,000] (Ahammed et al. 2013).

Cultivation of Plants and Fe Treatment

Plants received macro- and micronutrients using nutritive solution described by Pereira et al. (2019), with the Fe concentrations adjusted to each treatment. For Fe treatments, $FeCl_2 \cdot 4H_2O$ + EDTA was used at the concentrations of 2.5 µM (Fe deficiency) and 250 µM (Fe adequate) applied over 16 days (days 10–26 after the start of the experiment). On day 26 of the experiment, physiological and morphological parameters were measured for all plants, and leaf tissues were harvested for biochemical, anatomical and nutritional analyses.

Determining of Fe and Nutrients

Milled samples (100 mg) of root, stem and leaf tissues were pre-digested using conical tubes (50 mL) with 2 ml of sub boiled nitric acid (HNO_3). Subsequently, 8 ml of a solution containing 4 ml of hydrogen peroxide (H_2O_2) (30% v/v) and 4 ml of ultra-pure water were added, and transferred to a Teflon digestion vessel in agreement with Paniz et al. (2018). The determination of iron (Fe), phosphorus (P), potassium (K), magnesium (Mg), manganese (Mn), copper (Cu) and zinc (Zn) performed using an inductively coupled plasma mass spectrometer (model ICP-MS 7900; Agilent).

Measurement of Chlorophyll Fluorescence and Gas Exchange

Chlorophyll fluorescence was measured in fully expanded leaves under light using a modulated chlorophyll fluorometer (model OS5p; Opti-Sciences). Preliminary tests determined the location of the leaf, the part of the leaf and the time required to obtain the greatest F_v/F_m ratio; therefore, the acropetal third of the leaves, which was the middle third of the plant and adapted to the dark for 30 min, was used in the evaluation. The intensity and duration of the saturation light pulse were 7500 µmol m^{-2} s^{-1} and 0.7 s, respectively. Gas exchange was evaluated in all plants and measured in the expanded leaves in the middle region of the plant using an infrared gas analyser (model LCPro$^+$; ADC

BioScientific) in a chamber under constant CO_2, photosynthetically active radiation, air-flow rate and temperature conditions at 360 µmol mol^{-1} CO_2, 800 µmol photons m^{-2} s^{-1}, 300 µmol s^{-1} and 28 °C, respectively, between 10:00 and 12:00 h. The water-use efficiency (WUE) was estimated according to Ma et al. (2004), and the instantaneous carboxylation efficiency (P_N/C_i) was calculated using the formula that was described by Aragão et al. (2012).

Measurements of Anatomical Parameters

Samples were collected from the middle region of the leaf limb of fully expanded leaves of the third node and roots 5 cm from the root apex. Botanical material was fixed in FAA 70 for 24 h and then was dehydrated in a series of ethanol and butanol for inclusion in histological paraffin (Johansen 1940). Transverse sections were prepared in agreement with procedures described by Maia et al. (2018). For stomatal characterization, the epidermal impression method was used according to Segatto et al. (2004). The slides were observed and photomicrographed under an optical microscope (Motic BA 310; Motic Group Co. LTD.) coupled to a digital camera (Motic 2500; Motic Group Co., LTD.). The images were analysed using Moticplus 2.0 software. In both leaf faces, the stomatal density (SD) was calculated as the number of stomata per unit area and the stomatal functionality (SF) as the ratio PDS/EDS according to Castro et al. (2009). The stomatal index (SI%) was calculated as the percentage of stomata in relation to total epidermal cells by area.

Extraction of Antioxidant Enzymes, Superoxide and Soluble Proteins

Antioxidant enzymes (superoxide dismutase, catalase, ascorbate peroxidase and peroxidase), superoxide and soluble proteins were extracted from leaf tissues according to the method of (Badawi et al. 2004). The extraction mixture was prepared by homogenizing 500 mg of fresh plant material in 5 ml of extraction buffer, which consisted of 50 mM phosphate buffer (pH 7.6), 1.0 mM ascorbate and 1.0 mM EDTA. Samples were centrifuged at 14,000×*g* for 4 min at 3 °C, and the supernatant was collected. Quantification of the total soluble proteins was performed using the method described by (Bradford 1976). Absorbance was measured at 595 nm, using bovine albumin as a standard.

Superoxide Dismutase Assay

For superoxide dismutase (SOD) assay (EC 1.15.1.1), 2.8 ml of a reaction mixture containing 50 mM phosphate buffer (pH 7.6), 0.1 mM EDTA, 13 mM methionine (pH 7.6), 75 µM NBT, and 4 µM riboflavin was mixed with 0.2 ml of supernatant. The absorbance was then measured at 560 nm (Giannopolitis and Ries 1977).One SOD unit was defined as the amount of enzyme required to inhibit 50% of the NBT photoreduction. The SOD activity was expressed in unit mg^{-1} protein.

Catalase Assay

For Catalase (CAT) assay (EC 1.11.1.6), 0.2 ml of supernatant and 1.8 ml of a reaction mixture containing 50 mM phosphate buffer (pH 7.0) and 12.5 mM hydrogen peroxide were mixed, and the absorbance was measured at 240 nm (Havir and McHale 1987).The CAT activity was expressed in µmol H_2O_2 mg^{-1} protein min^{-1}.

Ascorbate Peroxidase Assay

For ascorbate peroxidase (APX) assay (EC 1.11.1.11), 1.8 ml of a reaction mixture containing 50 mM phosphate buffer (pH 7.0), 0.5 mM ascorbate, 0.1 mM EDTA, and 1.0 mM hydrogen peroxide was mixed with 0.2 ml of supernatant, and the absorbance was measured at 290 nm (Nakano and Asada 1981).The APX activity was expressed in µmol AsA mg^{-1} protein min^{-1}.

Peroxidase Assay

For peroxidase (POX) assay (EC 1.11.1.7), 1.78 ml of a reaction mixture containing 50 mM phosphate buffer (pH 7.0) and 0.05% guaiacol was mixed with 0.2 ml of supernatant, followed by addition of 20 µL of 10 mM hydrogen peroxide. The absorbance was then measured at 470 nm (Cakmak and Marschner 1992).The POX activity was expressed in µmol tetraguaiacol mg^{-1} protein min^{-1}.

Determination of Superoxide Concentration

For determination of superoxide (O_2^-), 1 ml of extract was incubated with 30 mM phosphate buffer [pH 7.6] and 0.51 mM hydroxylamine hydrochloride for 20 min at 25 °C. Then, 17 mM sulphanilamide and 7 mM α-naphthylamine were added to the incubation mixture for 20 min at 25 °C. After the reaction, ethyl ether was added in the identical volume and centrifuged at 3000×*g* for 5 min. The absorbance was measured at 530 nm (Elstner and Heupel 1976).

Extraction of Nonenzymatic Compounds

Nonenzymatic compounds (hydrogen peroxide and malondialdehyde) were extracted as described by Wu et al. (2006). Briefly, a mixture for extraction of H_2O_2 and MDA was prepared by homogenizing 500 mg of fresh leaf materials in 5 mL of 5% (w/v) trichloroacetic acid. Then, the samples

were centrifuged at 15,000×*g* for 15 min at 3 °C to collect the supernatant.

Determination of Hydrogen Peroxide Concentration

To measure hydrogen peroxide (H_2O_2), 200 µL of supernatant and 1800 µL of reaction mixture (2.5 mM potassium phosphate buffer [pH 7.0] and 500 mM potassium iodide) were mixed, and the absorbance was measured at 390 nm (Velikova et al. 2000).

Quantification of Malondialdehyde Concentration

Malondialdehyde (MDA) was determined by mixing 500 µL of supernatant with 1000 µL of the reaction mixture, which contained 0.5% (w/v) thiobarbituric acid (TBA) in 20% trichloroacetic acid. The mixture was incubated in boiling water at 95 °C for 20 min, with the reaction terminated by placing the reaction container in an ice bath. The samples were centrifuged at 10,000×*g* for 10 min, and the absorbance was measured at 532 nm. The nonspecific absorption at 600 nm was subtracted from the absorbance data. The MDA–TBA complex (red pigment) amount was calculated based on the method of Cakmak and Horst (1991), with minor modifications and using an extinction coefficient of 155 mM^{-1} cm^{-1}.

Determination of Electrolyte Leakage

Electrolyte leakage (EL) was measured according to the method of Gong et al. (1998) with minor modifications. Fresh tissue (200 mg) was cut into pieces 1 cm in length and placed in containers with 8 mL of distilled deionised water. The containers were incubated in a water bath at 40 °C for 30 min, and the initial electrical conductivity of the medium (EC_1) was measured. Then, the samples were boiled at 95 °C for 20 min to release the electrolytes. After cooling, the final electrical conductivity (EC_2) was measured (Gong et al. 1998). The percentage of electrolyte leakage was calculated using the formula $EL\ (\%) = (EC_1/EC_2) \times 100$.

Determination of Chloroplastic Pigments and Biomass

Chlorophyll and carotenoid determinations were performed using a spectrophotometer (model UV-M51; Bel Photonics) according to the methodology of Lichtenthaler and Buschmann (2001). Biomass of roots, stems and leaves was measured based on constant dry weights (g) after drying in a forced-air ventilation oven at 65 °C.

Data Analysis

Normality of residues was verified with Shapiro–Wilk test. Subsequently, data were submitted to one-way analysis of variance and applied Scott–Knott test at a probability level of 5% (Steel et al. 2006). All statistical procedures used the Assistat software.

Results

Fe Deficiency is Attenuated by EBR

Fe deficiency promoted negative changes in the Fe content in the root, stem and leaf tissues of soybean plants (Table 1), being also verified visual symptoms in leaves (Fig. 1). However, after the exogenous application of EBR (100 nM) in plants under Fe deficiency, substantial increases in Fe in the roots, stems and leaves equal to 91%, 66% and 26%, respectively, were induced compared with plants that received equal treatment without EBR (Fe deficiency and – EBR).

EBR Mitigates the Deleterious Effects Provoked by Fe Deficiency on Root Anatomy

Plants subjected to Fe deficiency showed reductions ($P < 0.05$) in RET, RDT, RCD, VCD and RMD (Fig. 2 and Table 2), whereas plants sprayed with 100 nM EBR and exposed to Fe deficiency exhibited increases of 26%, 20%, 9%, 23%, 205% for RET, RDT, RCD, VCD and RMD, respectively, compared with the same treatment without EBR (Fe deficiency and – EBR).

Table 1 Fe contents in soybean plants sprayed with EBR and exposed to Fe deficiency

Fe supply	EBR	Fe in root (µg g DM^{-1})	Fe in stem (µg g DM^{-1})	Fe in leaf (µg g DM^{-1})
Control	–	15,419.06 ± 469.11b	44.63 ± 0.67b	95.11 ± 1.30b
Control	+	18,878.61 ± 130.34a	54.22 ± 2.10a	103.17 ± 0.37a
Deficiency	–	6982.19 ± 512.40d	22.39 ± 0.76d	58.09 ± 0.87d
Deficiency	+	13,369.60 ± 289.67c	37.07 ± 1.73c	73.20 ± 1.22c

Columns with different letters indicate significant differences from the Scott–Knott test ($P < 0.05$). Values described corresponding to means from five repetitions and standard deviations

Fe = Iron

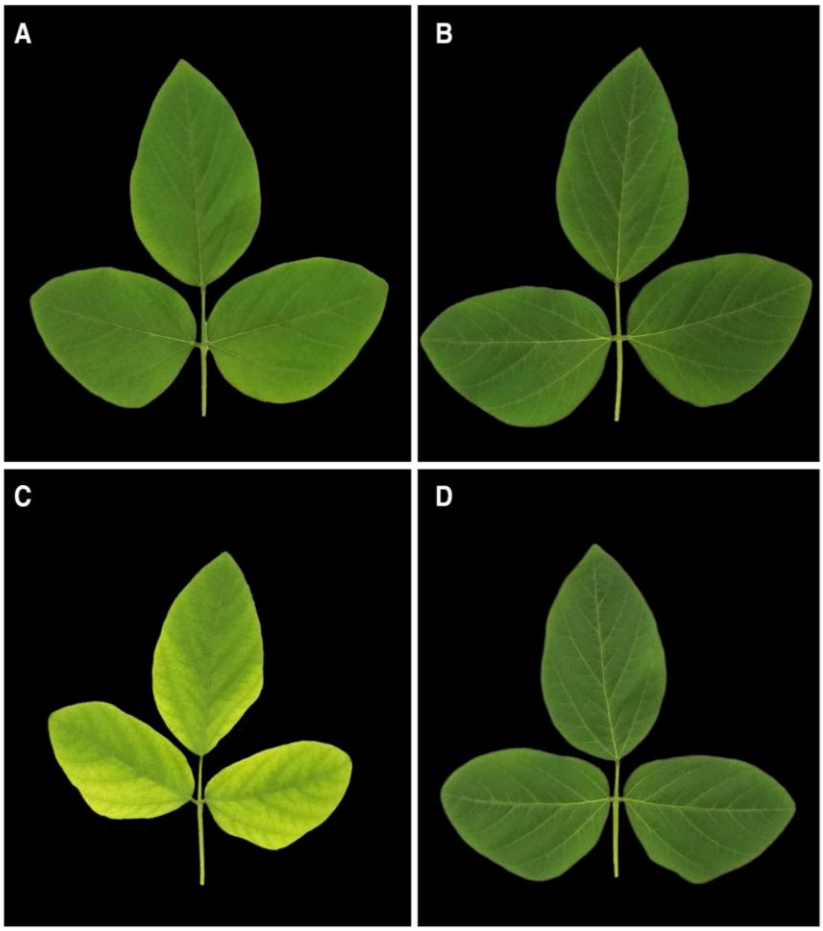

Fig. 1 Trifoliate leaves of soybean plants sprayed with EBR and exposed to Fe deficiency. Fe control/− EBR (**a**), Fe control/+EBR (**b**), Fe deficiency/− EBR (**c**), Fe deficiency/+EBR (**d**)

Steroid Treatment Enhances Homeostasis and the Nutrient Content

Soybean plants exposed to Fe deficiency showed reductions in the nutrient content (Table 3). However, plants subjected to Fe deficiency + 100 nM EBR showed increases in the P, K, Mg, Mn, Cu and Zn contents (root: 16%, 3%, 16%, 14%, 46% and 9%, respectively; stem: 8%, 2%, 18%, 5%, 5% and 18%, respectively; leaf: 5%, 7%, 7%, 16%, 15% and 4%, respectively) compared with treatment with Fe + 0 EBR deficiency (Table 3). The Fe^{2+}/Mg^{2+}, Fe^{2+}/Mn^{2+}, Fe^{2+}/Cu^{2+} and Fe^{2+}/Zn^{2+} ratios increased by 66%, 67%, 32% and 75% in the roots (Table 4), respectively, 41%, 58%, 58% and 40% in the stem, respectively, and 18%, 8%, 10% and 21% in the leaves, respectively, compared with the same treatment without EBR (Fe deficiency and – EBR).

EBR Improves the Performance of Photosystem II in Plants Exposed to Fe Restriction

Fe deficiency caused significant changes in F_o and F_v/F_m. However, EBR application induced a reduction of 16% in F_o and an increase of 6% in F_v/F_m (Fig. 3) compared with treatment without EBR and under Fe deficiency. Plants exposed to Fe deficiency showed significant decreases in Φ_{PSII}, q_P and ETR (Table 5), whereas EBR promoted significant increases of 14%, 25% and 17%, respectively, compared with plants without EBR and under Fe deficiency. Plants exposed to Fe deficiency showed increases in the variables NPQ, EXC and ETR/P_N; however, after receiving a spray with EBR, significant reductions of 23%, 6% and 15% (Table 5), respectively, were obtained compared with equal treatment without EBR (Fe deficiency and – EBR).

Negative Effects of Fe Deficiency and EBR on Gas Exchange

Plants subjected to Fe deficiency exhibited losses in gas exchange (Table 6), but the presence of EBR in plants under Fe deficiency provided significant increases in P_N, E, g_s, WUE and P_N/C_i of 38%, 12%, 16%, 22% and 61%, respectively, and a reduction of 13% in C_i, compared with plants without EBR and exposed to Fe deficiency.

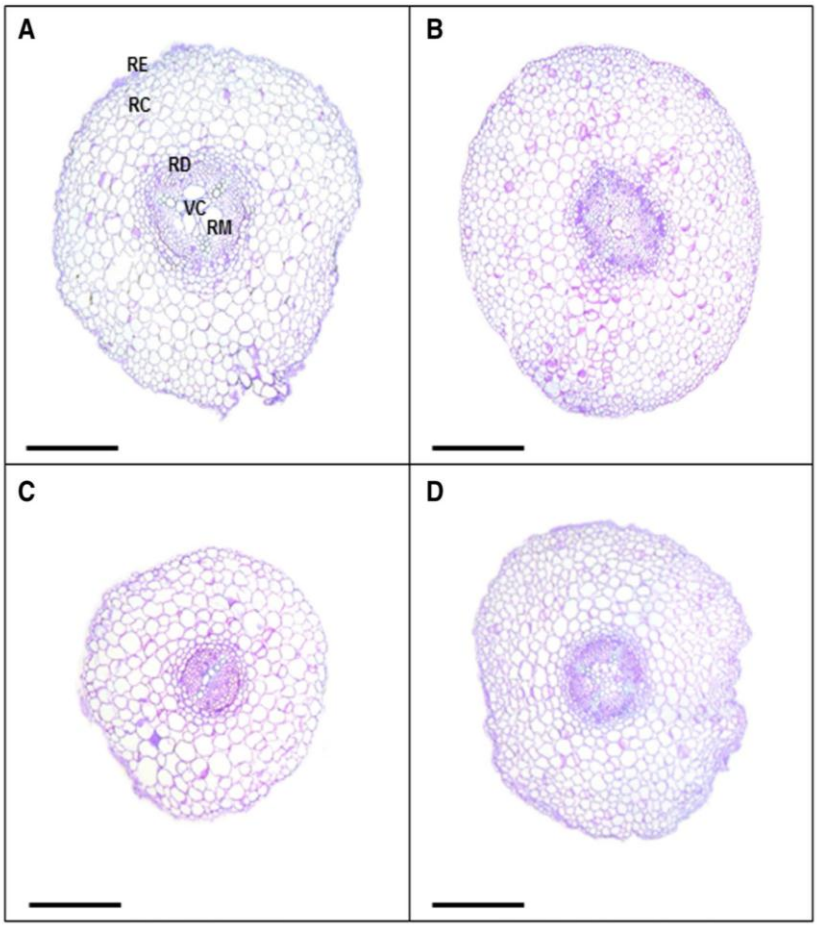

Fig. 2 Root cross sections in soybean plants sprayed with EBR and exposed to Fe deficiency. Fe control/− EBR (**a**), Fe control/+ EBR (**b**), Fe deficiency/− EBR (**c**), Fe deficiency/+ EBR (**d**). *RE* = root epidermis; *RC* root cortex; *RD* = root endodermis; *VC* = vascular cylinder; *RM* root metaxylem. Bars: 300 µm

Table 2 Root anatomy in soybean plants sprayed with EBR and exposed to Fe deficiency

Fe supply	EBR	RET (µm)	RDT (µm)	RCD (µm)	VCD (µm)	RMD (µm)
Control	−	12.74 ± 0.36b	16.89 ± 0.61a	288.91 ± 10.48b	284.53 ± 12.18a	80.75 ± 3.57a
Control	+	14.93 ± 0.83a	17.63 ± 0.61a	328.77 ± 26.15a	296.82 ± 17.46a	83.51 ± 6.17a
Deficiency	−	9.89 ± 0.39c	11.67 ± 0.64c	230.51 ± 10.27d	190.99 ± 10.49c	21.32 ± 1.18c
Deficiency	+	12.50 ± 0.19b	14.05 ± 0.67b	252.92 ± 10.07c	234.87 ± 15.40b	65.03 ± 3.96b

Columns with different letters indicate significant differences from the Scott–Knott test ($P < 0.05$). Values described corresponding to means from five repetitions and standard deviations

RET root epidermis thickness, *RDT* root endodermis thickness, *RCD* root cortex diameter, *VCD* vascular cylinder diameter, *RMD* root metaxylem diameter

EBR Positively Modulates Leaf Anatomy

Fe deficiency caused negative changes in SD, PDS, EDS, SF and IS on both leaf faces (adaxial and abaxial) (Table 7). However, the application of 100 nM EBR on the adaxial face produced increases in SD (7%), SF (2%) and SI (4%) and reductions in PDS (4%) and EDS (6%). Additionally, on the abaxial face exposed to Fe deficiency, EBR exogenous induced increases in SD (3%) and SI (0.4%), and decreases in PDS (13%) and EDS (7%) compared with equal treatment in the absence of EBR (Table 7). To leaf cross section, plants subjected to Fe deficiency showed significant declines in ETAd, ETAb, PPT and SPT (Fig. 4 and Table 8). However, foliar spraying of 100 nM EBR in Fe-deficient plants promoted increases in ETAd (16.2%), ETAb (16.5%), PPT (12%) and SPT (19.3%) compared with the same treatment without EBR.

Table 3 Nutrient contents in soybean plants sprayed with EBR and exposed to Fe deficiency

Fe supply	EBR	P (mg g DM^{-1})	K (mg g DM^{-1})	Mg (mg g DM^{-1})	Mn (µg g DM^{-1})	Cu (µg g DM^{-1})	Zn (µg g DM^{-1})
Contents in root							
Control	−	18.25 ± 0.81a	36.95 ± 0.48a	27.65 ± 0.71b	165.93 ± 2.68d	13.57 ± 0.74d	44.80 ± 1.10b
Control	+	19.03 ± 0.48a	37.50 ± 0.73a	27.82 ± 0.52b	193.20 ± 1.39c	16.35 ± 0.82c	46.56 ± 1.69b
Deficiency	−	12.15 ± 0.77c	32.65 ± 0.38c	27.90 ± 0.76b	303.68 ± 6.54b	24.20 ± 0.58b	45.92 ± 2.91b
Deficiency	+	14.09 ± 0.47b	33.72 ± 0.38b	32.30 ± 1.05a	347.21 ± 1.05a	35.24 ± 1.26a	50.00 ± 0.73a
Contents in stem							
Control	−	7.44 ± 0.21a	56.98 ± 0.60b	2.37 ± 0.11d	10.26 ± 0.42d	2.03 ± 0.03c	20.86 ± 0.61d
Control	+	7.51 ± 0.19a	58.57 ± 0.54a	2.76 ± 0.08c	11.20 ± 0.38c	2.12 ± 0.12c	23.42 ± 1.23c
Deficiency	−	6.56 ± 0.05c	52.73 ± 0.40d	3.33 ± 0.04b	25.84 ± 0.36b	3.72 ± 0.01b	26.93 ± 0.20b
Deficiency	+	7.06 ± 0.11b	53.94 ± 0.40c	3.91 ± 0.20a	27.03 ± 0.31a	3.89 ± 0.02a	31.84 ± 1.35a
Contents in leaf							
Control	−	7.32 ± 0.04a	27.02 ± 0.40b	4.60 ± 0.24b	24.34 ± 0.20b	1.84 ± 0.02d	30.90 ± 0.39c
Control	+	7.46 ± 0.12a	28.02 ± 0.36a	4.70 ± 0.20b	25.25 ± 0.39a	1.98 ± 0.01c	31.64 ± 0.84c
Deficiency	−	6.25 ± 0.09c	23.06 ± 0.70d	4.76 ± 0.11b	16.05 ± 0.05d	2.22 ± 0.03b	53.28 ± 0.82b
Deficiency	+	6.56 ± 0.10b	24.63 ± 0.10c	5.10 ± 0.11a	18.64 ± 0.10c	2.55 ± 0.04a	55.41 ± 0.97a

Columns with different letters indicate significant differences from the Scott–Knott test ($P < 0.05$).Values described corresponding to means from five repetitions and standard deviations

Mg = magnesium, P = phosphorus, K = potassium, Fe = iron, Cu = copper, Zn = zinc

Table 4 Metal ratios in soybean plants sprayed with EBR and exposed to Fe deficiency

Fe supply	EBR	Fe^{2+}/Mg^{2+}	Fe^{2+}/Mn^{2+}	Fe^{2+}/Cu^{2+}	Fe^{2+}/Zn^{2+}
Ratios in root					
Control	−	0.558 ± 0.017b	92.97 ± 1.92b	1138.86 ± 74.25a	344.38 ± 15.15b
Control	+	0.679 ± 0.016a	97.72 ± 1.28a	1156.97 ± 51.91a	405.90 ± 13.75a
Deficiency	−	0.250 ± 0.019d	23.00 ± 1.73d	288.45 ± 18.22c	152.68 ± 16.11d
Deficiency	+	0.414 ± 0.020c	38.51 ± 0.85c	379.64 ± 09.86b	267.38 ± 05.07c
Ratios in stem					
Control	−	0.019 ± 0.002a	4.30 ± 0.18b	21.94 ± 0.47b	2.14 ± 0.05b
Control	+	0.020 ± 0.002a	4.85 ± 0.16a	25.68 ± 1.07a	2.32 ± 0.05a
Deficiency	−	0.007 ± 0.001c	0.87 ± 0.03d	6.02 ± 0.23d	0.83 ± 0.03d
Deficiency	+	0.009 ± 0.001b	1.37 ± 0.06c	9.53 ± 0.42c	1.16 ± 0.04c
Ratios in leaf					
Control	−	0.021 ± 0.002a	3.91 ± 0.02b	51.97 ± 3.16a	3.08 ± 0.05b
Control	+	0.022 ± 0.003a	4.09 ± 0.03a	52.23 ± 1.21a	3.26 ± 0.06a
Deficiency	−	0.012 ± 0.001c	3.62 ± 0.05c	26.22 ± 0.44c	1.09 ± 0.03d
Deficiency	+	0.015 ± 0.001b	3.93 ± 0.08b	28.78 ± 0.88b	1.32 ± 0.07c

Columns with different letters indicate significant differences from the Scott–Knott test ($P < 0.05$).Values described corresponding to means from five repetitions and standard deviations

Fe = iron, Mg = magnesium, Mn = manganese, Cu = copper, Zn = zinc

Beneficial Actions of EBR on the Antioxidant System

Fe deficiency had negative effects on SOD, CAT, APX and POX activities (Fig. 5); however, plants exposed to Fe deficiency and sprayed with EBR showed increased values of 11%, 35%, 8% and 24%, respectively, compared with treatment without EBR and exposure to Fe deficiency.

Effects of EBR on Oxidant Compounds and Cell Damage

Regarding oxidative compounds (O_2^- and H_2O_2) and indicators of cellular damage (MDA and EL), plants subjected to Fe deficiency showed increases in their concentrations (Fig. 6). However, the application of 100 nM EBR provided

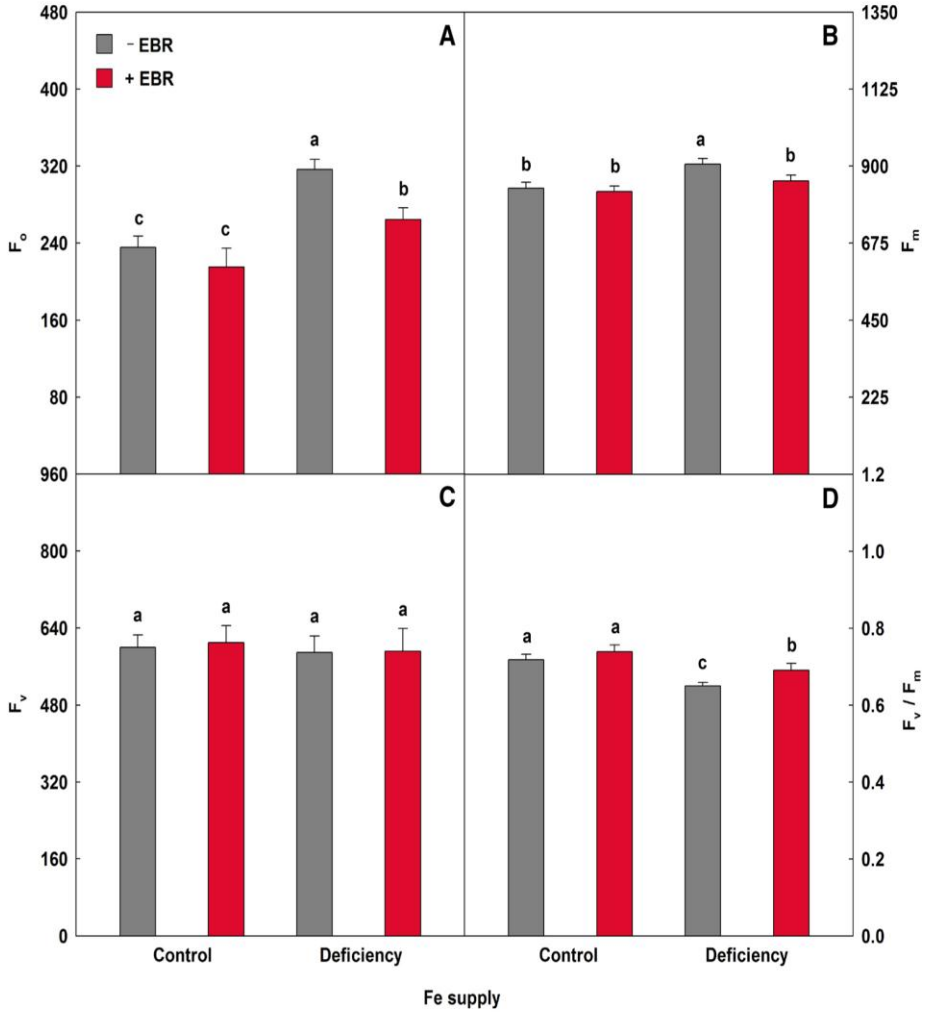

Fig. 3 Minimal fluorescence yield of the dark-adapted state (F_0), maximal fluorescence yield of the dark-adapted state (F_m), variable fluorescence (F_v) and maximal quantum yield of PSII photochemistry (F_v/F_m) in soybean plants sprayed with EBR and exposed to Fe deficiency. Columns with different letters indicate significant differences from the Scott–Knott test ($P < 0.05$). Columns corresponding to means from five repetitions and standard deviations

Table 5 Chlorophyll fluorescence in soybean plants sprayed with EBR and exposed to Fe deficiency

Fe supply	EBR	Φ_{PSII}	q_P	NPQ	ETR (μmol m^{-2} s^{-1})	EXC (μmol m^{-2} s^{-1})	ETR/P_N
Control	–	0.32 ± 0.01b	0.75 ± 0.06b	0.86 ± 0.07c	46.77 ± 1.24b	0.56 ± 0.01c	2.42 ± 0.08b
Control	+	0.35 ± 0.01a	0.87 ± 0.02a	0.74 ± 0.06c	50.90 ± 2.20a	0.53 ± 0.03c	2.45 ± 0.13b
Deficiency	–	0.24 ± 0.01d	0.40 ± 0.02d	1.49 ± 0.10a	34.56 ± 1.70d	0.64 ± 0.02a	2.91 ± 0.18a
Deficiency	+	0.28 ± 0.01c	0.50 ± 0.03c	1.13 ± 0.06b	40.54 ± 2.13c	0.60 ± 0.01b	2.47 ± 0.16b

Columns with different letters indicate significant differences from the Scott–Knott test ($P < 0.05$).Values described corresponding to means from five repetitions and standard deviations

Φ_{PSII} effective quantum yield of PSII photochemistry, q_P photochemical quenching coefficient, *NPQ* nonphotochemical quenching, *ETR* electron transport rate, *EXC* relative energy excess at the PSII level, *ETR*/P_N ratio between the electron transport rate and net photosynthetic rate

Table 6 Gas exchange in soybean plants sprayed with EBR and exposed to Fe deficiency

Fe supply	EBR	P_N (μmol m^{-2} s^{-1})	E (mmol m^{-2} s^{-1})	g_s (mol m^{-2} s^{-1})	C_i (μmol mol^{-1})	WUE (μmol $mmol^{-1}$)	P_N/C_i (μmol m^{-2} s^{-1} Pa^{-1})
Control	–	19.35 ± 0.65b	2.57 ± 0.25a	0.34 ± 0.02a	239 ± 10b	7.67 ± 0.60a	0.081 ± 0.005b
Control	+	20.79 ± 0.63a	2.60 ± 0.17a	0.34 ± 0.03a	216 ± 11c	8.01 ± 0.44a	0.097 ± 0.002a
Deficiency	–	11.87 ± 0.34d	2.25 ± 0.12b	0.22 ± 0.01c	297 ± 15a	5.32 ± 0.53c	0.040 ± 0.003d
Deficiency	+	16.46 ± 0.24c	2.53 ± 0.10a	0.26 ± 0.02b	258 ± 19b	6.52 ± 0.20b	0.065 ± 0.003c

Columns with different letters indicate significant differences from the Scott–Knott test ($P < 0.05$).Values described corresponding to means from five repetitions and standard deviations

P_N net photosynthetic rate, E transpiration rate, g_s stomatal conductance, C_i intercellular CO_2 concentration, *WUE* water-use efficiency, P_N/C_i carboxylation instantaneous efficiency

Table 7 Stomatal characteristics in soybean plants sprayed with EBR and exposed to Fe deficiency

Fe supply	EBR	SD (stomata per mm^2)	PDS (μm)	EDS (μm)	SF	SI (%)
Adaxial face						
Control	–	158.43 ± 3.15b	11.43 ± 0.37c	21.01 ± 0.59c	0.54 ± 0.00a	7.79 ± 0.33a
Control	+	168.57 ± 6.30a	11.06 ± 0.51c	19.50 ± 0.85d	0.57 ± 0.04a	7.84 ± 0.44a
Deficiency	–	140.00 ± 4.67d	12.98 ± 0.40a	26.26 ± 0.88a	0.49 ± 0.02c	6.14 ± 0.38c
Deficiency	+	151.86 ± 3.16c	12.17 ± 0.23b	23.15 ± 0.70b	0.53 ± 0.00b	6.90 ± 0.29b
Abaxial face						
Control	–	285.57 ± 3.13b	11.71 ± 0.43b	22.40 ± 0.59c	0.52 ± 0.01b	13.65 ± 0.55a
Control	+	292.86 ± 3.17a	10.88 ± 0.37c	19.64 ± 0.49d	0.55 ± 0.01a	13.94 ± 0.70a
Deficiency	–	258.71 ± 6.63d	13.09 ± 0.35a	27.85 ± 0.54a	0.47 ± 0.02c	12.01 ± 0.64b
Deficiency	+	271.57 ± 4.51c	12.03 ± 0.42b	23.46 ± 0.37b	0.51 ± 0.01b	12.46 ± 0.57b

Columns with different letters indicate significant differences from the Scott–Knott test ($P < 0.05$).Values described corresponding to means from five repetitions and standard deviations

SD stomatal density, *PDS* polar diameter of the stomata, *EDS* equatorial diameter of the stomata, *SF* stomatal functionality, *SI* stomatal index

reductions in the levels of O_2^- (35%), H_2O_2 (11%), MDA (10%) and EL (12%) compared with treatment without EBR and under Fe deficiency.

EBR Spray Modulates the Beneficial Effects on Photosynthetic Pigments

Plants exposed to Fe deficiency displayed negative changes in photosynthetic pigments (Table 9), but the presence of 100 nM EBR promoted significant increases in Chl *a* (14%), Chl *b* (23%), total Chl (15%) and Car (28%) compared with treatment in the absence of EBR combined with Fe deficiency. Additionally, reductions were found in the ratios of Chl *a*/Chl *b* and total Chl/Car at 6% and 11%, respectively.

Biomass of Soybean Plants Treated with EBR and Exposed to Fe Restriction

Plants exposed to Fe deficiency presented slight benefits regarding morphological parameters when sprayed with EBR, with increases of 0.2%, 1.4%, 0.3% and 0.6% in LDM, RDM, SDM and TDM, respectively, compared with treatment without EBR and under Fe deficiency (Fig. 7).

Discussion

The increase in the Fe content in plants exposed to Fe deficiency + 100 nM EBR suggests that this steroid improved the absorption, transport and accumulation of Fe in the evaluated tissues (Fig. 8). EBR induces Fe uptake by root epidermal cells, increasing the activity of the H^+-ATPase enzyme (Song et al. 2016), responsible for the release of protons (H^+) to the rhizosphere (Kim and Guerinot 2007). The acidification induced by this enzyme increases the iron solubility in the rhizosphere. Consequently, oxidized Fe^{3+} is reduced to the soluble form of Fe^{2+} through the reductase modulated by the *FRO2* gene (ferric reductase oxidase); thereafter, the iron is transported to the interior of the cell by the protein IRT1 (iron-regulated transporter) (Giehl et al. 2009). Vardhini et al. (2012) studied the effects of two brassinosteroid analogues (EBR and 28-homobrassinolide) on the mineral content and metabolites and observed that leaf spray of both forms increased the Fe content in the roots of *Raphanus sativus*.

EBR promoted beneficial effects on the root tissues (RET, RDT, RCD, VCD and RMD) of plants exposed to

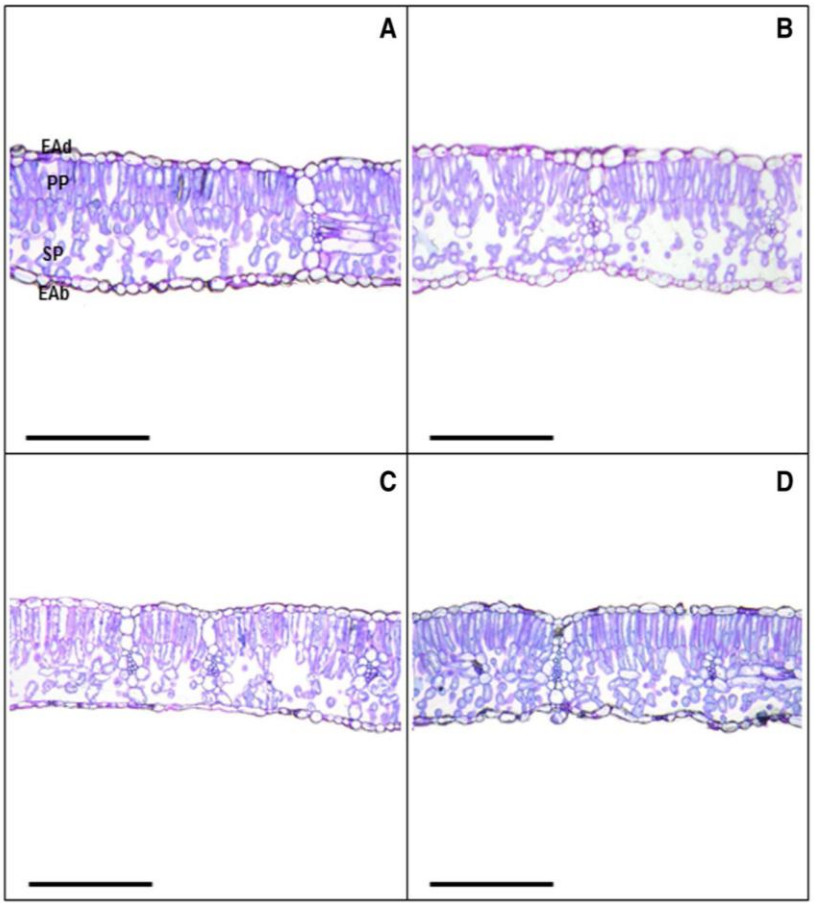

Fig. 4 Leaf cross sections in soybean plants sprayed with EBR and exposed to Fe deficiency. Fe control/− EBR (**a**), Fe control/+ EBR (**b**), Fe deficiency/− EBR **c**), Fe deficiency/+ EBR (**d**). *EAd* adaxial epidermis; *EAb* adaxial epidermis; *PP* palisade parenchyma; *SP* spongy parenchyma. Bars: 200 µm

Table 8 Leaf anatomy in soybean plants sprayed with EBR and exposed to Fe deficiency

Fe supply	EBR	ETAd (µm)	ETAb (µm)	PPT (µm)	SPT (µm)	Ratio PPT/SPT
Control	−	14.98 ± 0.39b	16.09 ± 0.59b	76.28 ± 2.99a	63.32 ± 2.12b	1.21 ± 0.08b
Control	+	16.96 ± 0.56a	18.08 ± 0.46a	77.48 ± 3.72a	68.44 ± 2.30a	1.13 ± 0.09b
Deficiency	−	12.13 ± 0.46d	11.26 ± 0.81d	62.41 ± 1.71c	39.71 ± 2.85d	1.58 ± 0.10a
Deficiency	+	14.09 ± 0.35c	13.12 ± 0.52c	69.90 ± 1.93b	47.39 ± 3.02c	1.48 ± 0.07a

Columns with different letters indicate significant differences from the Scott–Knott test ($P < 0.05$). Values described corresponding to means from five repetitions and standard deviations

ETAd epidermis thickness from adaxial leaf side, *ETAb* epidermis thickness from abaxial leaf side, *PPT* Palisade parenchyma thickness, *SPT* spongy parenchyma thickness

Fe deficiency. Increases in RET, RDT and RCD after the exogenous application of EBR (100 nM) indicated that this steroid stimulates the processes of cell division and elongation of the root meristem, specifically the epidermis (Gonzalez-Garcia et al. 2011; Hacham et al. 2011). The epidermis, endoderm and cortex are tissues that are associated with the mechanism of root protection and selectivity, and the increases detected in these tissues serve as a barrier against abiotic stresses, such as Fe deficiency (Cui 2015; Barberon et al. 2016). Increases in VCD and RMD induced by EBR suggest that higher densities of these tissues may facilitate water flow and nutrients in plant tissues. Maia et al. (2018) studied the responses induced by the exogenous application of EBR (100 nM) on root anatomy in contrasting *Solanum lycopersicum* genotypes (BRs-efficient and BRs-deficient) and observed increases in RET (9%), RDT (14%), RCD (12%), VCD (7%) and RMD (17%).

Plants with Fe deficiency and sprayed with EBR exhibited increased contents of macronutrients (P, K and Mg) and micronutrients (Mn, Cu and Zn) (Fig. 8). These results confirm that exogenous EBR (100 nM) mitigated the effects of Fe deficiency, optimizing the absorption and assimilation

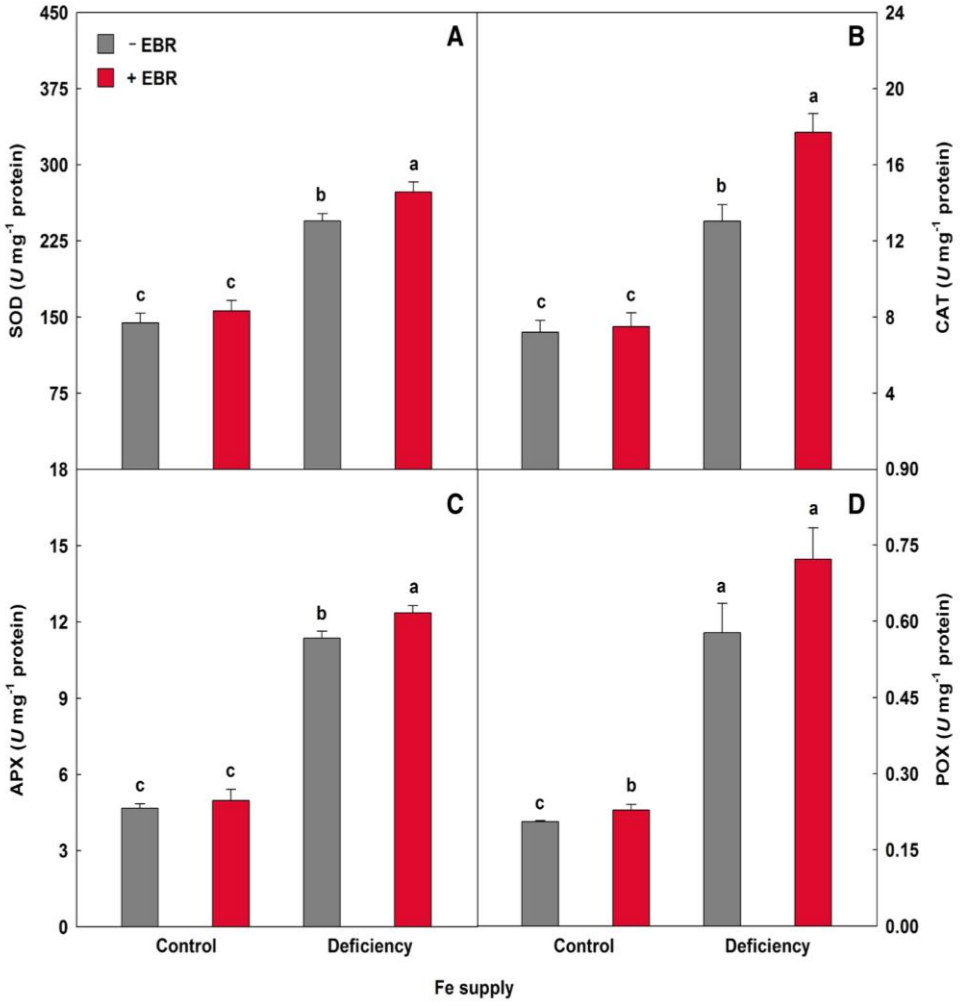

Fig. 5 Activities of superoxide dismutase (SOD), catalase (CAT), ascorbate peroxidase (APX) and peroxidase (POX) in soybean plants sprayed with EBR and exposed to Fe deficiency. Columns with different letters indicate significant differences from the Scott–Knott test ($P < 0.05$). Columns corresponding to means from five repetitions and standard deviations

processes of ions, also implying beneficial effects on nutritional balance (Talaat and Shawky 2013). Additionally, increases in the Fe^{2+}/Mg^{2+}, Fe^{2+}/Mn^{2+}, Fe^{2+}/Cu^{2+} and Fe^{2+}/Zn^{2+} ratios can be attributed to the simultaneous actions of the family transporters NRAMP, DMTI and IRT1, which function in Fe absorption and the intracellular transport of other metals, such as Mn, Cu and Zn (Kaiser et al. 2003; Colangelo and Guerinot 2006; Socha and Guerinot 2014). Tomasi et al. (2014) investigated the accumulation of nutrients in Fe-deficient *Cucumis sativus* leaves and observed that the Cu and Zn contents were higher in the leaf vascular system. Lima et al. (2018) proved that exogenous EBR provoked increments in the P (103%), K (8%), Mg (9%), Mn (21%), Cu (26%) and Zn (25%) contents by evaluating the nutritional status of *Eucalyptus urophylla* roots under Fe deficiency.

Exogenous EBR (100 nM) mitigated the negative effects caused by Fe deficiency on F_0, F_m, F_v and F_v/F_m, indicating that this plant steroid reduces photoinhibition and improves photochemical efficiency in soybean plants. A reduction in F_0 and increase in F_m indicate that EBR increased the proportion of oxidized quinone (Q_A), improving the capture of photons in PSII reaction centres and increasing the F_v/F_m values (Hertle et al. 2013; Li et al. 2017). Pestana et al. (2005) evaluated the physiological responses of *Citrus taiwanica* rootstocks under different Fe concentrations (0, 5, 10, 15 and 20 µM) and detected increased F_0 but reduced F_m and F_v/F_m. Xia et al. (2009) used *Cucumis sativus* to confirm that 0.1 µM EBR via foliar spraying elevated F_v/F_m values, optimizing the activity in PSII.

The increase in Φ_{PSII}, q_P and ETR values in plants exposed to Fe deficiency + 100 nM EBR (Fig. 8), being

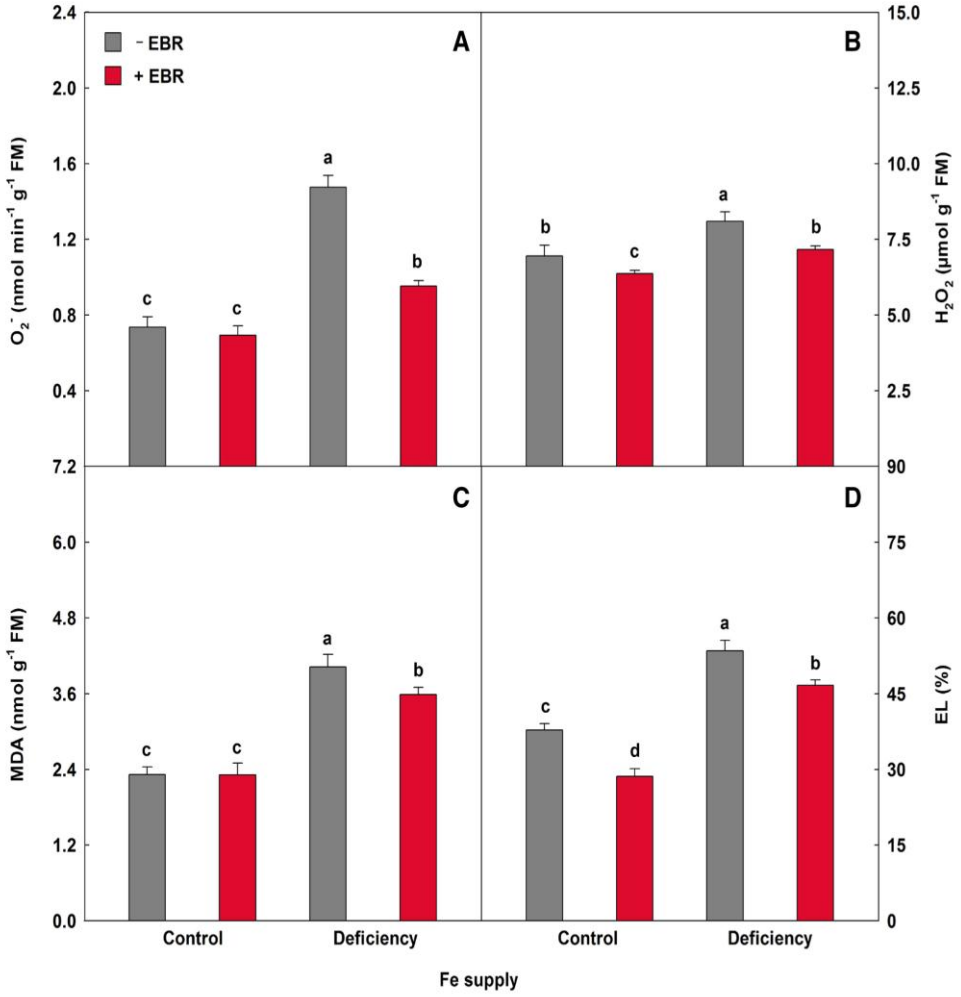

Fig. 6 Superoxide (O_2^-), hydrogen peroxide (H_2O_2), malondialdehyde (MDA) and electrolyte leakage (EL) in soybean plants sprayed with EBR and exposed to Fe deficiency. Columns with different letters indicate significant differences from the Scott–Knott test ($P < 0.05$). Columns corresponding to means from five repetitions and standard deviations

Table 9 Photosynthetic pigments in soybean plants sprayed with EBR and exposed to Fe deficiency

Fe supply	EBR	Chl *a* (mg g^{-1} FM)	Chl *b* (mg g^{-1} FM)	Total Chl (mg g^{-1} FM)	Car (mg g^{-1} FM)	Ratio Chl *a*/Chl *b*	Ratio Total Chl/Car
Control	–	8.45 ± 0.44a	2.00 ± 0.12a	10.41 ± 0.57a	1.53 ± 0.07a	4.37 ± 0.40a	6.82 ± 0.51b
Control	+	8.50 ± 0.48a	2.02 ± 0.19a	10.48 ± 0.52a	1.65 ± 0.12a	4.30 ± 0.35a	6.60 ± 0.65b
Deficiency	–	6.62 ± 0.28c	1.37 ± 0.12c	7.99 ± 0.32c	0.99 ± 0.04c	4.87 ± 0.45a	8.25 ± 0.41a
Deficiency	+	7.55 ± 0.37b	1.73 ± 0.13b	9.23 ± 0.56b	1.26 ± 0.11b	4.54 ± 0.44a	7.33 ± 0.45b

Columns with different letters indicate significant differences from the Scott–Knott test ($P < 0.05$). Values described corresponding to means from five repetitions and standard deviations

Chl a chlorophyll *a*, *Chl b* chlorophyll *b*, *Total chl* total chlorophyll, *Car* carotenoids

intrinsically related to increases in chloroplastic pigments and F_v/F_m. This result indicates a higher dissipation of fluorescence by processes related to electron transport in the chloroplasts and consequent generation of ATP and NADPH, reflected in increments in P_N (Rivero et al. 2010; Tikhonov 2013; Dumas et al. 2016). EBR also had a positive influence on q_P and ETR, increasing the activity of the cytochrome *b6f* complex (Cyt b6f) and ferredoxin (Fd), which are plant

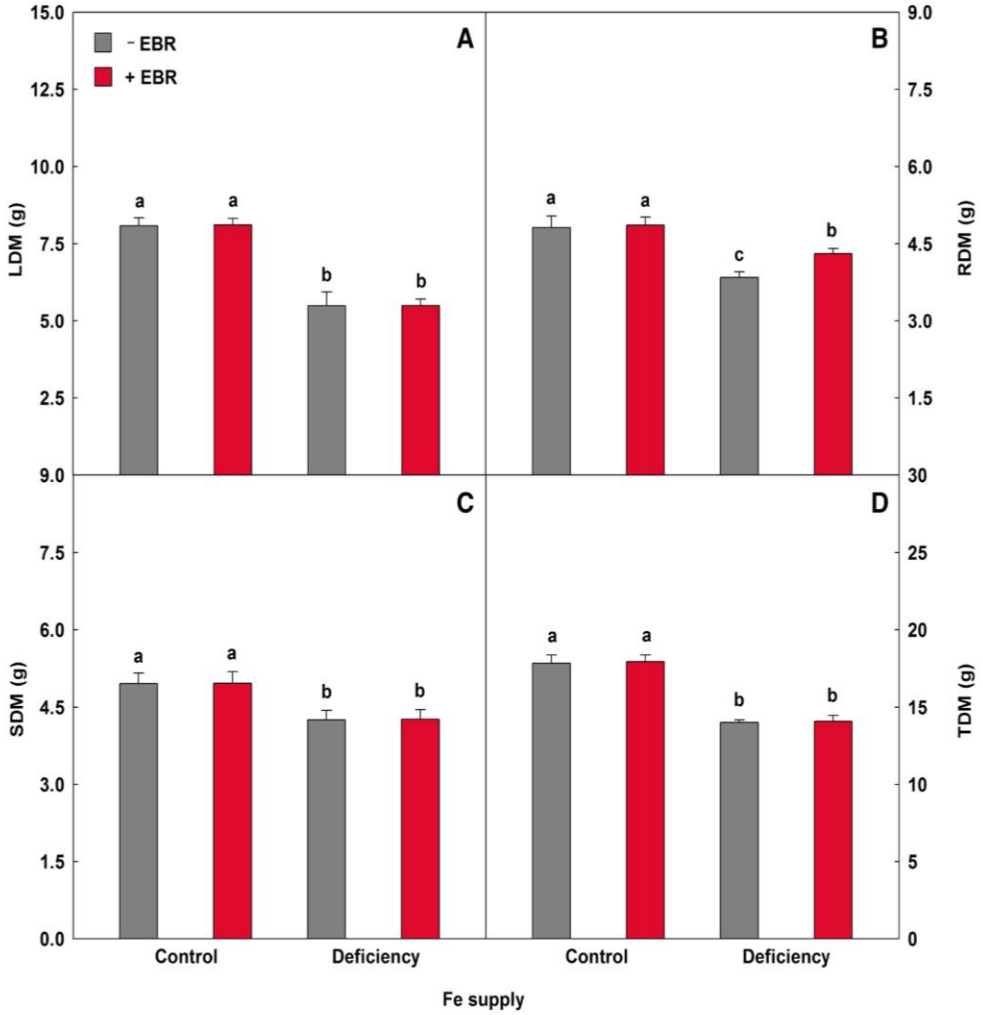

Fig. 7 Leaf dry matter (LDM), root dry matter (RDM), stem dry matter (SDM) and total dry matter (TDM) in soybean plants sprayed with EBR and exposed to Fe deficiency. Columns with different letters indicate significant differences from the Scott–Knott test ($P < 0.05$). Columns corresponding to means from five repetitions and standard deviations

proteins with vital functions in photosynthesis, both using Fe as a structural element (Buonasera et al. 2011). Roncel et al. (2016) investigated the impacts of Fe deficiency on photosynthetic electron transport in *Phaeodactylum tricornutum* plants and detected reductions in Φ_{PSII} and ETR. However, Siddiqui et al. (2018) studied chlorophyll fluorescence in *Brassica juncea* plants treated with 10^{-8} M EBR and showed increases in Φ_{PSII} (19%), q_P (17%) and ETR (19%); however, 10^{-8} M 28-homobrassinolide promoted increases of 17%, 16% and 18% for Φ_{PSII}, q_P and ETR, respectively.

EBR decreased the NPQ, EXC and ETR/P_N values in Fe-deficient plants, revealing that EBR improves the efficiency and conversion of energy absorbed by the PSII antenna, attenuating the photoinhibitory damage in the reaction centres (Ogweno et al. 2008; Zhang et al. 2015). The reduction of EXC is caused by the decrease in NPQ, indicating that this steroid reduces photochemical damage in PSII (Silva et al. 2012). Additionally, a reduction in ETR/P_N induced by EBR suggests the lower use of photochemical energy in other metabolic processes, such as photorespiration, nitrogen metabolism and the Mehler reaction (Silva et al. 2010; Krumova et al. 2013; Pociecha et al. 2017). Timperio et al. (2007) studied the effect of Fe deficiency on the pigment composition and organization of the thylakoid membrane and showed increased energy dissipation (NPQ) in *Spinacia oleracea* leaves exposed to 18 days of Fe deficiency.

In this study, EBR mitigated Fe deficiency in *Glycine max*, minimizing negative effects under gas exchange. EBR positively modulated *P*N, *E* and *C*i because of better performance in *g*s (Yu et al. 2004). Additionally, EBR improved the carboxylation rate of RuBisCO (Hasan et al. 2011), consequently promoting a better efficiency of CO_2 fixation in

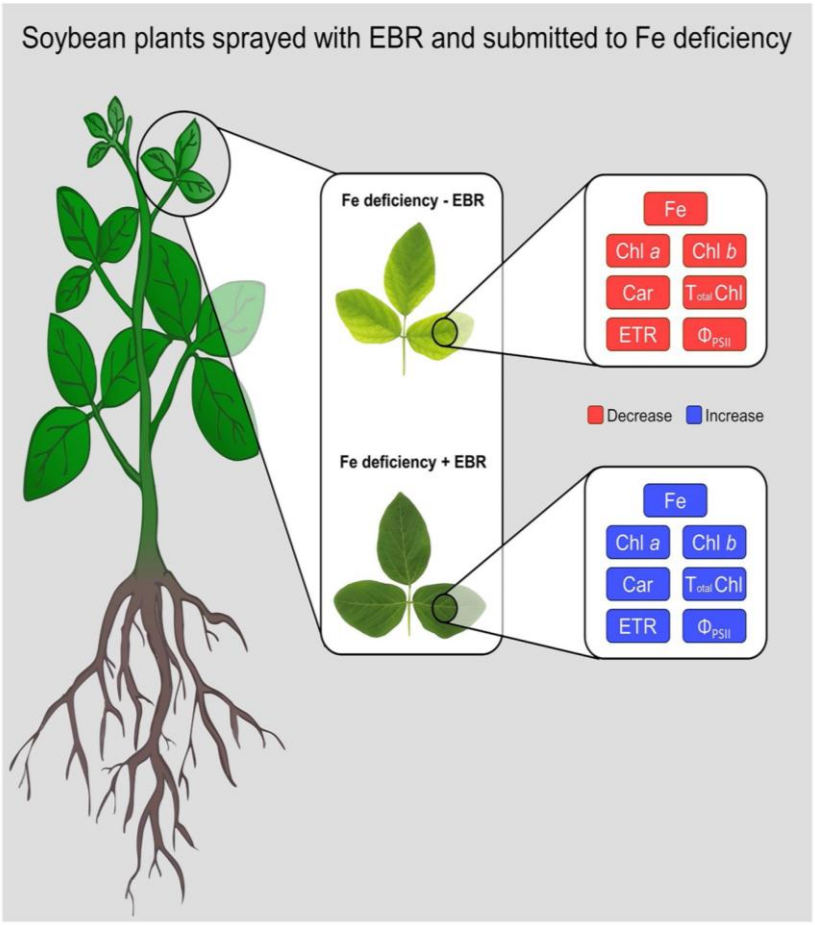

Fig. 8 Schematic representation connected to nutritional status, photosynthetic pigments and chlorophyll fluorescence in soybean plants sprayed with EBR and exposed to Fe deficiency, being variables focused on main results of this research

the Calvin–Benson cycle in chloroplasts and decreasing the intercellular CO_2 concentration (C_i) (Yu et al. 2004). The increases obtained for WUE are explained by the improvements promoted by EBR under P_N and E, with WUE calculated by the relationship between variables P_N and E (Barros Junior et al. 2017). Abiotic stresses, including the Fe deficiency, provoke negative interferences on gas exchange, affecting mainly P_N and WUE, and these modifications often delay growth and development (Sharma et al. 2020). Larbi et al. (2006) evaluated the effects of Fe deficiency on gas exchange and CO_2 assimilation in *Beta vulgaris, Pyrus communis* and *Prunus persica* plants and verified reductions in P_N and E, as well as an increase in C_i, in leaves under extreme chlorosis induced by Fe deficiency in all species studied. Additionally Ogweno et al. (2010), confirmed, using *Solanum lycopersicum*, that 1.0 mg L^{-1} of EBR maximized the CO_2 uptake, inducing a significant increase in P_N.

EBR positively modulates the stomatal characteristics (SD, PDS, EDS, SF and SI) of plants subjected to Fe deficiency. Increases detected in SD, SF and SI demonstrated that exogenous EBR (100 nM) optimizes stomatal performance (g_s), probably regulating the development of stomata through the activation of protein kinase in the stomatal intracellular signalling pathway (Kim et al. 2012; Casson and Hetherington 2012). Concomitantly, higher concentrations of CO_2 were absorbed by the mesophyll cells (PPT and SPT) (Flexas et al. 2008, 2012). Regarding PDS and EDS, EBR promoted reductions in PDS and EDS, indicating that smaller stomata have greater functionality and beneficial effects on gas exchange, presenting a decrease in pore size and a lower loss of water via E (Eburneo et al. 2017). Fernández et al. (2008) detected structural alterations associated with chlorosis by Fe deficiency in *Pyrus communis* and *Prunus persica*, demonstrating a significant decrease in the stomatal pore length in both species.

Plants treated with EBR (100 nM) and exposed to Fe deficiency showed beneficial effects on leaf anatomy (ETAd, ETAb, PPT and SPT). The increases in PPT and SPT are associated with increases verified in P_N and P_N/C_i because the photosynthetic process is regulated by the intrinsic transport capacity of the mesophyll and conductance of CO_2 of ambient air to the carboxylation sites in the chloroplasts (Ennajeh et al. 2010). The high values of ETAd and ETAb in plants sprayed with EBR can be explained by the higher

values in *E* and WUE, in which the epidermis is a coating tissue, clearly contributing to water use and avoiding excessive water loss during the transpiration process (Javelle et al. 2011). Yuan et al. (2018) investigated the anatomical and ultrastructural responses in *Capsicum annuum* leaves at four Fe concentrations (0, 0.05, 0.1 and 2.0 mM Fe L^{-1}) and described that leaves exposed to Fe deficiency (0 mM Fe L^{-1}) presented mesophyll cells weakly compressed and few chloroplasts.

The exogenous application of EBR contributed to increased activities of the SOD, CAT, APX and POX enzymes of plants exposed to Fe deficiency, revealing an intrinsic action of this steroid on the antioxidant system. Additionally, EBR promotes photochemical efficiency, as evidenced by the increases in F_v/F_m and ETR. Song et al. (2016) evaluated the enzymatic activities and growth of *Arachis hypogea* seedlings exposed to Fe deficiency in combination with EBR and detected increases in SOD, POX and CAT. EBR up-regulated the expressions of the POX and CAT genes, mitigating the adverse impacts on *Brassica juncea* seedlings exposed to Pb toxicity (Kohli et al. 2018b). Bajguz (2010) studied the exogenous effects of EBR on the culture of *Chlorella vulgaris* exposed to Cu, Cd and Pb and observed beneficial effects on the antioxidant system, promoting increases in the activities of antioxidant enzymes (SOD, CAT and APX).

The EBR application promoted reductions in the ROS levels (O_2^- and H_2O_2) and mitigated membrane damage (EL and MDA). These results are attributed to increases in antioxidant enzyme activities (SOD, CAT, APX and POX) previously detected in this study. These enzymes are responsible for cell detoxification (Ahmad et al. 2010; Rattan et al. 2020), alleviation of oxidative stress and cell death generated by ROS (Bajguz 2010; El-Beltagi and Mohamed 2013). Additionally, high concentrations of O_2^- and H_2O_2 frequently promote lipid peroxidation (MDA), inducing electrolyte leakage (EL) and negatively interfering with membrane functions (Kumari et al. 2010; Gallego et al. 2012). Kohli et al. (2019) found significant reductions of O_2^-, H_2O_2 and MDA in *Brassica juncea* treated with EBR and Pb-stress. Tewari et al. (2013) evaluated the induction of ROS under Fe deficiency and the mechanism of programmed cell death in *Brassica napus* leaves and detected significant accumulations of O_2^- and H_2O_2 in chloroplasts. Abdelmajid et al. (2008) evaluated the symbiotic response of two varieties of *Phaseolus vulgaris* exposed to Fe deficiency and found accumulated MDA of 24% in ARA14 and 44% in Coco blanc, indicating oxidative stress and lipid peroxidation in the cell membrane of the nodules of both varieties. However, Choudhary et al. (2011) evaluated *Raphanus sativus* seedlings subjected to three concentrations of EBR (10^{-11}, 10^{-9} and 10^{-7} M) and exposed to Cu and showed a significant decrease in the MDA content (44%) with 10^{-9} M EBR.

EBR induced increases in the Chl *a*, Chl *b*, Chl total and Car levels of plants under Fe deficiency (Fig. 8), suggesting that this steroid improves the function of the enzyme ferrochelatase in the route of chlorophyll biosynthesis. Ferrochelatase is an enzyme present in the thylakoid membrane, where it is responsible for inserting Fe into protoporphyrinogen IX oxidase (PPO), which acts as a catalyst during the oxidation reaction of protoporphyrinogen IX to protoporphyrin IX to form the chlorophyll molecule (Lermontova et al. 1997; Suzuki et al. 2002). Molassiotis et al. (2005) investigated the oxidative stress, antioxidant activity and activity of Fe(III) chelate reductase in *Prunus* rootstocks exposed to Fe deficiency and detected reductions in the Chl total levels. Bajguz (2011) analysed the contents of chlorophylls and phytochelatins, as well as growth, in *Chlorella vulgaris* treated with EBR (10^{-8} M) and exposed to Cd, Pb and Cu and detected an increase in the Chl total content positively induced by the action of this steroid. Kaya et al. (2020) evaluating *Capsicum annuum* plants sprayed with EBR and subjected to Cd toxicity reported that this steroid mitigated the deleterious effects on Chl *a* and Chl *b*, being these results explained by the improvements on antioxidant system and subsequent lower oxidative stress.

EBR application reduced the deleterious effects caused by iron deficiency on the plant biomass (LDM, RDM, SDM and TDM). These increases are explained by EBR stimulating the processes of cell division and elongation, combined with adequate nutrient contents and higher photosynthetic rates (Shahbaz and Ashraf 2007), resulting in the accumulation of dry matter (Bhardwaj et al. 2007). Mahmoudi et al. (2007) reported that Fe deficiency significantly inhibits the biomass in two *Cicer arietinum* varieties. However, Swamy and Rao (2009) proved that exogenous application of EBR (0.5, 1.0 and 3.0 µM) improved the growth of *Pelargonium graveolens* plants, promoting increases in LDM, RDM, and SDM. Jan et al. (2018) working with *Pisum sativum* seedlings under Cd stress described significant increments in dry matter and length of root and shoot after EBR treatment, being associated by these authors to stimulation promoted by this steroid on elongation rate and cell division. In relation next steps, future research using contrasting genotypes to EBR biosynthesis (deficient and efficient) and focusing on gene expression related to Fe transporters are necessary to expand the knowledge on EBR roles in higher plants.

Conclusion

Exogenous EBR minimizes the damage caused by Fe deficiency. This steroid maximized the Fe content in the leaf, stem and root, suggesting that EBR enhances the uptake and transport of Fe and other essential nutrients, improving the nutritional status. In parallel, EBR benefits metallic

homeostasis, as confirmed by the increments detected in the Fe^{2+}/Mg^{2+}, Fe^{2+}/Mn^{2+} and Fe^{2+}/Cu^{2+} ratios in plants exposed to Fe deficiency. Steroid mitigates the negative effects of Fe deficiency on chlorophylls, being modulated by antioxidant enzymes (superoxide dismutase, catalase, ascorbate peroxidase and peroxidase) and corroborated by reductions in the malondialdehyde levels and electrolyte leakage, revealing a protective action of EBR against damage provoked by oxidative stress in chloroplast pigments. Concomitantly, plants treated with EBR exhibited fewer deleterious effects caused by photoinhibition in PSII (Photosystem II), minimizing the relative energy excess at the PSII level and nonphotochemical quenching. However, EBR increased the electron transport rate and photochemical quenching, indicating a higher photochemical efficiency. Therefore, our results demonstrate that EBR spray improved the nutrient content and physiological performance of soybean plants under the conditions of Fe limitation.

Acknowledgements This research was funded by Fundação Amazônia de Amparo a Estudos e Pesquisas (FAPESPA/Brazil), Conselho Nacional de Desenvolvimento Científico e Tecnológico (CNPq/Brazil), Programa de Pós-Graduação em Agronomia (PGAGRO/Brazil) and Universidade Federal Rural da Amazônia (UFRA/Brazil) to AKSL. Additionally, LRS was supported by a scholarship from Coordenação de Aperfeiçoamento de Pessoal de Nível Superior (CAPES/Brazil). Authors would like to extend their sincere appreciation to the Researches Supporting Project Number (RSP 2020/236) from King Saud University, Riyadh, Saudi Arabia.

Author Contributions AKSL was the advisor of this project, planning all phases of this research. LRS, LSP and YCP conducted the experiment in the greenhouse and performed physiological, biochemical and morphological determinations, while BRSS measured anatomical parameters and BLB performed nutritional determinations and helped in drafting the manuscript and in interpreting the results. AAA critically revised and edited the manuscript. All authors read and approved final version of manuscript.

Data Availability Data are available upon request to the corresponding author.

Compliance with Ethical Standards

Conflict of interest The authors declare that they have no competing interests.

References

Abdelmajid K, Karim BH, Chedly A (2008) Symbiotic response of common bean (*Phaseolus vulgaris* L.) to iron deficiency. Acta Physiol Plant 30:27–34. https://doi.org/10.1007/s11738-007-0087-5

Ahammed GJ, Choudhary SP, Chen S et al (2013) Role of brassinosteroids in alleviation of phenanthrene–cadmium co-contamination-induced photosynthetic inhibition and oxidative stress in tomato. J Exp Bot 64:199–213. https://doi.org/10.1093/jxb/ers323

Ahanger MA, Ashraf M, Bajguz A, Ahmad P (2018) Brassinosteroids regulate growth in plants under stressful environments and crosstalk with other potential phytohormones. J Plant Growth Regul 37:1007–1024. https://doi.org/10.1007/s00344-018-9855-2

Ahanger MA, Mir RA, Alyemeni MN, Ahmad P (2020) Combined effects of brassinosteroid and kinetin mitigates salinity stress in tomato through the modulation of antioxidant and osmolyte metabolism. Plant Physiol Biochem 147:31–42. https://doi.org/10.1016/j.plaphy.2019.12.007

Ahmad P, Jaleel CA, Salem MA et al (2010) Roles of enzymatic and nonenzymatic antioxidants in plants during abiotic stress. Crit Rev Biotechnol 30:161–175. https://doi.org/10.3109/07388550903524243

Ahmad P, Abd_Allah EF, Alyemeni MN et al (2018a) Exogenous application of calcium to 24-epibrassinosteroid pre-treated tomato seedlings mitigates NaCl toxicity by modifying ascorbate–glutathione cycle and secondary metabolites. Sci Rep 8:13515. https://doi.org/10.1038/s41598-018-31917-1

Ahmad P, Ahanger MA, Egamberdieva D et al (2018b) Modification of osmolytes and antioxidant enzymes by 24-epibrassinolide in chickpea seedlings under mercury (Hg) toxicity. J Plant Growth Regul 37:309–322. https://doi.org/10.1007/s00344-017-9730-6

Aksoy E, Maqbool A, Tindas İ, Caliskan S (2017) Soybean: a new frontier in understanding the iron deficiency tolerance mechanisms in plants. Plant Soil 418:37–44. https://doi.org/10.1007/s11104-016-3157-x

Alam P, Albalawi TH, Altalayan FH et al (2019) 24-epibrassinolide (EBR) confers tolerance against NaCl stress in soybean plants by up-regulating antioxidant system, ascorbate-glutathione cycle, and glyoxalase system. Biomolecules. https://doi.org/10.3390/biom9110640

Anwar F, Kamal GM, Nadeem F, Shabir G (2016) Variations of quality characteristics among oils of different soybean varieties. J King Saud Univ Sci 28:332–338. https://doi.org/10.1016/j.jksus.2015.10.001

Aragão RM, Silva EN, Vieira CF, Silveira JAG (2012) High supply of NO3—mitigates salinity effects through an enhancement in the efficiency of photosystem II and CO2 assimilation in *Jatropha curcas* plants. Acta Physiol Plant 34:2135–2143. https://doi.org/10.1007/s11738-012-1014-y

Badawi GH, Yamauchi Y, Shimada E et al (2004) Enhanced tolerance to salt stress and water deficit by overexpressing superoxide dismutase in tobacco (*Nicotiana tabacum*) chloroplasts. Plant Sci 166:919–928. https://doi.org/10.1016/j.plantsci.2003.12.007

Bai G, Jenkins S, Yuan W et al (2018) Field-based scoring of soybean iron deficiency chlorosis using RGB imaging and statistical learning. Front Plant Sci 9:1–12. https://doi.org/10.3389/fpls.2018.01002

Bajguz A (2010) An enhancing effect of exogenous brassinolide on the growth and antioxidant activity in *Chlorella vulgaris* cultures under heavy metals stress. Environ Exp Bot 68:175–179. https://doi.org/10.1016/j.envexpbot.2009.11.003

Bajguz A (2011) Suppression of *Chlorella vulgaris* growth by cadmium, lead, and copper stress and its restoration by endogenous brassinolide. Arch Environ Contam Toxicol 60:406–416. https://doi.org/10.1007/s00244-010-9551-0

Baker HM, Anderson BF, Baker EN (2003) Dealing with iron: common structural principles in proteins that transport iron and heme. Proc Natl Acad Sci USA 100:3579–3583. https://doi.org/10.1073/pnas.0637295100

Barberon M, Dubeaux G, Kolb C et al (2014) Polarization of iron-regulated transporter 1 (IRT1) to the plant-soil interface plays

crucial role in metal homeostasis. Proc Natl Acad Sci USA 111:8293–8298. https://doi.org/10.1073/pnas.1402262111

Barberon M, Vermeer JEM, De Bellis D et al (2016) Adaptation of root function by nutrient-induced plasticity of endodermal differentiation. Cell 164:447–459. https://doi.org/10.1016/j.cell.2015.12.021

Barros Junior UO, Barbosa MAM, Lima MDR et al (2017) Short-time of rehydration is not effective to re-establish chlorophyll fluorescence and gas exchange in two cowpea cultivars submitted to water deficit. Not Bot Horti Agrobot Cluj-Napoca 45:238–244. https://doi.org/10.15835/nbha45110569

Bhardwaj R, Arora N, Sharma P, Arora HK (2007) Effects of 28-homobrassinolide on seedling growth, lipid peroxidation and antioxidative enzyme activities under nickel stress in seedlings of *Zea mays* L. Asian J Plant Sci 6:765–772. https://doi.org/10.3923/ajps.2007.765.772

Bishop GJ, Koncz C (2002) Brassinosteroids and plant steroid hormone signaling. Plant Cell 14:S97–S110. https://doi.org/10.1105/tpc.001461

Borges KLR, Hippler FWR, Carvalho MEA et al (2019) Nutritional status and root morphology of tomato under Cd-induced stress: comparing contrasting genotypes for metal-tolerance. Sci Hortic (Amsterdam) 246:518–527. https://doi.org/10.1016/j.scienta.2018.11.023

Bradford MM (1976) A rapid and sensitive method for the quantitation of microgram quantities of protein utilizing the principle of protein-dye binding. Anal Biochem 72:248–254. https://doi.org/10.1016/0003-2697(76)90527-3

Buonasera K, Lambreva M, Rea G et al (2011) Technological applications of chlorophyll a fluorescence for the assessment of environmental pollutants. Anal Bioanal Chem 401:1139–1151. https://doi.org/10.1007/s00216-011-5166-1

Cakmak I, Horst WJ (1991) Effect of aluminium on lipid peroxidation, superoxide dismutase, catalase, and peroxidase activities in root tips of soybean (*Glycine max*). Physiol Plant 83:463–468. https://doi.org/10.1111/j.1399-3054.1991.tb00121.x

Cakmak I, Marschner H (1992) Magnesium deficiency and high light intensity enhance activities of superoxide dismutase, ascorbate peroxidase, and glutathione reductase in bean leaves. Plant Physiol 98:1222–1227. https://doi.org/10.1104/pp.98.4.1222

Casson SA, Hetherington AM (2012) GSK3-like kinases integrate brassinosteroid signaling and stomatal development. Sci Signal 5:1–3. https://doi.org/10.1126/scisignal.2003311

Castro EM, Pereira FJ, Paiva R (2009) Plant histology: structure and function of vegetative organs. Federal University of Lavras, Lavras, p 234

Chen L, Ding C, Zhao X et al (2015) Differential regulation of proteins in rice (*Oryza sativa* L.) under iron deficiency. Plant Cell Rep 34:83–96. https://doi.org/10.1007/s00299-014-1689-1

Choudhary SP, Bhardwaj R, Gupta BD et al (2011) Enhancing effects of 24-epibrassinolide and putrescine on the antioxidant capacity and free radical scavenging activity of *Raphanus sativus* seedlings under Cu ion stress. Acta Physiol Plant 33:1319–1333. https://doi.org/10.1007/s11738-010-0665-9

Clouse SD (2002) Brassinosteroids Plant counterparts to animal steroid hormones? In: Litwack G (ed) Vitamins and hormones, 1st edn. Academic Press, United States, pp 195–223. https://doi.org/10.1016/S0083-6729(02)65065-4

Colangelo EP, Lou GM (2006) Put the metal to the petal: metal uptake and transport throughout plants. Curr Opin Plant Biol 9:322–330. https://doi.org/10.1016/j.pbi.2006.03.015

Cui H (2015) Cortex proliferation in the root is a protective mechanism against abiotic stress. Plant Signal Behav 10:e1011949. https://doi.org/10.1080/15592324.2015.1011949

da Silveira VC, de Oliveira AP, Sperotto RA et al (2007) Influence of iron on mineral status of two rice (*Oryza sativa* L.) cultivars. Braz J Plant Physiol 19:127–139. https://doi.org/10.1590/S1677-04202007000200005

Dumas L, Chazaux M, Peltier G et al (2016) Cytochrome b6f function and localization, phosphorylation state of thylakoid membrane proteins and consequences on cyclic electron flow. Photosynth Res 129:307–320. https://doi.org/10.1007/s11120-016-0298-y

Eburneo L, Ribeiro-Júnior NG, Karsburg IV et al (2017) Anatomy and micromorphometric analysis of leaf *Catasetum x apolloi Benelli* & Grade with addition of potassium silicate under different light sources. Braz J Biol 77:140–149. https://doi.org/10.1590/1519-6984.12015

Ekpei P, Bedford D, Claro J et al (2018) Food outlook. FAO, Rome

El-Beltagi HS, Mohamed HI (2013) Reactive oxygen species, lipid peroxidation and antioxidative defense mechanism. Not Bot Horti Agrobot Cluj-Napoca 41:44–57. https://doi.org/10.15835/nbha4118929

Elstner EF, Heupel A (1976) Inhibition of nitrite formation from hydroxylammoniumchloride: a simple assay for superoxide dismutase. Anal Biochem 70:616–620. https://doi.org/10.1016/0003-2697(76)90488-7

Ennajeh M, Vadel AM, Cochard H, Khemira H (2010) Comparative impacts of water stress on the leaf anatomy of a drought-resistant and a drought-sensitive olive cultivar. J Hortic Sci Biotechnol 85:289–294. https://doi.org/10.1080/14620316.2010.11512670

Fariduddin Q, Yusuf M, Chalkoo S et al (2011) 28-Homobrassinolide improves growth and photosynthesis in *Cucumis sativus* L. through an enhanced antioxidant system in the presence of chilling stress. Photosynthetica 49:55–64. https://doi.org/10.1007/s11099-011-0022-2

Fernández V, Eichert T, Del Río V et al (2008) Leaf structural changes associated with iron deficiency chlorosis in field-grown pear and peach: physiological implications. Plant Soil 311:161–172. https://doi.org/10.1007/s11104-008-9667-4

Flexas J, Ribas-Carbó M, Diaz-Espejo A et al (2008) Mesophyll conductance to CO_2: current knowledge and future prospects. Plant Cell Environ 31:602–621. https://doi.org/10.1111/j.1365-3040.2007.01757.x

Flexas J, Barbour MM, Brendel O et al (2012) Mesophyll diffusion conductance to CO_2: an unappreciated central player in photosynthesis. Plant Sci 193–194:70–84. https://doi.org/10.1016/j.plantsci.2012.05.009

Gallego SM, Pena LB, Barcia RA et al (2012) Unravelling cadmium toxicity and tolerance in plants: insight into regulatory mechanisms. Environ Exp Bot 83:33–46. https://doi.org/10.1016/j.envexpbot.2012.04.006

Giannopolitis CN, Ries SK (1977) Superoxide dismutases: I. Occurrence in higher plants. Plant Physiol 59:309–314

Giehl RF, Meda AR, Wirén NV (2009) Moving up, down, and everywhere: signaling of micronutrients in plants. Curr Opin Plant Biol 12:320–327. https://doi.org/10.1016/j.pbi.2009.04.006

Gong M, Li Y-J, Chen S-Z (1998) Abscisic acid-induced thermotolerance in maize seedlings is mediated by calcium and associated with antioxidant systems. J Plant Physiol 153:488–496. https://doi.org/10.1016/S0176-1617(98)80179-X

Gonzalez-Garcia M-P, Vilarrasa-Blasi J, Zhiponova M et al (2011) Brassinosteroids control meristem size by promoting cell cycle progression in Arabidopsis roots. Development 138:849–859. https://doi.org/10.1242/dev.057331

Hacham Y, Holland N, Butterfield C et al (2011) Brassinosteroid perception in the epidermis controls root meristem size. Development 138:839–848. https://doi.org/10.1242/dev.061804

Hasan SA, Hayat S, Ahmad A (2011) Brassinosteroids protect photosynthetic machinery against the cadmium induced oxidative stress in two tomato cultivars. Chemosphere 84:1446–1451. https://doi.org/10.1016/j.chemosphere.2011.04.047

Havir EA, McHale NA (1987) Biochemical and developmental characterization of multiple forms of catalase in tobacco leaves. Plant Physiol 84:450–455. https://doi.org/10.1104/pp.84.2.450

Hertle AP, Blunder T, Wunder T et al (2013) PGRL1 is the elusive ferredoxin-plastoquinone reductase in photosynthetic cyclic electron flow. Mol Cell 49:511–523. https://doi.org/10.1016/j.molcel.2012.11.030

Hoagland DR, Arnon DI (1950) The water-culture method for growing plants without soil, 2nd edn. California Agricultural Experiment Station, Berkeley

Jan S, Alyemeni MN, Wijaya L et al (2018) Interactive effect of 24-epibrassinolide and silicon alleviates cadmium stress via the modulation of antioxidant defense and glyoxalase systems and macronutrient content in *Pisum sativum* L. seedlings. BMC Plant Biol 18:146. https://doi.org/10.1186/s12870-018-1359-5

Janeczko A, Gruszka D, Pociecha E et al (2016) Physiological and biochemical characterisation of watered and drought-stressed barley mutants in the HvDWARF gene encoding C6-oxidase involved in brassinosteroid biosynthesis. Plant Physiol Biochem 99:126–141. https://doi.org/10.1016/j.plaphy.2015.12.003

Javelle M, Vernoud V, Rogowsky PM, Ingram GC (2011) Epidermis: the formation and functions of a fundamental plant tissue. New Phytol 189:17–39. https://doi.org/10.1111/j.1469-8137.2010.03514.x

Jeong J, Connolly EL (2009) Iron uptake mechanisms in plants: functions of the FRO family of ferric reductases. Plant Sci 176:709–714. https://doi.org/10.1016/j.plantsci.2009.02.011

Jin CW, You GY, He YF et al (2007) Iron deficiency-induced secretion of phenolics facilitates the reutilization of root apoplastic iron in red clover. Plant Physiol 144:278–285. https://doi.org/10.1104/pp.107.095794

Johansen DA (1940) Plant microtechnique, 1st edn. McGraw-Hill, New York

Kaiser BN, Moreau S, Castelli J et al (2003) The soybean NRAMP homologue, GmDMT1, is a symbiotic divalent metal transporter capable of ferrous iron transport. Plant J 35:295–304. https://doi.org/10.1046/j.1365-313X.2003.01802.x

Kaya C, Ashraf M, Wijaya L, Ahmad P (2019) The putative role of endogenous nitric oxide in brassinosteroid-induced antioxidant defence system in pepper (*Capsicum annuum* L.) plants under water stress. Plant Physiol Biochem 143:119–128. https://doi.org/10.1016/j.plaphy.2019.08.024

Kaya C, Ashraf M, Alyemeni MN, Ahmad P (2020) The role of nitrate reductase in brassinosteroid-induced endogenous nitric oxide generation to improve cadmium stress tolerance of pepper plants by upregulating the ascorbate-glutathione cycle. Ecotoxicol Environ Saf 196:110483. https://doi.org/10.1016/j.ecoenv.2020.110483

Keino L, Baijukya F, Ng'etich W et al (2015) Nutrients limiting soybean (*Glycine max* L.) growth in acrisols and ferralsols of Western Kenya. PLoS ONE 10:1–20. https://doi.org/10.1371/journal.pone.0145202

Kim SA, Lou GM (2007) Mining iron: iron uptake and transport in plants. FEBS Lett 581:2273–2280. https://doi.org/10.1016/j.febslet.2007.04.043

Kim T-W, Michniewicz M, Bergmann DC, Wang Z-Y (2012) Brassinosteroid regulates stomatal development by GSK3-mediated inhibition of a MAPK pathway. Nature 482:419–422. https://doi.org/10.1038/nature10794

Kohli SK, Handa N, Sharma A et al (2018a) Combined effect of 24-epibrassinolide and salicylic acid mitigates lead (Pb) toxicity by modulating various metabolites in *Brassica juncea* L. seedlings. Protoplasma 255:11–24. https://doi.org/10.1007/s00709-017-1124-x

Kohli SK, Handa N, Sharma A et al (2018b) Interaction of 24-epibrassinolide and salicylic acid regulates pigment contents, antioxidative defense responses, and gene expression in *Brassica juncea* L. seedlings under Pb stress. Environ Sci Pollut Res 25:15159–15173. https://doi.org/10.1007/s11356-018-1742-7

Kohli SK, Bali S, Tejpal R et al (2019) In-situ localization and biochemical analysis of bio-molecules reveals Pb-stress amelioration in *Brassica juncea* L. by co-application of 24-epibrassinolide and salicylic acid. Sci Rep 9:1–15. https://doi.org/10.1038/s41598-019-39712-2

Krumova S, Zhiponova M, Dankov K et al (2013) Brassinosteroids regulate the thylakoid membrane architecture and the photosystem II function. J Photochem Photobiol B 126:97–104. https://doi.org/10.1016/j.jphotobiol.2013.07.008

Kumari A, Sheokand S, Swaraj K (2010) Nitric oxide induced alleviation of toxic effects of short term and long term Cd stress on growth, oxidative metabolism and Cd accumulation in chickpea. Braz J Plant Physiol 22:271–284. https://doi.org/10.1590/S1677-04202010000400007

Larbi A, Abadía A, Abadía J, Morales F (2006) Down co-regulation of light absorption, photochemistry, and carboxylation in Fe-deficient plants growing in different environments. Photosynth Res 89:113–126. https://doi.org/10.1007/s11120-006-9089-1

Lermontova I, Kruse E, Mock H-P, Grimm B (1997) Cloning and characterization of a plastidal and a mitochondrial isoform of tobacco protoporphyrinogen IX oxidase. Proc Natl Acad Sci USA 94:8895–8900. https://doi.org/10.1073/pnas.94.16.8895

Li J, Cang Z, Jiao F et al (2017) Influence of drought stress on photosynthetic characteristics and protective enzymes of potato at seedling stage. J Saudi Soc Agric Sci 16:82–88. https://doi.org/10.1016/j.jssas.2015.03.001

Lichtenthaler HK, Buschmann C (2001) Chlorophylls and carotenoids: measurement and characterization by UV-VIS spectroscopy. Current protocols in food analytical chemistry. Wiley, Hoboken, NJ, pp 431–438

Lima JV, Lobato AKS (2017) Brassinosteroids improve photosystem II efficiency, gas exchange, antioxidant enzymes and growth of cowpea plants exposed to water deficit. Physiol Mol Biol Plants 23:59–72. https://doi.org/10.1007/s12298-016-0410-y

Lima MDR, Barros Junior UO, Batista BL, Lobato AKS (2018) Brassinosteroids mitigate iron deficiency improving nutritional status and photochemical efficiency in *Eucalyptus urophylla* plants. Trees 32:1681–1694. https://doi.org/10.1007/s00468-018-1743-7

López-Millán A-F, Grusak MA, Abadía A, Abadía J (2013) Iron deficiency in plants: an insight from proteomic approaches. Front Plant Sci 4:1–8. https://doi.org/10.3389/fpls.2013.00254

Ma JF, Mitani N, Nagao S et al (2004) Characterization of the silicon uptake system and molecular mapping of the silicon transporter gene in rice. Plant Physiol 136:3284–3289. https://doi.org/10.1104/pp.104.047365

Mahmoudi H, Labidi N, Ksouri R et al (2007) Differential tolerance to iron deficiency of chickpea varieties and Fe resupply effects. C R Biol 330:237–246. https://doi.org/10.1016/j.crvi.2007.02.007

Maia CF, Silva BRS, Lobato AKS (2018) Brassinosteroids positively modulate growth: physiological, biochemical and anatomical evidence using two tomato genotypes contrasting to dwarfism. J Plant Growth Regul 37:1–14. https://doi.org/10.1007/s00344-018-9802-2

Molassiotis AN, Diamantidis GC, Therios IN et al (2005) Oxidative stress, antioxidant activity and Fe(III)-chelate reductase activity of five *Prunus* rootstocks explants in response to Fe deficiency. Plant Growth Regul 46:69–78. https://doi.org/10.1007/s10725-005-6396-z

Morrissey J, Lou GM (2009) Iron uptake and transport in plants: the good, the bad, and the ionome. Chem Rev 109:4553–4567. https://doi.org/10.1021/cr900112r.Iron

Nakano Y, Asada K (1981) Hydrogen peroxide is scavenged by ascorbate-specific peroxidase in spinach chloroplasts. Plant Cell Physiol 22:867–880

Ogweno JO, Song XS, Shi K et al (2008) Brassinosteroids alleviate heat-induced inhibition of photosynthesis by increasing carboxylation efficiency and enhancing antioxidant systems in *Lycopersicon esculentum*. J Plant Growth Regul 27:49–57. https://doi.org/10.1007/s00344-007-9030-7

Ogweno JO, Hu WH, Song XS et al (2010) Photoinhibition-induced reduction in photosynthesis is alleviated by abscisic acid, cytokinin and brassinosteroid in detached tomato leaves. Plant Growth Regul 60:175–182. https://doi.org/10.1007/s10725-009-9439-z

Oliveira VP, Lima MDR, Silva BRS et al (2019) Brassinosteroids confer tolerance to salt stress in *Eucalyptus urophylla* plants enhancing homeostasis, antioxidant metabolism and leaf anatomy. J Plant Growth Regul 38:557–573. https://doi.org/10.1007/s00344-018-9870-3

Osório J, Osório ML, Correia PJ et al (2014) Chlorophyll fluorescence imaging as a tool to understand the impact of iron deficiency and resupply on photosynthetic performance of strawberry plants. Sci Hortic (Amsterdam) 165:148–155. https://doi.org/10.1016/j.scienta.2013.10.042

Paniz FP, Pedron T, Freire BM et al (2018) Effective procedures for the determination of As, Cd, Cu, Fe, Hg, Mg, Mn, Ni, Pb, Se, Th, Zn, U and rare earth elements in plants and foodstuffs. Anal Methods 10:4094–4103. https://doi.org/10.1039/c8ay01295d

Pereira YC, Rodrigues WS, Lima EJA et al (2019) Brassinosteroids increase electron transport and photosynthesis in soybean plants under water deficit. Photosynthetica 57:1–11

Pestana M, de Varennes A, Abadía J, Faria EA (2005) Differential tolerance to iron deficiency of citrus rootstocks grown in nutrient solution. Sci Hortic (Amsterdam) 104:25–36. https://doi.org/10.1016/j.scienta.2004.07.007

Pociecha E, Dziurka M, Oklestkova J, Janeczko A (2016) Brassinosteroids increase winter survival of winter rye (*Secale cereale* L.) by affecting photosynthetic capacity and carbohydrate metabolism during the cold acclimation process. Plant Growth Regul 80:127–135. https://doi.org/10.1007/s10725-016-0149-z

Pociecha E, Dziurka M, Waligórski P et al (2017) 24-Epibrassinolide pre-treatment modifies cold-induced photosynthetic acclimation mechanisms and phytohormone response of perennial ryegrass in cultivar-dependent manner. J Plant Growth Regul 36:618–628. https://doi.org/10.1007/s00344-016-9662-6

Rattan A, Kapoor D, Kapoor N et al (2020) Brassinosteroids regulate functional components of antioxidative defense system in salt stressed maize seedlings. J Plant Growth Regul 39:1–11. https://doi.org/10.1007/s00344-020-10097-1

Ribeiro DGS, Silva BRS, Lobato AKS (2019) Brassinosteroids induce tolerance to water deficit in soybean seedlings: contributions linked to root anatomy and antioxidant enzymes. Acta Physiol Plant 41:1–11. https://doi.org/10.1007/s11738-019-2873-2

Rivero RM, Gimeno J, Van Deynze A et al (2010) Enhanced cytokinin synthesis in tobacco plants expressing PSARK:IPT prevents the degradation of photosynthetic protein complexes during drought. Plant Cell Physiol 51:1929–1941. https://doi.org/10.1093/pcp/pcq143

Roncel M, González-Rodríguez AA, Naranjo B et al (2016) Iron deficiency induces a partial inhibition of the photosynthetic electron transport and a high sensitivity to light in the diatom *Phaeodactylum tricornutum*. Front Plant Sci 7:1–14. https://doi.org/10.3389/fpls.2016.01050

Rout GR, Sahoo S (2015) Role of iron in plant growth and metabolism. Rev Agric Sci 3:1–24. https://doi.org/10.7831/ras.3.1

Santos CS, Roriz M, Carvalho SMP, Vasconcelos MW (2015) Iron partitioning at an early growth stage impacts iron deficiency responses in soybean plants (*Glycine max* L.). Front Plant Sci 6:1–12. https://doi.org/10.3389/fpls.2015.00325

Segatto FB, Bisognin DA, Benedetti M et al (2004) A technique for the anatomical study of potato leaf epidermis. Ciência Rural 34:1597–1601. https://doi.org/10.1590/S0103-84782004000500042

Shahbaz M, Ashraf M (2007) Influence of exogenous application of brassinosteroid on growth and mineral nutrients of wheat (*Triticum Aestivum* L.) under saline conditions. Pak J Bot 39:513–522

Sharma A, Thakur S, Kumar V et al (2016) Pre-sowing seed treatment with 24-epibrassinolide ameliorates pesticide stress in *Brassica juncea* L. Through the modulation of stress markers. Front Plant Sci 7:1–12. https://doi.org/10.3389/fpls.2016.01569

Sharma A, Kumar V, Shahzad B et al (2020) Photosynthetic response of plants under different abiotic stresses: a review. J Plant Growth Regul 39:509–531. https://doi.org/10.1007/s00344-019-10018-x

Siddiqui H, Ahmed KBM, Hayat S (2018) Comparative effect of 28-homobrassinolide and 24-epibrassinolide on the performance of different components influencing the photosynthetic machinery in *Brassica juncea* L. Plant Physiol Biochem 129:198–212. https://doi.org/10.1016/j.plaphy.2018.05.027

Silva EN, Ferreira-Silva SL, Fontenele AV et al (2010) Photosynthetic changes and protective mechanisms against oxidative damage subjected to isolated and combined drought and heat stresses in *Jatropha curcas* plants. J Plant Physiol 167:1157–1164. https://doi.org/10.1016/j.jplph.2010.03.005

Silva EN, Ribeiro RV, Ferreira-Silva SL et al (2012) Coordinate changes in photosynthesis, sugar accumulation and antioxidative enzymes improve the performance of *Jatropha curcas* plants under drought stress. Biomass Bioenerg 45:270–279. https://doi.org/10.1016/j.biombioe.2012.06.009

Singh P, Kumar R, Sabapathy SN, Bawa AS (2008) Functional and edible uses of soy protein products. Compr Rev Food Sci Food Saf 7:14–28. https://doi.org/10.1111/j.1541-4337.2007.00025.x

Socha AL, Lou GM (2014) Mn-euvering manganese: the role of transporter gene family members in manganese uptake and mobilization in plants. Front Plant Sci 5:1–16. https://doi.org/10.3389/fpls.2014.00106

Song YL, Dong YJ, Tian XY et al (2016) Role of foliar application of 24-epibrassinolide in response of peanut seedlings to iron deficiency. Biol Plant 60:329–342. https://doi.org/10.1007/s10535-016-0596-4

Steel RG, Torrie JH, Dickey DA (2006) Principles and procedures of statistics: a biometrical approach, 3rd edn. Academic Internet Publishers, Moorpark

Suzuki T, Masuda T, Singh DP et al (2002) Two types of ferrochelatase in photosynthetic and nonphotosynthetic tissues of cucumber. J Biol Chem 277:4731–4737. https://doi.org/10.1074/jbc.M105613200

Swamy KN, Rao SSR (2009) Effect of 24-epibrassinolide on growth, photosynthesis, and essential oil content of *Pelargonium graveolens* (L.) Herit. Russ J Plant Physiol 56:616–620. https://doi.org/10.1134/S1021443709050057

Talaat NB, Shawky BT (2013) 24-Epibrassinolide alleviates salt-induced inhibition of productivity by increasing nutrients and compatible solutes accumulation and enhancing antioxidant system in wheat (*Triticum aestivum* L.). Acta Physiol Plant 35:729–740. https://doi.org/10.1007/s11738-012-1113-9

Tewari RK, Hadacek F, Sassmann S, Lang I (2013) Iron deprivation-induced reactive oxygen species generation leads to non-autolytic PCD in *Brassica napus* leaves. Environ Exp Bot 91:74–83. https://doi.org/10.1016/j.envexpbot.2013.03.006

Tikhonov AN (2013) The cytochrome b6f complex at the crossroad of photosynthetic electron transport pathways. Plant Physiol Biochem 81:163–183. https://doi.org/10.1016/j.plaphy.2013.12.011

Timperio AM, D'Amici GM, Barta C et al (2007) Proteomics, pigment composition, and organization of thylakoid membranes in iron-deficient spinach leaves. J Exp Bot 58:3695–3710. https://doi.org/10.1093/jxb/erm219

Tomasi N, Mimmo T, Terzano R et al (2014) Nutrient accumulation in leaves of Fe-deficient cucumber plants treated with natural Fe complexes. Biol Fertil Soils 50:973–982. https://doi.org/10.1007/s00374-014-0919-6

Tsai HH, Schmidt W (2017) Mobilization of iron by plant-borne coumarins. Trends Plant Sci 22:538–548. https://doi.org/10.1016/j.tplants.2017.03.008

Vardhini BV, Sujatha E, Rao SSR et al (2012) Studies on the effect of brassinosteroids on the qualitative changes in the storage roots of radish. Bulg J Agric Sci 18:63–69

Velikova V, Yordanov I, Edreva A (2000) Oxidative stress and some antioxidant systems in acid rain-treated bean plants protective role of exogenous polyamines. Plant Sci 151:59–66. https://doi.org/10.1016/S0168-9452(99)00197-1

Wu Q-S, Xia R-X, Zou Y-N (2006) Reactive oxygen metabolism in mycorrhizal and non-mycorrhizal citrus (*Poncirus trifoliata*) seedlings subjected to water stress. J Plant Physiol 163:1101–1110. https://doi.org/10.1016/j.jplph.2005.09.001

Wu X, Yao X, Chen J et al (2014) Brassinosteroids protect photosynthesis and antioxidant system of eggplant seedlings from high-temperature stress. Acta Physiol Plant 36:251–261. https://doi.org/10.1007/s11738-013-1406-7

Xia X-J, Huang L-F, Zhou Y-H et al (2009) Brassinosteroids promote photosynthesis and growth by enhancing activation of Rubisco and expression of photosynthetic genes in *Cucumis sativus*. Planta 230:1185–1196. https://doi.org/10.1007/s00425-009-1016-1

Xiong H, Guo X, Kobayashi T et al (2014) Expression of peanut Iron regulated transporter 1 in tobacco and rice plants confers improved iron nutrition. Plant Physiol Biochem 80:83–89. https://doi.org/10.1016/j.plaphy.2014.03.021

Yu JQ, Huang L-F, Hu WH et al (2004) A role for brassinosteroids in the regulation of photosynthesis in *Cucumis sativus*. J Exp Bot 55:1135–1143. https://doi.org/10.1093/jxb/erh124

Yuan J, Chen Y, Li H et al (2018) New insights into the cellular responses to iron nanoparticles in *Capsicum annuum*. Sci Rep 8:3228. https://doi.org/10.1038/s41598-017-18055-w

Zhang Y, Xu S, Yang S, Chen Y (2015) Salicylic acid alleviates cadmium-induced inhibition of growth and photosynthesis through upregulating antioxidant defense system in two melon cultivars (*Cucumis melo* L.). Protoplasma 252:911–924. https://doi.org/10.1007/s00709-014-0732-y

Zhiponova MK, Vanhoutte I, Boudolf V et al (2013) Brassinosteroid production and signaling differentially control cell division and expansion in the leaf. New Phytol 197:490–502. https://doi.org/10.1111/nph.12036

CONCLUSÃO GERAL

Os resultados de ambos os estudos demonstraram que suprimentos baixos e altos de Zn e Fe produziram efeitos deletérios em plantas de soja. Contudo, nossas pesquisas revelaram claramente que EBR pode desempenhar papéis múltiplos e benéficos em plantas de soja expostas aos efeitos negativos de Zn e Fe.

EBR aliviou o impacto produzido pelo estresse do zinco no sistema radicular agindo positivamente sobre a epiderme radicular, endoderme radicular, córtex, cilindro vascular e metaxilema, melhorando intrisecamente a homeostase dos nutrientes nas plantas.

As repercussões benéficas da EBR no crescimento, manutenção dos pigmentos fotossintéticos, maquinário fotossintético e trocas gasosas estavam intrinsecamente ligados à menor produção de compostos oxidantes e danos às células.

A aplicação exógena do EBR em plantas expostas ao estresse de Zn e Fe melhorou, de modo geral, os parâmetros anatômicos, nutricionais, fisiológicos, bioquímicos e morfológicos, com 100 nM EBR como concentração ótima. Isso pode ser recomendado para a utilização prática em plantas expostas a deficiência de Zn e Fe e ao excesso de Zn.